SUMMARY OF T-28 PARTICIPATION IN VORTEX/MIGHT, 1994-1995

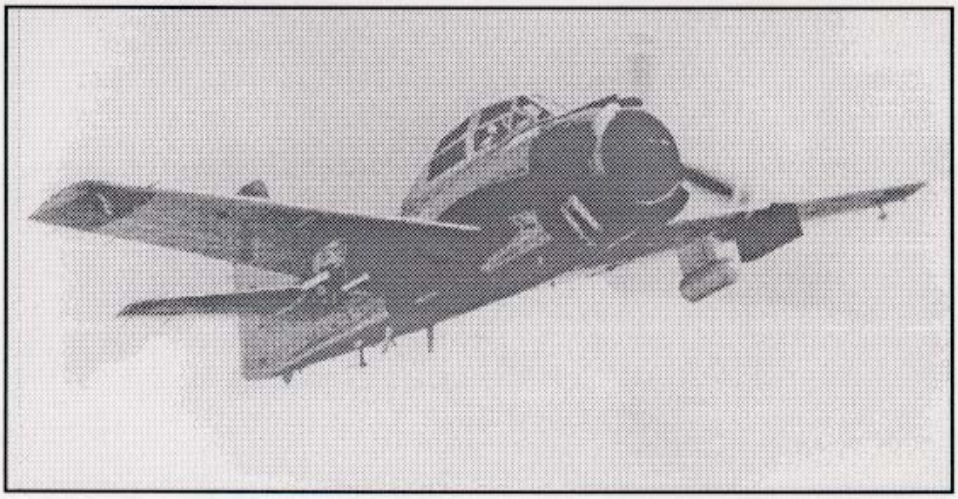

By:
Andrew G. Detwiler, Kenneth R. Hartman, and Paul L. Smith

Report SDSMT/IAS/R-96/01
January 1996

Prepared for:
Division of Atmospheric Sciences
National Science Foundation
4201 Wilson Blvd.
Arlington, VA 22203-9966

Institute of Atmospheric Sciences
South Dakota School of Mines and Technology
501 East Saint Joseph Street
Rapid City SD 57701-3995

TABLE OF CONTENTS

LIST OF FIGURES

LIST OF TABLES

I. INTRODUCTION

The South Dakota School of Mines and Technology (SDSMT) armored T-28 storm-penetrating research aircraft was deployed to the central Great Plains for portions of the 1994 and 1995 spring storm seasons at the request of Prof. Jerry Straka, University of Oklahoma (OU), and Dr. Dusan Zrnic, National Severe Storms Laboratory (NSSL). Its mission was to penetrate convective clouds and provide *in situ* observations of the precipitation particle population in regions simultaneously being scanned by a multi-parameter meteorological radar. The T-28 observations will be used in conjunction with multi-parameter radar signatures to improve algorithms for inferring cloud microphysical characteristics from multi-parameter radar signatures. A list of the hypotheses being investigated using T-28 and multi-parameter radar observations is given in Table 1.

Oklahoma flight operations were conducted from Westheimer Field in Norman during the month of May in both 1994 and 1995 in coordination with the NSSL Cimarron meteorological radar. An additional three weeks of operations were also conducted in Colorado in June, 1995, from Ft. Collins/Loveland Airport in coordination with the Colorado State University (CSU) CHILL meteorological radar located northeast of Greeley, Colorado. For the 1995 Colorado operations Drs. Straka and Zrnic were joined by Drs. Steve Rutledge (Dept. Atmospheric Sciences, CSU) and V. N. Bringi (Dept. Electrical Engineering, CSU), as co-requestors for the T-28 deployment. These deployments were funded by the National Science Foundation (NSF) Division of Atmospheric Sciences (ATM) facilities deployment pool and were made possible by base support for the T-28 research aircraft facility under cooperative agreements ATM-9104474 and ATM-9401117 between NSF and the South Dakota School of Mines and Technology.

The Oklahoma portions of T-28 operations were in loose coordination with the Verification of Rotation in Tornadoes Experiment (VORTEX; see Rasmussen *et al.*, 1994). VORTEX was conducted from 1 April through 15 June in both 1994 and 1995. It was hosted by NSSL and OU with collaboration from a large group of university and government organizations. VORTEX operations involved a fleet of instrumented automobiles, mobile research balloon launchers, and mobile surface and airborne radars, that deployed to intercept tornadic storms occurring anywhere within the broad region from southern Kansas through Oklahoma through northern Texas. The primary goals of VORTEX were related to identification of precursors to tornado development in convective storms.

TABLE 1. MIGHT Hypotheses

Specific Differential phase (K_{DP})

Values of K_{DP} in rain/hail mixtures are due almost entirely to rain. The rain contribution to Z_H can be separated from the hail contribution if the presence of mixed phase hydrometeors is limited.

Pairs of K_{DP} and Z_H delineate the ice/liquid boundary better than pairs of Z_{DR} and Z_H if the presence of mixed phase hydrometeors is limited.

Positive signatures of K_{DP} in ice clouds can be produced by oriented dendrites. The concentrations of these dendrites might be more accurately determined using K_{DP} than K_H.

Triplets of K_{DP}, Z_{DR}, and Z_H, might be used to identify oriented dendrites from other ice forms.

Cross-polar correlation (ρ_{HV})

Values of $\rho_{HV}(0)$ decrease with increasing diversity of hydrometeor type, orientation, size, and shape. Thus $\rho_{HV}(0)$ should decrease near the melting level where there are mixtures of liquid and ice phase hydrometeors and where there are large hailstones.

Values of $\rho_{HV}(0)$ decrease with increasing hail/aggregate size.

Values of $\rho_{HV}(0)$ decrease with increasing protuberance to diameter ratio of hailstones.

Values of $\rho_{HV}(0)$ are at a minimum when the contributions to Z_H from hail, and graupel/rain are similar.

Backscatter differential phase (δ)

Backscatter differential phase can be used to determine aggregate and hail size.

Differential reflectivity (Z_{DR})

Values of Z_{DR} are about -0.5 to -2.0 dB, and values of Z_H are greater than 55 dBZ in regions of hail with maximum sizes of 2 to 4 cm.

Values of Z_{DR} are more negative in hail cores with oblate hailstones and are near-zero in storms than produce more spherical hailstones.

Large values of Z_{DR} (1.5 to 5.5 dB) with small Z_H (5 to 35 dBZ) and non-trivial attenuation indicate low concentrations of very large drops (3 to 8 mm diameter)

The T-28 operations were restricted by radar beamwidth limitations to roughly 50 n mi range from the Cimarron radar, located just west of Oklahoma City. To distinguish T-28 Oklahoma operations from the much more extensive VORTEX operations, the T-28-based program was dubbed Measure, Interpret, and Ground-truth Hydrometeors in Thunderstorms (MIGHT). MIGHT depended on the VORTEX forecasting infrastructure, but conducted operations independently of the larger experiment due to its unique goals and the limitation of operating closely enough to the Cimarron radar to obtain good quality multi-parameter data. It turned out that only one of the T-28 missions during the two Oklahoma deployments was in coordination with a VORTEX deployment, and that occurred on 17 May 1995.

The CSU-CHILL radar has some performance characteristics superior to those of the Cimarron radar. Both are 10-cm wavelength radars with 1 deg beamwidths and the capability of transmitting and receiving both horizontal and vertical linearly-polarized radiation. However, CHILL has better antenna beam characteristics and can receive reflected radiation cross-polar to the transmitted polarization, which Cimarron cannot. In order to obtain a collection of multi-parameter observations in convective storms that includes cross-polar quantities, such as linear depolarization ratio (LDR), a Colorado deployment was added to the originally-planned MIGHT deployments to Oklahoma. In addition, the drier Colorado climate produces storms which might be expected to differ somewhat microphysically from Oklahoma storms due to higher and colder cloud bases, among other differences, in Colorado. Thus multi-parameter signatures in Colorado might be different, or the interpretation of the same signature might be different, in Colorado compared to observations obtained in Oklahoma.

The T-28 armored storm-penetrating research aircraft has been conducting operations in convective storms since 1969. Over the years it has played a pivotal role in important studies of thunderstorm structure and evolution in the North American Great Plains, southeastern US, and Switzerland. It carries a suite of state-of-the-art instrumentation that can accurately characterize microphysical populations ranging from cloud droplets a few micrometers in diameter to hailstones the size of tennis balls. In addition it records standard meteorological variables and electrostatic fields within and around thunderstorms. Finally, vertical winds can be estimated from recorded aircraft motion, acceleration, and attitude variables. A table describing instruments carried during the MIGHT deployments is given in Appendix A. Quantities routinely recorded and/or computed from readings of these instruments are described in Appendix B, organized by a unique "tag" number by which they are indexed in the reduced data files. Basic information concerning the algorithms used in these computations is given in Appendix C. Further information, along with software that can be used to extract and analyze specific data from the recorded datasets, can be obtained through the Institute of Atmospheric Sciences at SDSMT.

II. FLIGHT OPERATIONS

A list of all flights conducted during MIGHT operations in 1994 and 1995 is given in Table 2. Maps showing the operational areas in Oklahoma and Colorado are provided in Figures 1 and 2.

A summary of daily operations on those days with research flights is given below. All times are local daylight time (CDT in May, 1994 and 1995, and MDT in June, 1995), with T-28 takeoff and landing times indicated under the "Operations" subheadings. The level of detail in the summaries varies somewhat from day-to-day, due to changes in operational configuration and personnel. It is felt useful to include details helpful for interpreting the aircraft observations if they are available, rather than leave out all but the most general observations in order to maintain a consistent style throughout.

✈Flight 620, Friday, 6 May 1994

Weather

VORTEX teams left in morning for KS. Strong storms with tornadoes and hail developed in NE OK, just south of the KS border, about 1700, roughly 150 km NNE of Cimmaron. Predominantly positive CG lightning discharges for some periods.

Late in the day, when it was clear that there would be no significant convection within range of the Cimarron radar, the T-28 did a clear air test flight out to 65 n mi west of Will Rogers VORTAC. This was roughly 80 n mi from Norman. The highest altitude reached was 21 kft (6.4 km).

Operations
1719 - 1822

Telemetry worked well for the whole flight. Some problems were experienced with the handheld VHF transceiver used on the ground for ground-air communications, but problems were no worse at 65 n mi than at 20 n mi from Will Rogers. Pilot could not hear ground but ground could hear him, sometimes.

TABLE 2. T-28 FLIGHTS during MIGHT

Date	Flt No.	Time (h)	Purpose
(1994)			
30 April	617	0.3	test flight (local)
1 May	618	2.6	ferry to ICT
3 May	619	1.5	ferry to OUN
6 May	620	1.3	test flight
9 May	621	1.1	research
23 May	622	1.7	research
24 May	623	1.9	research
25 May	624	1.8	research
29 May	625	1.8	research
1 June	626	1.3	ferry to EWK
1 June	627	1.4	ferry to MCK
2 June	628	1.6	ferry to RAP
Total hrs		*18.3*	
(1995)			
28 April	651	1.2	test flight (local)
1 May	652	1.4	ferry to LBF
1 May	653	3.0	ferry to OUN
3 May	654	1.2	test flight
5 May	655	1.9	research
7 May	656	1.8	research/test (land at OKC)
7 May	657	0.4	ferry to OUN
17 May	658	1.9	research
20 May	659	1.6	pilot proficiency
21 May	660	2.2	research
23 May	661	1.2	research
23 May	662	2.2	ferry to MCK
23 May	663	1.7	ferry to RAP
11 June	664	2.1	ferry to FNL
12 June	665	0.9	test
17 June	666	1.7	research
20 June	667	1.5	research
22 June	668	1.2	research
25 June	669	1.3	test
27 June	670	1.7	research
28 June	671	2.0	research
1 July	672	1.7	ferry to RAP
Total hrs:		*35.8*	

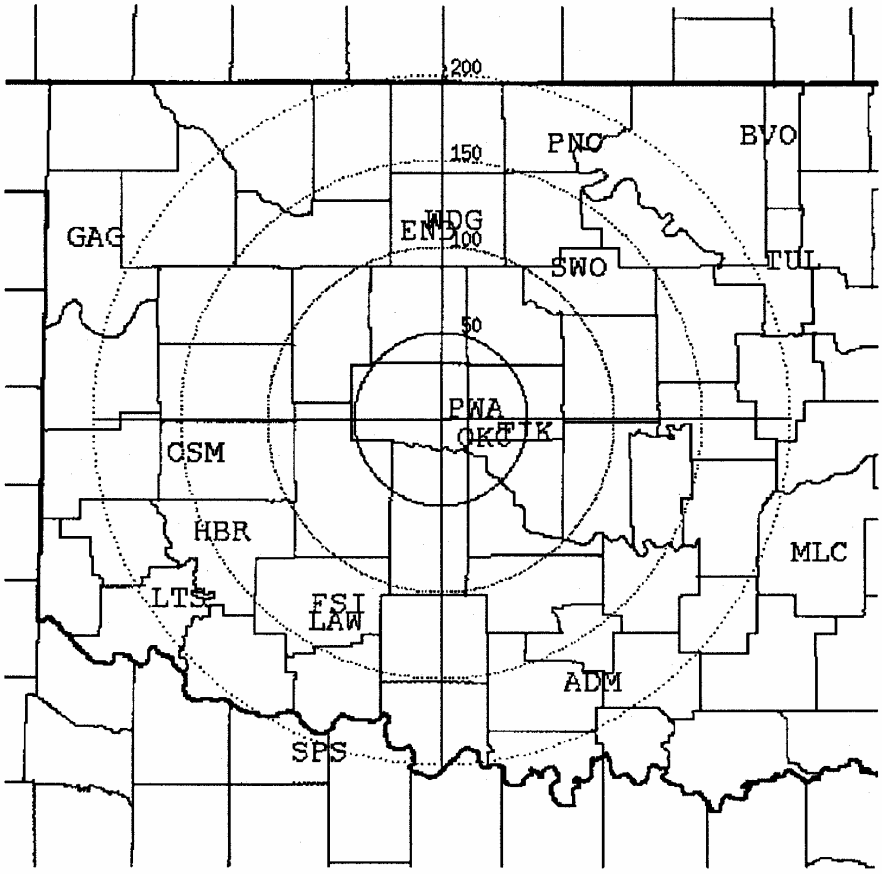

Figure 1. MIGHT operational area surrounding the Cimarron radar location NW of Oklahoma City (OKC). Range rings are at 50 km intervals. (Figure produced by Dave Priegnitz, SDSM&T.)

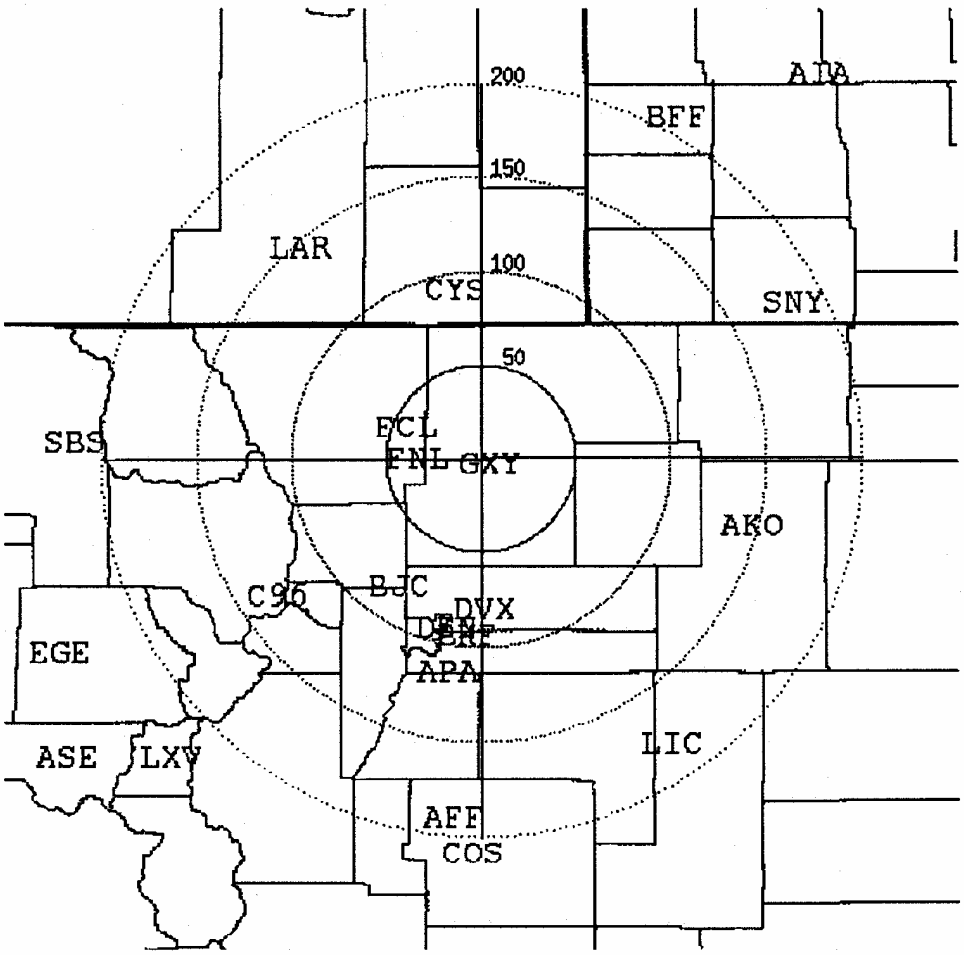

Figure 2 MIGHT operational area surrounding the CSU-CHILL radar site near Greeley, Colorado (GXY). Range rings are at 50 km intervals. (Figure produced by Dave Priegnitz, SDSM&T.)

Observations

Most data looked good at initial glance. Rosemount and reverse-flow temperatures were up to 2°C apart. The aircraft penetrated some shallow Cu just below inversion that showed up on the FSSP but not the J-W. Heater current reading looked good. No precipitation images in 150+ buffers of 2D-P data but just speckles, stuck bits, etc.

✈Flight 621, Monday, 9 May, 1994

Weather

It was very hazy and overcast, with light drizzle at Westheimer in the morning. Radar showed some echo extending to 5 km AGL to the S. VORTEX teams took off at 1030 to the west for something that they hoped would develop in the Texas panhandle region. T-28 remained in Norman, and carried out a melting layer mission in coordination with the Cimmaron radar.

Operations
1239-1322

T-28 took off at 1239 with conditions just above minimums at Westheimer. Climbed out ~ 20 n mi to the SW to 9500 ft (2.9 km); then turned SE and penetrated a mass of cloud with some embedded echo rolls and cores in which reflectivities reached the high 30's dBZ. The aircraft reversed course after 20 n mi or so and returned at 11500 ft (3.5 km). After this leg, it was due S of Cimmaron radar about 60 km out. At this point it returned to base as fuel reserves were just sufficient to reach Tulsa, the nearest alternate, if conditions were still below minimum at Westheimer on arrival there. It turned out that landing was possible at Westheimer.

The ARTCC transponder worked reasonably well following a recent repair. Radio communications were not high quality. Air-to-ground was good; ground-to-air was not so good.

Observations

The pilot reported light precipitation through most of the flight. The 2D-P showed small drizzle at 9500 ft (7°C) and large aggregates at 11500 ft (2°C). Precipitation particle number concentrations were slightly lower at the lower altitude. The 2D-P images were somewhat corrupted. Many of the time bars were corrupted, making concentration analysis somewhat laborious. It is still possible to do a reasonably accurate size and concentration estimate using the data. The only cloud droplets encountered were in some

elements just below the inversion. The J-W and FSSP appeared to respond consistently. It would seem that the hail spectrometer should have picked up some of the larger aggregates at 11500 ft, but it didn't. It did pick up some particles on landing. Images were obtained, but were too small to show much detail. A field mill test was conducted from 124444 for one minute; it turned out to be corrupted by aircraft charging.

✈Flight 622, Monday, 23 May 1994

Weather

After a two-week hiatus in the weather, the goal was to make a test flight into any echo within range in which precipitation might be found, to test probe performance and also radar display and tracking in the operations room.

By about 1600 nature obliged as some multicellular storms were in progress about 80 mi NW of Norman. They were making copious lightning on the NLDN, were relatively stationary, and new development looked like it was occurring on the SW end. This system eventually grew in size and complexity and moved over the OKC region late in the evening.

Operations
1724-1824

The aircraft climbed to the SW, then headed W of Cimarron radar, then turned N. Cruise altitude was 14 kft (4.3 km). There are some control problems with the radar and at 1756 Cimarron is still not under control. At 1758 the aircraft headed through the target storm to the N, at 105 km NW of Cimarron. Once through it did a 180 deg turn to come back through and head for home.

Observations

At 1802 the pilot reported icing and precipitation in the clouds he penetrated. Data review shows RFT ~-3°C; ~1/2 g/m^3 peak J-W cloud water concentration; mostly streak images on the 2D-P; and artifacts on the hail spectrometer. There are questionable hail counts at 175537 and near the beginning of descent at 180943. There is good foil, showing that the largest particles were few mm drops near the end of the first penetration and few mm imprints during the last penetration. Peak updrafts were ±7.5 m/s with computations using the Cooper and Kopp methods in good agreement with each other. There were signs of a polarimetric radar signa-

ture of insects at 600-700 m AGL, but it was weak. There were no obvious insect images in our probe data, but the data are so noisy that insects could not be ruled out. The 2D-P recorded good images when precipitation particles were present, but there is a background of noise due to stuck bits, etc. The FSSP recorded no droplets after 175830, possibly due to interference from icing.

✈Flight 623, Tuesday, 24 May 1994

Weather

Remnants of previous day's MCS were still in the region in the morning. Active shower bands were N and S of Norman. Lightning was over by 0800 or so. The operations decision was to go for remnants to the S. Tops had subsided to 15 kft and maximum reflectivity to 50 dBZ as of 0830.

Operations
0913-1044

The aircraft performed multiple penetrations of convective storm remnants initially ~60 n mi to S of the Cimarron radar. The data system crashed briefly at 094331 but was back on at 094546. Penetration levels ranged between 3.8 to 4.5 km MSL. The predominant particle types were graupel, both roundish and conical, and aggregates. Peak J-W cloud water concentrations approached 0.7 g m^{-3}. Strong vertical electric fields, ranging from -60 to +40 kV m^{-1}, were encountered, generally associated with peaks in graupel concentration at the penetration level. For the final penetration the T-28 had to descend with the cloud tops from 4.5 to 3.8 km MSL. Particle sizes and concentrations, and electric fields, diminished during the later penetrations.

Observations

The 2D-P recorded low continuous counts on climbout. There are a few raindrops but most of the images were artifacts. Leaving de-ice heat on until approach on descent seemed to minimize spurious images in 2D-P data and spurious counts in hail spectrometer data. This 2D-P seems very prone to streaking! It was recording streakers with only 0.5 g m^{-3} indicated cloud water concentration from the J-W. There was noise in the image data, but good images should be separable.

Very good foil impressions were obtained, in basic agreement with 2D-P, except that aggregates didn't make clear impressions on the foil. Due to the long time spent in-cloud, a large length of foil was exposed. After

the flight the foil was broken into 2 segments. The first segment was marked off in 1 ft increments from the punch marks. It ended at the end of penetration 4 at the position of the trailing edge of the window (about $9^5/_8$ in past the punch mark). The second portion of the foil was marked in 1 ft increments from this trailing edge of the window position. The E-field pattern of variation from penetration to penetration was consistent with a cloud-top positive charge layer falling through the aircraft level during the flight, as the cloud collapsed.

✈Flight 624, Wednesday, 25 May 1994

Weather

It was warm and relatively (for this year) humid. The VORTEX mobile mesonet went south, expecting convection to develop along the Red River (which did occur later).

Cimarron was turned on at 1506. Large storm(s) were detectable out in NW OK, near Gage. Cimarron showed some >67 dBZ patches in it, along with a distinct weak echo region ~90 miles from Cimarron. Storm evolution was followed for several hours prior to launch. At 1550 there was not much storm movement. New cells had been forming on the E side, but this process seemed to have ceased, at this time. By 1600 one of the middle echos in the group intensified with >67 dBZ extending to 18 kft. At 1630 operators switched Cimarron from recording basic parameters to recording in polarimetric mode. New echo was developing SEwd from old at 297 deg/65 mi from Cimarron. At 1645 operators switched to sector scans of the storm. A line of feeders/daughters extended SEwd from the main echo. Echo tops over the main echo region extended to 45 kft. Closest development was still 61 mi from Cimarron. By 1700 could visually see some convective development to ENE of Norman, but echo was not visible on OKC WSR-57 in that direction. The line of convection to NW was filling in and the closest portions were within 40 mi of Cimarron. Decision was made to go for 1800 launch of T-28.

At 1724 the main storm was 70 mi NW of Cimarron. Peak reflectivity was >67 dBZ with 55 dBZ echo extending to 25 kft.

Operations
1821 - 1942

At 1753 the Cimarron computer clock was noted to be ~17 s ahead of WWV.

The critical problem with operations on this day developed at 1827. Operators lost control of Cimarron and could no longer change the azimuth limits of the sector scan. Later during the flight the radar computer was re-booted, and the data recorded up to that time were overwritten.

The T-28 made 4 passes through a convective storm 50 to 60 km to the NW of Cimarron at altitudes ranging from 10 to 12 kft (3.0 to 3.7 km) MSL. The ground generally could be seen during penetration at 10 kft. Moderate precipitation, p-static, lightning, light turbulence, and modest updrafts were encountered.

Observations

The clouds got progressively more vigorous and contained higher concentrations of precipitation as the flight progressed and reached higher altitudes. The pilot didn't clearly recognize any hail during his flight, although there could have been some smaller stones. The foil was clear and little-wrinkled. All punch marks came through. There were very high concentrations of particles on all but the first pass. Biggest impressions were < 5 to 6 mm. The depth of the impressions varied. The biggest particles were probably heavily rimed aggregates. There may have been lightly-rimed aggregates of similar size that just didn't make complete impressions. The lowest pass (1st) probably was characterized by rain as indicated by round impressions. Hail images were recorded until 185959 and were mostly small. The 2D-P probe performance was vastly improved over previous VORTEX flights. There were still some stuck bits, but not nearly so many empty buffers as on previous flights. The first halves of buffers again suffered from enhanced electronic noise. The electric field variations were quite interesting. There were fairly large values (many 10's of kV m^{-1}) with much shifting of sign. According to the National Lightning Detection Network, this storm was producing predominantly positive cloud-to-ground lightning during its most vigorous phase (prior to arrival of T-28). There was a successful field mill test 182426-183102, showing that the field mill suite was operating normally.

✈Flight 625, Sunday, 29 May 1994

Weather

The leading edge of a squall line was passing over Norman by 6 AM. It had been working its way south from the Kansas border since midnight. As it passed there was heavy rain, frequent lightning, and some areas with severe winds and small hail. It accelerated as it passed Norman heading S and was at the Red River by 10 AM.

Operations
0820-0945

This was to be the final flight of the 1994 campaign. At 0825 there was a brief cloud encounter 60 km S Cimarron, ~1.5 km MSL, 13°C. No precipitation particles were detected. Again at 0832 there was a brief cloud penetration 95 km S Cimarron at 3 km MSL. Again there was no precipitation.

The T-28 made multiple penetrations through the decaying squall line ~100 to 170 km S and SE of Cimarron. Penetration temperatures ranged from 7 to 0°C. At 0837 the data acquisition system crashed; it was successfully rebooted. Moderate rain, moderate turbulence, lightning, and p-static were encountered. Communications were poor due to the p-static and great range, leading to some mis-direction of the penetrations.

Observations

This storm slipped out of radar range before a good job of sampling it could be accomplished. The first two passes should have good, if somewhat distant, radar coverage of the penetration regions. Hail imaging quit after first pass. The spectrometer was dumping 10 buffers/s to the data acquisition system at the time of the crash. It may have been a factor contributing to the crash.

The foil had its largest impressions on the first pass. There were large prolate impressions up to 7-8 mm, denser in the middle than on the edges. The 2D-P images were prolate, too, with many splashes and bursts. This is consistent with partially melted/frozen particles. Negligible cloud water was found on all passes. The south side of the line was generally 3-4°C warmer than the north side, at all levels.

✈Flight 654, Wednesday, 3 May 1995

Weather

Very sporadic drizzle drops were noted while walking outside around Westheimer Field near the time of the flight.

Operations
1720 - 1813

This was the first operation of the 1995 season. The aircraft departed Norman to the south, taking off into strong southerly winds. It went into cloud almost immediately, then turned northwestward. It flew northwest of Oklahoma City, orbitted for a while, and returned. Cloud and precipitation particle encounters were as follows:

1722 - while climbing from 800-1200 m heading NW from Norman. Encountered cloud water only.

1725 - while climbing from 1800-2200 m heading NW from Norman. Encountered cloud water only.

1744→1747 - while orbitting 40 km NW of Twin Lakes radar and descending from 2200→1700 m. Encountered cloud water and drizzle drops.

1802→1810 - a long leg at 950 m flying SW from 10 to 20 km from Twin Lakes radar. Encountered cloud water. There may have been a very few drizzle drops. The radar signature was suggestive of oriented insects near this altitude. If there were images of insects in the 2D-P data, it would be hard to distinguish them from the shed drop (streak) images, as both would be elongated in the horizontal. (The 2D-P samples ~1 m^3 every 6 s, or ~10 m^3 min^{-1}.)

Observations

The telemetered positions were flawlessly transmitted into the radar display workstation and displayed on top of a Twin Lakes operational WSR-88D radar reflectivity display. However, there was an error in the position calculation relative to the radar within the telemetry receiving software. This problem was fixed after the flight. As little precipitation was expected, the foil impactor was not loaded for the flight. The NCAR King Probe (borrowed from NCAR for use in VORTEX 95) worked flawlessly. Liquid water concentrations were in the neighborhood of a few tenths of a gram per cubic meter during the two layers encountered on climb out and during descent through the upper of these layers. This was greater than those indicated by the J-W but less than those computed from the FSSP. The 2D-P seems to shed prolifically even when cloud water concentrations are in the neighborhood of only a few tenths of a gram per cubic meter. No valid 1-D hail spectrometer data were obtained. The hail spectrometer pylon field meter data show spikes due to radio communications, of the order of many kilovolts per meter. Other than the problems noted, research instrumentation appeared to work normally.

✈Flight 655, Friday, 5 May 1995

Weather

Echoes developed to the W by afternoon. By 1515 precipitation area was within usable range from Cimarron Radar.

Operations
1547 - 1716

The T-28 maintained 9 kft (2.7 km) MSL altitude throughout the flight, penetrating embedded convective cells within a general area of precipitation west of Oklahoma City and Norman that moved north-northeastward during the flight. Precipitation was heavy in spots and there was frequent lightning. The precipitation type encountered at 9 kft (~5°C) was predominantly rain drops, but in a few locations it appeared to be partially-melted graupel. Updrafts were mild at this relatively low altitude, with peak updraft estimates less than 10 m s^{-1}.

Observations

Instrumentation worked generally well. About 2 minutes of good hail spectrometer image data were obtained from 1559 - 1601. The foil impactor data were very clean, but the roll of foil was exhausted by ~1700 (after about 45 min of "in-cloud" data were obtained). The 2D-P data suffered from various stuck bits and random "speckles" (which were fixed during preliminary processing). King Probe, FSSP, and J-W cloud liquid water estimates agreed for very narrow droplet spectra encountered near cloud bases on climbout and return. At 9 kft the J-W estimates were roughly 1/2 those based on the other two instruments, presumably due to the fact that the J-W responds incompletely to the broader droplet spectra encountered further above cloud base. The pilot's voice notes were unusable due to low battery power in the audio-cassette unit. No field mill test was performed. The bottom mill failed near the very end of the flight.

✈Flight 656, Sunday, 7 May 1995

Weather

Storms were already forming to the W in the morning. After solving some problems with the operations display of KTLX radar, the call went out for an 1100 takeoff.

Operations
1118 - 1242

After some delays encountered in re-installing a bad field mill that had been removed for repair, and due to air traffic congestion in the region, the aircraft departed at 1118. The aircraft departed Norman to the S, then headed W for a line of convective cells west of Norman and Oklahoma City. This line extended southward into Texas. The data acquisition computer crashed at 113144, possibly due to a failure in the hail spectrometer caused by a circuit card coming loose. The system was successfully rebooted by 113549. All penetrations were at an altitude near 13 kft (4.0 km), where the temperature was ~0°C. Many individual convective cells within a general line of storms were penetrated. Data were obtained in updrafts, downdrafts, and quiescent stratiform regions. The most vigorous convection was encountered over Norman as the aircraft diverted northward to Will Rogers Airport due to poor landing conditions at Norman, after 1220, when the fuel was running low. Unfortunately, the 2D-P had apparently iced or fogged over by this time, and the foil impactor had jammed due to ice collected between layers of foil on the take-up spool. Thus no precipitation data were obtained in this region.

Data system was turned off at 124149 on approach to Will Rogers. After landing and refueling, a break in the weather at Norman occurred. The aircraft returned to Norman at ~1400.

Observations

Precipitation particle types were predominantly graupel and aggregates. The graupel generally was less than 5 mm in diameter, while some aggregates exceeded the span of the 2D-P (6.4 mm). Updrafts encountered were less than 10 m s^{-1} with peak cloud water concentrations of 2 g m^{-3}. The pilot noted lightning as frequently as 6 times per minute. 2D-P data were good until 122000. The foil registered denser particles well, but incomplete impressions were obtained in regions where aggregates predominated. The high concentrations of ice particles and rime ice build-up within the impactor itself during sampling caused some wrinkling of the foil through much of the flight, and led to the jamming of the impactor near 1217. Unfortunately, the hail spectrometer did not obtain good data after 1131. Other items of note concerning instrumentation include: (1) the hail pylon field mill was switched into the bottom fuselage position. The bottom mill had failed on the previous flight and had not yet been repaired. The nonworking mill was carried in the hail pylon to fill the hole, there. Appropriate changes were made in the data reduction equations, (2) 2D-P images con-

tinued to suffer from "speckles" (random bits turned on during imaging) in the last-halves of buffers. These speckles and also continuously stuck bits were fixed during processing of the image data, (3) An attempted field mill test (112220 - 112350) was covered by ambient fields and aircraft charging.

✈Flight 658, Wednesday, 17 May 1995

Weather

Storms went by in the morning, but operators couldn't get the Twin Lakes radar display on the operations work station. Storms were relatively small and moved rapidly NEwd. By the time the radar display problem was fixed, it was decided to wait for more active and larger storms in the afternoon. Storms developed N and E of OKC in afternoon. The T-28 targeted a group of storms N of OKC.

Operations
1544 - 1717

The aircraft departed Norman to the south, then headed north for a line of convective cells N of Norman and Oklahoma City. These were classic High Plains cumulonimbi. They were visible from the roof of the NSSL building during the first hour of the flight (see Fig. 3), after which they moved so far N and E that only portions of their anvils were visible from NSSL. The T-28 penetrated several storms in the region at a pressure altitude of 17 kft (5.2 km), encountering updrafts to 30 m s^{-1}, cloud liquid water concentrations approaching 5 g m^{-3}, and hail exceeding 2 cm diameter. The storms were forming near a strong local jet maximum, and the temperature at flight level varied by almost 10°C from the east side (warmer) to the west side (colder) of this maximum. Cells at a variety of stages of evolution were penetrated, providing detailed *in situ* measurements in strong nearly precipitation-free updrafts and in hail growth regions. The 1st and 4th penetrations were through the same echo maximum; the 2nd and 3rd were through another, and the 5th and 6th were through yet another. A third storm was penetrated on the way home. A sample of a radar view of the storms with flight track overlain is shown in Fig. 4.

Figure 3. Thunderstorms N of Norman, 1637 CDT, 17 May 1995.

Observations

One optical window shield on the 2D-P was lost on the 4th penetration during an encounter with a very high concentration of graupel and the probe provided unreliable data after that. The foil also ripped at this time, so that no foil data were obtained for the remainder of the flight. Hail image data were obtained only up to the 1st penetration. However, the hail spectrometer obtained good 1D (particle size) data throughout the flight, with detection of particles a cm or more in size corroborated by hail reports by the pilot. The King liquid water probe was also bent during the flight, but provided good data throughout. The first good field mill self-charge tests of the month were completed on this flight, and this was also the first flight with observations from two discharge probes, fore and aft, on the underside of the fuselage. These storms were electrically active, with pilot reports of lightning as frequent as once every 5 to 10 s.

✈Flight 660, Sunday, 21 May 1995

Weather

Personnel scrambled early for some stratiform clouds. These were remnants of clouds that had developed overnight and moved across Oklahoma. At 0830 some parts of the echo had tops to 5 km; in spots there were tops to 8 km. Cimarron ϕ_{dp} shows signal of oriented crystals.

Operations
0847 - 1011

Clouds to the S were worked initially in a block 12-15 kft (3.7-4.6 km), but eventually in the block 19-21 kft (5.8-6.4 km). They were worked in an area behind a more active convective region near the Red River, which was beyond operational range for the radar and aircraft. There was lightning in this more active region, but not in area where T-28 was working. Penetrations were generally NW-SE.

Observations

The pilot reported that he was in light rain at 13.5 kft (4.1 km) and indistinct cloud at 20 kft (6.1 km). There was quite a bit of ice inside the cowling when the aircraft landed. There were electric fields reaching 10's of

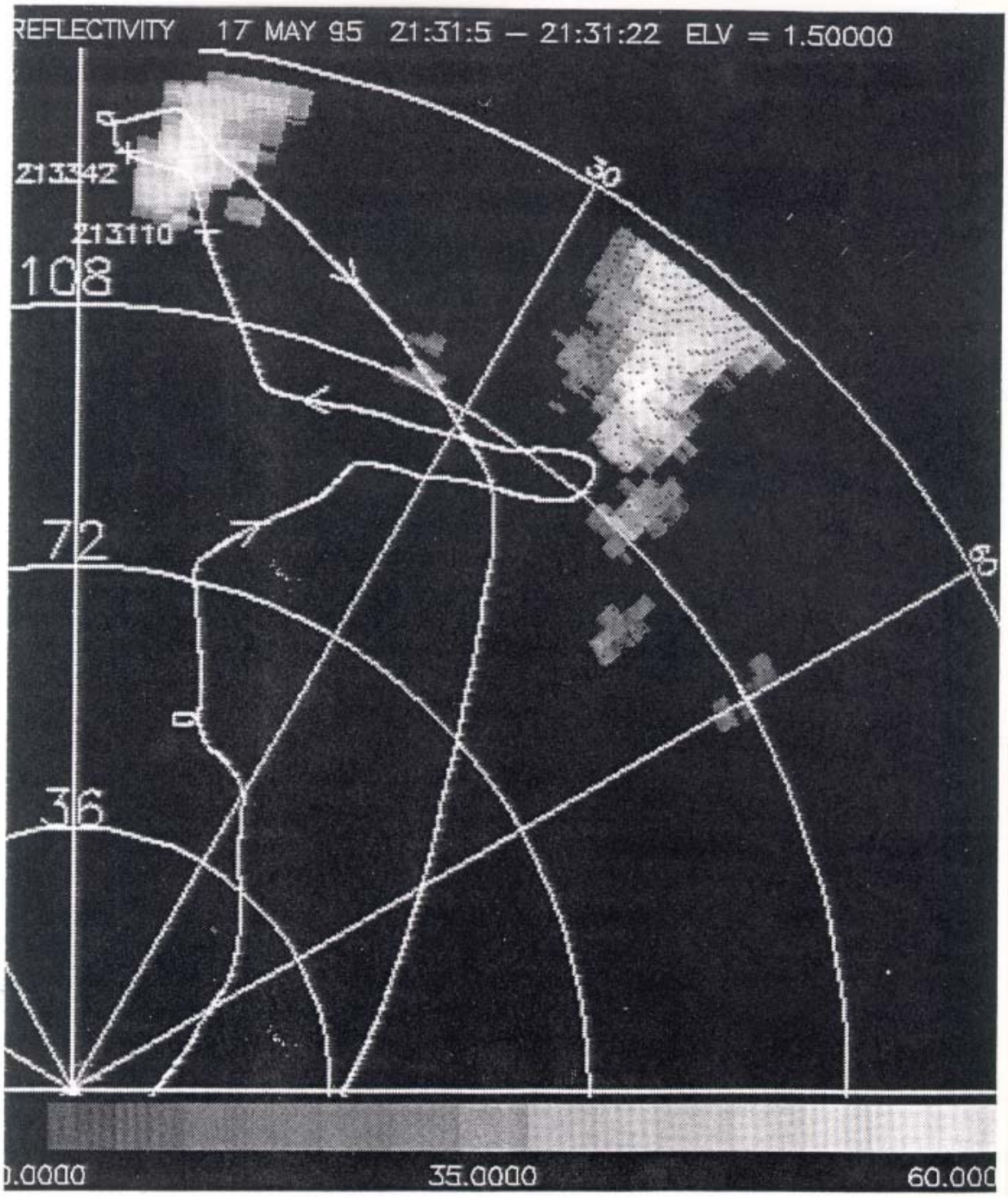

Figure 4. Cimarron radar reflectivity at 1.5° elevation at 1631 CDT on 17 May 1995. T-28 track for entire flight superimposed. Radar display spiderweb entered on radar, range in km, azimuth in deg. (Figure produced by Brent Gordon, OU.)

kV m^{-1} in places, and there were also two episodes of high counts from the hail spectrometer (probably due to large aggregates).

✈Flight 661, Tuesday, 23 May 1995

Weather

Convective storms developed just across the border in TX to the SW. They moved towards Norman beginning at 1400. There was some problem getting the KTLX display for operations; the display became available after 1500. By the time the T-28 took off the storm had had 55 dBZ echo to 6 km, but was already weakening as it approached central OK.

Operations
1548 - 1704

The T-28 reached the initial storm target, SW of Cimarron, at 1610. By this time the storm had decayed. The T-28 made one pass through, from 1607-1613, then headed N for a newly-formed cell. The aircraft spent the period 1622-1640 penetrating this newer cell NW of Cimarron, then turned SE, then headed back to Norman. On the way home another echo region was penetrated extending from 1645 until landing at 1704, although the in-cloud switch was not activated and thus there was no foil exposed during this period. All penetrations were near the 3 km MSL (7°C) level, until descent began at 1652.

Observations

Particle types were predominantly ice and rimed aggregates, probably beginning to melt. The largest particles, exceeding 5 mm across, were found in the newer cell NW of Cimarron, in which cloud water concentrations approached 1 g m^{-3} and updraft/downdrafts exceeded 5 m s^{-1}. The first and last echo regions penetrated had generally smaller precipitation particles, very small vertical motions and little cloud water, although some larger particles appeared in the 3rd echo region penetrated on the way home. All three echo regions penetrated were electrified, with peak field magnitudes reaching 10's of kV m^{-1}. The 2D-P probe mysteriously failed to record images between 161109-163630, although apparently valid shadow/or counts were being recorded during this period. A few hail spectrometer images were recorded just after 161109 and around 162655. Good hail spectrometer images were obtained during the pass through the 3rd echo region beginning at 1645. No field mill test was performed.

✈Flight 665, Monday, 12 June 1995

Weather

Generally sunny and clear.

Operations
1510 - 1600

This was the first day of operations in conjunction with the CSU-CHILL radar. A short test flight was made that actually involved a brief cloud penetration. The aircraft flew out to the Greeley area from its base at Ft. Collins-Loveland Airport (FNL), then headed away from the radar to test radio and telemetry. Several problems were noted, including problems in passing aircraft track information from the T-28 telemetry computer to the CHILL radar display computer (improper data format), problems with radio communications (volume turned down on pilot's headset for his second radio), and minor problems in filing a flight plan. The cable used to activate the turbocharger also failed when the pilot attempted to activate the turbocharger. The aircraft penetrated the edge of a storm north of CHILL, briefly, providing a good test of the SPEC, Inc., HVPS particle imaging device.

Observations

No foil was run. There were some problems with the 1-D response of the hail spectrometer, which are attributed to moisture that got into the probe during rainy weather in Rapid City. The HVPS images were excellent, and covered the whole penetration.

✈Flight 666, Saturday, 17 June 1995

Weather

There were strong S winds with nearly overcast mid-level clouds all day. Convective cells start moving off the mountains to the SW of DEN after 1600. Call T-28 crew at 1650. Rain at FNL at the time.

Operations
1718 - 1840

Some operational problems developed while switching CHILL and operations van to generator power, then back again when problems developed with the generator. The T-28 telemetry ground computer ended up rebooting with an older version of the telemetry software and sent track position in the wrong format to the radar display computer. The CHILL crew even-

tually activated a different radar display package that displayed the ARTCC transponder position. In the meantime, operations were guided by looking at separate radar and aircraft track displays. The aircraft worked a storm to the W of CHILL, penetrating at the 12 kft (3.7 km) level initially, then climbing to 15 kft (4.6 km) and then to 17 kft (5.2 km). The storm was moving rapidly NNE during the penetration period.

Observations

The HVPS again functioned well. Hail spectrometer 2D images were obtained after takeoff (rain), but imaging failed after storm penetrations began; the last hail images obtained came near 1748. The foil bunched up and jammed, and foil data were not obtained after the 4th pass. Radio communication spikes appeared in many variables, causing large spikes in the Kopp updraft calculation. A field mill test beginning at 171845 was lost in noise due to aircraft charging in rain and fields encountered while maneuvering around charged clouds. The J-W LWC was ~ 1/2 of King Probe LWC. FSSP spectra were somewhat broader than on the previous flight.

✈Flight 667, Tuesday, 20 June 1995

Weather

The aircraft was launched in the mid-afternoon as new convective cells were forming on an outflow boundary from an earlier storm. These new storms were near and E of CHILL, moving NEwd, at the time of the launch.

Operations
1600 - 1714

There were 13 penetrations, most on radials toward or away from CHILL, between 14 and 17 kft (4.3-5.2 km), in the small thunderstorm E of CHILL. The predominant precipitation type was low-density graupel and mushy clumps of aggregates, some reaching 2 cm across. Updrafts had 1-2 degrees of positive buoyancy. HVPS, foil, and 1-D hail spectrometer data are good. (There are a few minor glitches in the 1-D data, but they are easily recognizable as artifacts.) Impressions on foil are light but large. There were a few large artificial spikes in the reverse-flow temperature, but no large ones in Rosemount temperature or in pressure records. There were some indications in the electric field data of vertical screening layers of positive charge on entry and/or exit from several penetrations.

✈Flight 668, Thursday, 22 June 1995

Weather

Storms formed on the foothills even before noon. Low level winds were light and E; upper level winds strong SW. These conditions continued into the afternoon. Operations deployed instrumented vans to E at 1500 in anticipation of new development in this region, although nothing was forming there at the time.

Operations
1712 - 1806

The NCAR Sailplane took off at 1500. It went hunting for updrafts in the foothills west of FNL. CHILL received sailplane tracks for a while, but the aircraft apparently switched transponder codes and CHILL lost its track at 1608. Eventually the sailplane released at 1617 right over the CSU airfield. Operations received an update on sailplane transponder at 1628. It had climbed to 20 kft (6.1 km) from ~12 kft (3.7 km) in a storm ~50 km N of CHILL. The sailplane left the storm when its pitot iced up.

Operations called to launch the T-28 at 1650. Reflectivities reaching 35 dBZ extended to 40 kft (12.2 km) in a storm to N of CHILL at the time. The T-28 eventually made 5 penetrations along a SW-NE direction in a storm moving SEwd and passing N and E of CHILL, encountering large hail on several of the passes. See Fig. 5 for an example of the radar view during one pass. There was significant damage to the un-armored surfaces of the airframe and to the cooling fins on 3 cylinders. The FSSP forward hemisphere was badly pushed-in. The King probe element was damaged.

The flight was brought to an early conclusion when the oil filler door flapped open during the 5th pass. At the time, there were also communication problems on one of the two communications radios on the aircraft, making it impossible for the pilot to easily monitor both air traffic control and communications from the CHILL user van.

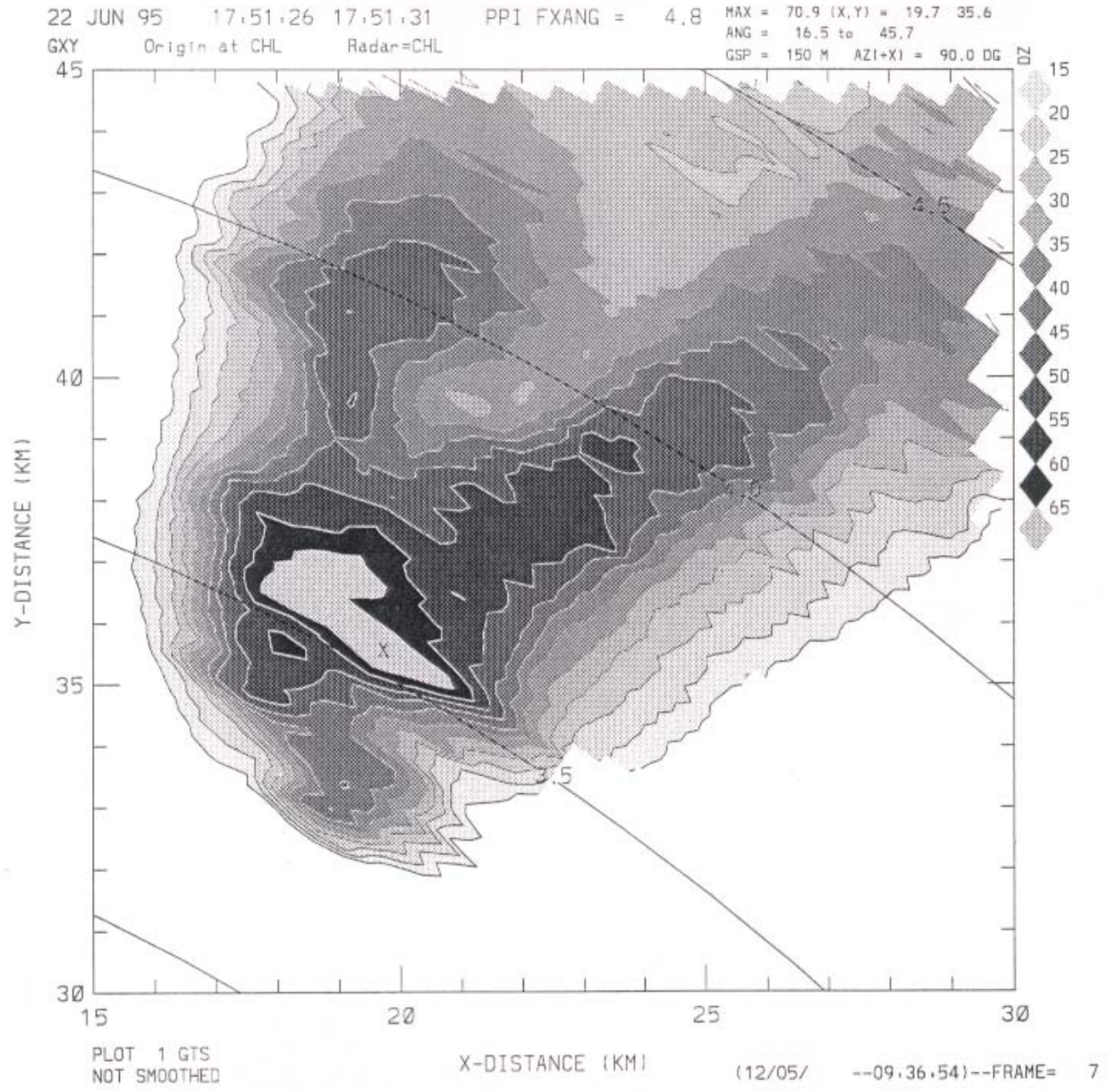

Figure 5. CHILL radar reflectivity at 48° elevation at 1751 MDT, 22 June 1995. The T-28 passed along the SE side of the reflectivity maximum. (Figure produced by Pat Kennedy, CSU.)

Observations

Large hail was encountered, sometimes outside of visible cloud. Maximum sizes detected by the hail spectrometer were 3-4 cm, while the largest impressions on the foil were ~1 1/2 cm. Observations from the mobile vans under the same storm confirmed maximum sizes of 3-4 cm. The cockpit audio tape recorded both muffled and sharp hail impacts from the windscreen microphone. Some hail could be heard even through the voice microphone. The King probe was not turned on until part way into the 1st penetration. It failed near 173630, part way in to the 3rd penetration. The hail spectrometer imaging worked until the beginning of the second penetration. All other instruments, including the HVPS, appeared to work well during the entire flight. There is some drift in the baseline of E_Z; this needs further investigation. There was a good field mill test from 171358-171617.

✈Flight 669, Sunday, 25 June 1995

Weather

Sunny and VFR.

Operations

A short low-level 30-min test flight (Flt 669) was run from FNL out over the CHILL radar and back. Two field mill tests were performed. The aircraft returned with the remains of many insects splatted on it.

Observations

A quick survey of the HVPS data revealed no obvious insect images. Based on the density of insect remains at several locations along leading edges, the average insect concentration in the air through which the aircraft flew was estimated to be one insect per 50 to 100 m^3.

✈Flight 670, Tuesday, 27 June 1995

Weather

High-base small Cb's developed by noon.

Operations
1510 - 1630

The call to launch came at 1430. Many potential targets were around the radar at the time. A storm was finally selected. It organized and intensified much more than expected initially. The T-28 made multiple penetrations between 15 and 17 kft (4.6 and 5.2 km, -2 to -6°C), finding soft hail that was generally pea to marble size, but occasionally ping-pong ball size. Later, the T-28 crew observed similar cells making cloud-to-ground lightning at the rate of 1-2 flashes/min. Storms remained active in the Ft. Collins area until well past 2200, with much wind but little rain.

Observations

The foil lasted until ~1603. Slushy-looking splats were the norm, with sizes in agreement with the pilot's observations. The final ~20 ft of foil were badly wrinkled as the take-up reel filled and eventually jammed, causing the motor to burn out. The HVPS worked well, with images in the same size range as noted by the pilot and on the foil. The King probe element was bent at some point during the flight, but the probe operated throughout the flight. Hail spectrometer 2D images were obtained only up to 1 min into the 1st pass, although 1D data were good through the entire flight. Spikes continued to appear in static pressure data, causing dramatic spikes in the updraft computations. Field mill test was unsuccessful.

✈Flight 671, Wednesday, 28 June 1995

Weather

"Stratiform" rain developed in the afternoon. Very sporadic lightning was observed later in the afternoon from an occasional embedded cell.

Operations
1758 - 1940

At 1710 the decision was made to launch for a bright band study. Rain ended at FNL, facilitating a T-28 takeoff. CHILL was still in the midst of a wide area of light rain. The aircraft made multiple long passes, E-W, through a large area of precipitation to the E of CHILL (see Fig. 6). It covered the altitude range 10 - 16 kft (3.0-4.9 km, +6 to -8°C). The T-28 ARTCC transponder, and one of its communications radios, both failed during the flight.

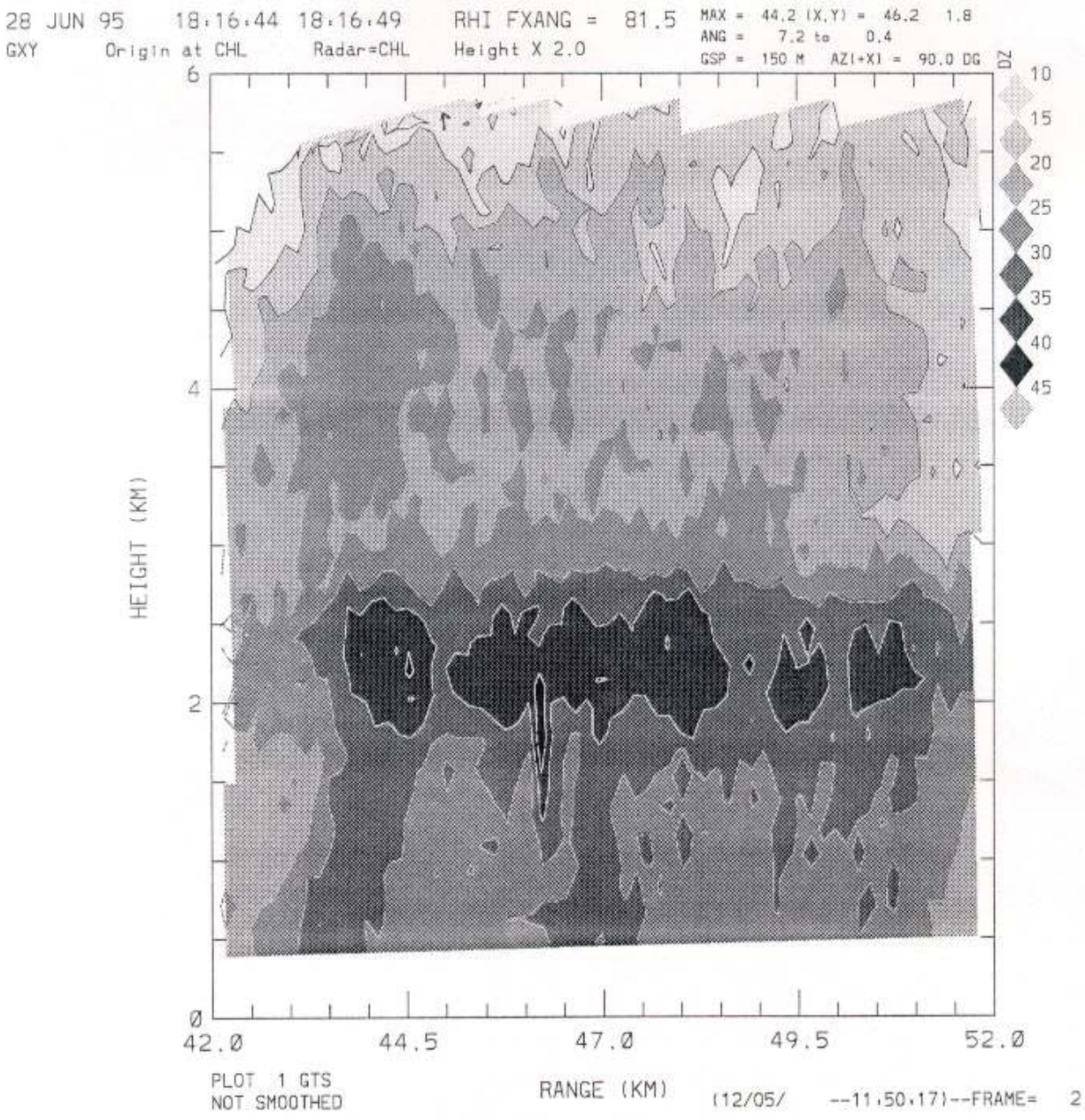

Figure 6. Vertical cross-section of CHILL radar reflectivity along the radial corresponding to the T-28 legs on 28 June 1995. Successive legs spanned in altitude the bright band centered at 2.25 km. (Figure produced by Pat Kennedy, CSU.)

Observations

Large particles were seen at and below the bright band; few 1D hail counts (indicating particles larger than 5 mm) were seen at the highest penetration level, above the bright band. There was a strong inversion between 14 and 16 kft (4.3 and 4.9 km). No foil data were obtained because the motor on the impactor had burned out on the previous day's flight and could not be replaced in time. Both HVPS and 1D hail spectrometer data were good. No field mill test was performed.

III. SUMMARY OF DATA COLLECTED

3.1 STORM-PENETRATION SUMMARY

A pass-by-pass summary of microphysical characteristics is given in Table 3. (Radar-relative flight tracks are shown in Appendix D.) The variables shown in Table 3 are described below.

Time in - times, in local daylight time, 24-hour format, when the aircraft began a cloud penetration. Attempts are made to keep the aircraft data system clock set to WWV. Only small deviations (plus or minus a second) may be present on any given flight, unless otherwise noted in daily summaries.

Dur - duration, in seconds, of the cloud penetration. At a typical true airspeed of ~90 m s^{-1}, the aircraft goes 1 km every 11 s.

GPS Alt - average geometric altitude, above mean sea level, during the penetration period as computed by the GPS.

Hdng - average direction of penetration, relative to magnetic north, in deg. A pattern of successive penetration headings differing by 180° is typical of successive penetrations of the same cell.

T - average temperature, in degrees Celsius, during the penetration as determined from the Rosemount aircraft temperature sensor. This sensor is subject to wetting effects and the average temperature may be biased low by a degree or more on many penetrations.

Max J-W, Max King - maximum 1-s value of total cloud liquid water concentration, in g m^{-3}, as determined by the J-W cloud water meter, or King Probe. The J-W instrument has been shown to respond mainly to droplets with diameters less than 30 micrometers; the King probe (available for 1995 flights) probably gives the truest reading under the broadest range of conditions.

Max Down, Max Up - Preliminary tabulation of peak negative and positive vertical winds, in m/s, during the period, estimated from changes in aircraft pressure altitude computed from centered 2-s differences with some corrections applied. The peak downdrafts tended to occur near the beginnings of penetrations and are not always reliable estimates of the actual air motion as the aircraft is not always in steady-state flight attitude at these times. As the aircraft rolls out of a turn, there is a period of ~ 30 s where the pilot regains altitude lost in the turn. Updraft estimates are only reliable at steady-state constant attitude flight settings.

Max Sh/Or - maximum precipitation particle count rate, observed during the penetration by the PMS 2D-P probe. The probe sweeps out ~ 1/6 m^3s^{-1}. This probe responds to particles larger than roughly 200 micrometers diameter. Only the edge of a particle need be in the sample volume to trip the probe, so the effective volume sampling rate for larger particles is larger than 1/6 m^3s^{-1}. A rough estimate of total concentration (ℓ^{-1})can be made by dividing this count by 160. The 2D-P was not flown during June, 1995.

Hail Mx C and Hail Mx D - Peak concentration (m^{-3}) of particles with diameters larger than ~5 mm and maximum-size particle (mm) detected by the hail spectrometer during the penetration. This estimate is based on counts from the non-imaging, one-dimensional part of the probe circuitry. Large liquid drops may be counted by this probe as well as snow, graupel, and hail. Timing criteria are used in an attempt to reject counts due to water streaming off the probe housing, although this has been observed to be insufficient to eliminate all artifacts from the data. The maximum measurable size is 45 mm. Values this large in the presence of rain are probably artifacts due to water streaming off the housing. Detailed examination of the measured size spectra should be done in order to further verify the maximum sizes listed here.

2D-P C and 2D-P D - Peak (1 s) concentration (m^{-3}) and size (mm) determined by preliminary analysis of 2D-P image data, along with a rough characterization of predominant particle type for 1994 data, only. The 2D-P was not flown during June, 1995.

TABLE 3
VORTEX/MIGHT CLOUD PENETRATION SUMMARY

Flight	Time In	Dur	GPS Alt	Hdng	T (C)	Max J-W	Max King	Max Down	Max Up	Max Sh/Or	Hail Mx C	Hl Mx D	2D-P C	2D-P D
	(LDT)	(s)	(m)	(deg)		($g\ m^{-3}$)	($g\ m^{-3}$)	($m\ s^{-1}$)	($m\ s^{-1}$)	(s^{-1})	(m^{-3})	(mm)	(ℓ^{-1})	(mm)
620	18:04:45	101	5661	111.3	-10.7	0.2		-3	2	296	0	0		
5/6/94	18:11:00	41	2197	133	17	0.4		-1	3	209	0	0		
621	12:44:00	156	2334	234.7	9.7	0.5		-5	5	366	0	0	1.0	1.4
5/9/94	12:56:08	133	2814	120.8	6	0		-4	4	352	0	0	2.1	2.6
	13:00:45	275	3155	296.9	3.4	0		-8	4	375	0	0	2.5	14.4 snow after 130423
	13:08:50	66	3494	305.8	1.7	0		-2	3	287	0	0	1.1	31.0 snow
622	17:55:26	155	4445	321.2	-3.8	0.6		-3	3	117	0.5	45	0.4	2.0 streakers
5/23/94	17:59:43	37	4540	162.7	-3.8	0.7		-5	5	112	0	0	0.2	2.2 streakers
	18:01:06	48	4541	138.7	-4.1	0.7		-3	1	174	0	0	0.3	2.6 streakers
623	9:24:07	94	2686	263.7	9	0.2		-9	4	48	0	0		streakers
5/24/94	9:26:12	94	2953	358.2	7.3	0.4		-8	4	66	0	0		streakers
	9:32:50	156	3153	78.8	5.5	0.6		-9	4	89	0	0		strealers
	9:36:04	45	3166	302.5	4.5	0.3		-6	2	82	0.1	6		streakers
	9:39:55	151	3176	89.4	5.9	0.5		-9	4	74	0	0	0.2	2.0
	9:50:00	153	3802	267.3	1.5	0.6		-8	3	837	5.1	20	3.9	4.0
	9:55:04	267	4419	73.8	-2.7	0.6		-7	6	5795	0	0	19.0	7.4 more jagged after 095800
	10:02:40	185	4521	257	-2.7	0.1		-4	3	4004	0	0	17.3	8.0 snow & graupel
	10:08:23	208	4429	79.7	-2.7	0.7		-5	3	3814	0	0	15.6	8.2 snow & graupel
	10:15:03	267	4534	267.5	-2.5	0.3		-5	4	5422	0.1	40	14.5	9.8 snow & graupel
	10:22:15	118	4419	90.8	-2.4	0.1		-4	3	1576	0	0	7.1	1.6 snow & graupel
	10:29:20	56	3744	279.7	1.3	0.2		-3	2	747	0	0	3.0	2.2 snow & graupel
624	18:51:56	367	3189	41.7	4.9	0		-5	4	426	2.7	29	2.1	4.4 ice & streakers
5/25/94	19:00:30	197	3795	227.7	-0.6	0.1		-5	6	4206	5.8	17	6.6	7.0 ice
	19:06:26	294	3853	49.3	-0.9	0.8		-6	5	3667	23	36	16.8	10.0 ice
	19:14:26	294	4480	231.2	-3.9	0.8		-9	12	7429	8.5	45	36.0	6.0 ice
625	8:32:20	21	3205	173.1	7.1	0.4		-3	2	70	0	0		artifacts, rain at end
5/29/94	8:37:00	120	3235	168.5	7.7	0.1		-7	3	648	5	45	2.8	5.4 rain/graupel
	8:42:00	141	3513	349	4.5	0.1		-11	4	1114	4.9	45	5.1	4.4 rain/graupel
	8:52:10	96	3581	174.4	5.4	0.1		-15	3	430	3.6	45	2.0	4.8 graupel
	8:55:00	171	3551	26.3	4.9	0.1		-6	2	532	3.3	45	2.0	4.4 graupel
	9:04:10	241	3845	241.4	2.2	0		-15	3	877	17.7	45	4.7	5.4 graupel
	9:10:51	192	4236	60.5	1.1	0		-6	3	1033	0.5	9	4.7	5.8 graupel

Table 3. VORTEX/MIGHT CLOUD PENETRATION SUMMARY (continued)

Flight	Time In	Dur	GPS Alt	Hdng	T (C)	Max J-W	Max King	Max Down	Max Up	Max Sh/Or	Hail MxC	Hl Mx D	2D-P C	2D-P D
	(LDT)	(s)	(m)	(deg)		($g\ m^{-3}$)	($g\ m^{-3}$)	($m\ s^{-1}$)	($m\ s^{-1}$)	(s^{-1})	(m^{-3})	(mm)	(ℓ^{-1})	(mm)
654	17:24:30	61	1944	329.2	7.5	0.2	0.5	-3	2	48	0	0	< 0.1	3.6 streakers
5/4/95	18:01:35	56	1000	193.2	12	0.4	0.7	-3	3	17	0	0	< 0.1	2.4 streakers
655	15:58:51	463	2858	272.2	5.6	0.4	2.2	-9	7	2999	12.7	45	5.7	4.8 rain
5/5/95	16:09:03	418	2832	103.4	5.4	0.1	1.6	-9	8	1784	3.6	29	5.5	8.8 rain
	16:16:00	281	2846	160.2	5.9	0.3	1.7	-7	7	948	6.3	45	3.8	8.2 rain/graupel
	16:20:50	81	2850	239.4	6.3	0.6	2.7	-5	6	1456	0	0	5.1	7.4 rain/graupel
	16:22:52	164	2858	239.9	5.8	0.5	1.8	-4	4	327	0	0	1.5	4.2 graupel/rain
	16:27:03	209	2861	18.9	5.6	0.1	1.3	-12	2	662	8.9	45	2.5	4 graupel/rain
	16:30:36	326	2907	20.6	5.3	0.2	1.7	-4	5	618	6	45	2.5	8.4 graupel/rain
	16:37:06	175	2894	20.8	4.3	0.4	1.5	-3	3	670	0	0	2.9	7.6 rain/graupel
	16:41:31	344	2809	199.8	4.4	0.4	1.4	-6	4	1308	3	45	6.3	6.8 rain/graupel/streakers
	16:48:58	96	2924	205.1	4.3	0.2	1.1	-4	4	887	0	0	4.4	5.8 graupel/rain
	16:52:36	199	2867	134	5.6	0.3	2	-7	6	1279	0	0	3.8	4.8 graupel/rain
	16:59:49	295	2803	133.5	5.8	0.3	1.9	-4	4	503	0	0	2.3	6.4 graupel/rain
	17:08:20	81	2821	83.2	6.3	0.7	2.9	-4	7	339	0	0	0.4	2.6 streakers
656	11:37:12	429	4125	277.3	-0.1	0.1	1.4	-12	5	6263	0.5	1	38.3	9.4 snow/graupel
5/7/95	11:48:20	498	4465	143.7	-2.5	0.1	2.2	-10	10	3502	0	0	13.1	9.2 snow/graupel
	11:58:43	233	4433	282.7	-2.5	0.2	2.4	-10	9	4189	0	0	16.3	9.8 snow/graupel
	12:03:55	195	4357	281.4	-2.8	0.1	1.5	-9	5	3440	0	0	17.2	11.4 snow/graupel
	12:08:54	194	4477	99.9	-2.6	-0.1	0.5	-5	1	3700	0	0	19.7	7.6 graupel
	12:13:25	396	4449	144.7	-2.6	0.3	3.1	-7	14	4809	0	0	21.5	6.8 graupel
	12:24:38	343	2788	350.1	6.9	0	3.8	-9	9	272	0	0	----	----
658	16:11:46	123	5437	68.7	-8.4	0.8	2.9	-11	7	5730	0.4	45	18.7	7.8 streakers/graupel
5/17/95	16:16:25	91	5447	114.7	-6.9	1.2	4.8	-8	17	1989	0	0	6.4	11.2 graupel
	16:19:41	146	5498	271.8	-7.2	1.7	5.4	-15	27	2249	0.4	1	7.9	10 graupel/streakers
	16:24:15	103	5228	265.4	-8	0.1	1.9	-9	3	4806	0	0	17.7	2.6 graupel/streakers
	16:31:23	41	5288	326.4	-9.8	0	0.8	-5	9	4318	2.6	29	12.4	4.3 graupel
	16:32:17	74	5320	269.4	-9.5	0.8	4.1	-15	20	3546	26.4	45	11.4	data poor after 163220
	16:36:15	169	5202	137.7	-9.4	0.1	2.6	-9	6	3482	8.7	17	13.4	data poor after 163220
	16:46:37	92	5124	162.4	-8.2	0.5	2.8	-24	11	1552	0	0	6.2	data poor after 163220

TABLE 3. VORTEX/MIGHT CLOUD PENETRATION SUMMARY (Continued)

Flight	Time In	Dur	GPS Alt	Hdng	T (C)	Max J-W	Max King	Max Down	Max Up	Max Sh/Or	Hail Mx C	Hl Mx D	2D-P C	2D-P D
	(LDT)	(s)	(m)	(deg)		($g\ m^{-3}$)	($g\ m^{-3}$)	($m\ s^{-1}$)	($m\ s^{-1}$)	(s^{-1})	(m^{-3})	(mm)	(ℓ^{-1})	(mm)
660	9:04:52	305	4135	194.8	-2.7	0	0.6	-8	5	6853	0.5	10	18.8	8.6 snow
5/21/95	9:11:54	177	4142	88.8	-2.7	0	0.4	-9	3	6651	3.7	12	24.6	7.2 snow
	9:15:00	481	4351	327.8	-4	0	0.5	-15	11	5439	17.4	10	29.3	10.4 snow
	9:26:00	421	6307	152.3	-15.5	0	0.5	-7	5	12458	0	0	47.9	4.8 graupel
	9:34:00	256	6351	323.9	-15.7	0	0.4	-13	14	14459	0	0	50.6	5.0 snow
	9:41:16	175	6312	124.2	-15.6	0	0.3	-5	3	12818	0	0	51.1	6.4 snow
	9:45:00	531	6349	297.8	-15.8	0	0.3	-6	5	10921	0	0	51.3	7.6 snow/graupel
	9:55:00	200	5706	151	-12.7	0	0.2	-14	11	4484	0.5	6	18.4	13.8 snow
	10:01:15	55	4888	308.6	-7.2	0	0	-10	-2	2197	0.1	4	5.1	5.4 snow
661	16:09:40	86	0	19.8	7.2	0.1	0.9	-11	0	1003	1.3	29	3.8	2.4 rain
5/23/95	16:22:38	60	0	351.3	7	0.3	1.4	-7	2	0	0	0	----	Missing data
	16:24:06	98	0	350.2	6.8	0.2	1.2	-7	4	60946	0	0	----	Missing data
	16:26:12	103	0	19.2	6.2	0.6	1.9	-13	8	62800	0.1	4	----	Missing data
	16:29:32	111	0	196.7	6.9	0.3	1.7	-9	4	790	0.8	10	----	Missing data
	16:31:35	29	0	240	6.5	0.1	0.2	-3	2	181	0.1	4	----	Missing data
	16:34:52	34	0	64.5	6.5	0.1	0.7	-12	-2	925	0	0	----	Missing data
	16:37:08	48	0	276.1	7.7	0.1	1.1	-14	-5	385	0	0	2	5.6 graupel/rain
665	15:36:13	259	0	2.9	-4.4	1	0.9	-7	7		152.3	29		
6/12/95														
666	17:44:15	29	3968	286.9	2	0.3	0.5	-13	-8		0	0		
6/17/95	17:45:01	47	3943	258.4	2	0.3	0.4	-8	1		0	0		
	17:47:00	56	3938	261.6	2.1	0.2	0.4	-27	28		0	0		
	17:48:30	362	4006	171.2	1.9	0.6	1.3	-32	44		1.5	36		
	17:57:36	163	4739	11.3	-1.9	0.4	0.6	-32	26		0	0		
	18:00:25	196	4718	14.3	-2.1	0.7	1.7	-24	22		0	0		
	18:06:00	161	4797	163	-1.9	0.6	1.3	-30	2		0	0		
	18:12:00	145	5454	1	-5.2	0.3	1.1	-28	23		0	0		
	18:16:00	131	5398	278.5	-5.1	0.2	0.7	-10	4		0	0		
	18:20:46	165	5323	20.4	-5.6	0.5	1.6	-33	32		0.2	6		
	18:23:58	169	5434	181.9	-5.1	0.1	1.2	-13	4		0	0		

Table 3. VORTEX/MIGHT CLOUD PENETRATION SUMMARY (continued)

Flight	Time In	Dur	GPS Alt	Hdng	T (C)	Max J-W	Max King	Max Down	Max Up	Max Sh/Or	Hail Mx C	Hl Mx D	2D-P C	2D-P D
	(LDT)	(s)	(m)	(deg)		(g m^{-3})	(g m^{-3})	(m s^{-1})	(m s^{-1})	(s^{-1})	(m^{-3})	(mm)	(ℓ^{-1})	(mm)
667	16:15:40	162	5256	103.3	-4.1	1.1	2.1	-7	12		29.1	45		
6/20/95	16:20:30	172	5494	277.3	-7.4	1.4	1.4	-9	5		5.1	45		
	16:25:32	186	5520	80.5	-7.9	1.3	1.3	-8	8		14.1	45		
	16:30:35	139	5619	252.4	-8.7	0.7	1.1	-9	5		27.5	45		
	16:34:42	133	5524	67	-8.7	0.8	1	-9	7		6	45		
	16:37:44	116	5649	253	-8.3	1.2	1.5	-9	5		16.4	45		
	16:41:08	175	5672	63.8	-8.9	1.3	1.7	-14	5		13.3	36		
	16:45:06	165	5590	232.8	-8.9	0.6	1.5	-10	10		27.7	36		
	16:49:16	153	5656	63	-8.5	1.3	1.4	-20	9		32.5	45		
	16:52:41	134	5652	232.6	-8.7	0.6	1.3	-12	13		26.7	36		
	16:56:03	173	5589	62	-8.6	1	1.5	-15	7		21.1	36		
	17:00:06	179	5602	233.1	-8.7	1.1	1.3	-14	8		12.6	36		
668	17:27:47	116	4192	50.7	0.4	1.4	2.9	-13	15		7.1	36		
6/22/95	17:31:53	104	4167	231	0.5	1.2	2.8	-15	12		6.2	29		
	17:35:43	133	4156	67.9	0.2	1.2	1.4	-18	23		9.2	36		
	17:44:00	90	4805	233.3	-3.8	1.8	-1.3	-1	20		5.5	29		
	17:50:45	76	4938	32.6	-4.2	1.7	-1.2	-1	19		0.9	36		
	17:52:30	78	4543	176.6	-3	0.5	-1.3	-20	20		0	0		
670	15:26:21	105	4655	288.7	-2.5	0.8	1.2	-9	12		10.1	36		
6/27/95	15:29:10	56	4411	85.1	0.9	0.3	0.7	-4	13		16.9	36		
	15:32:50	145	4511	276.2	-0.9	0.3	0.8	-9	13		10.4	36		
	15:37:40	162	4729	95.4	-1.2	0.7	1.1	-11	7		35.2	36		
	15:40:54	37	4885	272.5	-3.9	0.7	0.9	-6	8		0.4	12		
	15:42:00	134	4823	4.2	-2.6	0.2	0.4	-9	5		23.6	45		
	15:45:08	113	4810	189	-2.4	0.2	0.6	-11	3		34.4	36		
	15:48:05	174	4868	3	-2.5	0.2	0.4	-19	17		15.7	36		
	15:53:20	254	5117	203.5	-4.9	0.5	1.2	-9	8		47.1	36		
	15:59:08	223	5407	13.1	-6.6	0.2	0.8	-26	19		31.5	36		
	16:03:15	235	5411	170.2	-6	0.8	1.8	-12	7		67.9	36		
	16:07:17	81	5523	188.2	-7.6	0.5	0.9	-6	5		0	0		
	16:09:10	101	5363	6.6	-7.5	0.4	0.9	-13	0.6		0.1	4		
	16:11:10	186	5632	44.3	-6.3	0.6	2.4	-9	23.4		68.7	36		
	16:16:44	142	4793	233.3	-3.3	0.7	0.9	-10	18		35.2	36		

Table 3. VORTEX/MIGHT CLOUD PENETRATION SUMMARY (continued)

Flight	Time In	Dur	GPS Alt	Hdng	T (C)	Max J-W	Max King	Max Down	Max Up	Max Sh/Or	Hail Mx C	Hl Mx D	2D-P C	2D-P D
	(LDT)	(s)	(m)	(deg)		($g\ m^{-3}$)	($g\ m^{-3}$)	($m\ s^{-1}$)	($m\ s^{-1}$)	(s^{-1})	(m^{-3})	(mm)	(ℓ^{-1})	(mm)
671	18:14:35	376	3232	82	5.8	0.2	0.8	-7	5		0.8	2		
6/28/95	18:23:30	151	3112	190.3	5	0.2	0.4	-14	3		1.2	14		
	18:26:18	235	3176	268.8	5.6	0.2	0.7	-5	4		1	24		
	18:36:45	399	3548	91.6	2.9	0.1	1.1	-9	9		1.8	36		
	18:44:00	281	3753	272.4	1	0.3	0.9	-10	8		2.9	36		
	18:50:15	358	4432	90.9	-1.8	0.2	0.4	-13	4		4.8	29		
	18:57:05	361	5060	271.6	-5.2	0.2	0.4	-12	6		0.1	04		
	19:05:40	439	5512	93.4	-8	0.2	0.4	-11	8		0.3	04		
	19:14:55	351	3698	263.6	1.9	0.3	0.4	-13	9		0.5	14		
	19:30:30	121	1593	263.5	12.8	0.2	0.7	-7	7		0	0		

3.2 INSTRUMENTATION PERFORMANCE

The evaluation and interpretation of airborne measurements obtained in clouds is a small but rich field of scientific endeavor. Brief summaries of basic principles relevant to the instrumentation employed in this field work are given below, along with selected references to representative work in the literature that are intended to serve as pointers to more detailed discussions.

3.2.1 CLOUD WATER

FSSP

The T-28 flew during its VORTEX/MIGHT deployments as many as three instruments capable of giving independent estimates of cloud droplet population characteristics. The first was a Particle Measuring Systems, Inc. (PMS) Forward-Scattering Spectrometer Probe (FSSP) on a long-term borrowing arrangement with NCAR. In fact, this probe is serial number 1 of the FSSP series, first flown in 1975. This probe was flown throughout all 1994 and 1995 deployments. Its optical configuration is somewhat different than later FSSP models, but when properly calibrated it can produce very good data on cloud droplet concentrations and size distributions. The interpretation of data from FSSP's has been extensively discussed in the literature (e.g. Cooper, 1988; Baumgardner and Spowart, 1990).

The T-28 FSSP is routinely tested by passing glass beads of two different sizes through the instrument on the ground, using a vacuum cleaner to draw air and beads through the sample volume. Periodic calibrations were done during the field campaigns, and bench tests were done in the off-season, to monitor FSSP performance. Calibration dates and results are shown in Table 4. The channel size assignments computed from these results and applicable to the three deployment periods are presented in Table 5. These size assignments are based on Mie-scattering calculations using as reference the channel into which glass beads of 32 μm and 8 μm diameter were assigned when passed through the FSSP during tests on the ground. Briefly, the glass bead diameter is converted to a water droplet diameter with the same near-forward scattering characteristics (a glass bead, due to its higher index of refraction compared to that of water, "looks like" a smaller water droplet to the FSSP). Knowing the photomultiplier output voltage for the channel in which the majority of these beads were assigned, and the relationship of this voltage to that of the other channels, the equivalent water droplet sizes that would fall in the other channels can be

computed by moving up and down the Mie scattering curve of relative output versus droplet diameter.

Droplets greater than the minimum size indicated for a given channel, but less than the minimum size indicated for the next higher channel, will be counted in the given channel. The size assigned to these droplets is the average between the minimum sizes of the adjacent channels. When two channels are assigned the same minimum size, the counts in both channels are effectively lumped together and assigned the same size. This is sometimes the most reasonable treatment of the data, and is applicable where the Mie scattering curves indicate a scattering signal rapidly oscillating up and down with increasing droplet size.

The computed size is shifted down one channel to account for undersizing of droplets passing through the sample volume due to limited response speed of the FSSP electronics. A particle is through the beam while the photomultiplier amplifier signal is still rising at typical T-28 true airspeed. Thus a smaller pulse height is produced than would be for a slower-moving particle of a given size during the bead tests on the ground.

The droplet concentration is adjusted upward to account for the inability of the probe to respond to subsequent droplets passing through the sample volume while it is processing a previous droplet. This adjustment is described in Appendix C.

When beads of two different sizes are used, the calibration based on one size is usually not strictly compatible with that based on the other size over the complete range of droplet sizes to which the FSSP is sensitive. In this case, a hybrid calibration curve is estimated "by eye", with more consideration given to the estimate based on the smaller beads for the lower channels, and to that based on the larger beads for the upper channels.

These size assignments are tested by comparing computed FSSP total cloud water concentration measured in flight to simultaneous measurements made by the J-W and/or King probes in regions where good agreement might be expected. If the agreement is not reasonable, then the size assignments are adjusted in an iterative manner until suitable agreement is obtained.

It can be seen that the calibration shifted significantly between the last two phases of VORTEX/MIGHT. The probe was re-aligned early in the summer of 1994. Its behavior was consistent throughout August, 1994 during a field project in Texas, and had essentially the same response when tested again in April, 1995. There appears to have been a shift in response that occurred sometime during May, or between the May and June deploy-

ments, that dramatically reduced the ability of the probe to count smaller droplets. A preliminary examination of the May, 1995, data suggests that the relative responses of the FSSP, J-W, and King probe were consistent throughout the Oklahoma deployment, and consistent, but using a different calibration, during the Colorado deployment in June, 1995. If more detailed analysis verifies this, then the shift in response must have occurred during the interval between the Oklahoma and Colorado deployments.

The optical train, as well as some of the pulse-shaping electronics, deteriorated following the 1995 Oklahoma deployment. It appears that during the 1995 Colorado deployment, droplets smaller than ~10 um were not detected, and there is the possibility of more-serious-than-normal undercounting of the larger droplets that were detected.

J-W

The T-28 Johnson-Williams cloud water meter (J-W) was built in the late 1960's. This type of probe has seen more than three decades of service to the cloud physics community, but is currently out-of-production. Its performance characteristics have been extensively discussed in the literature (e.g. Spyers-Duran, 1968; Strapp and Schemenauer, 1982; Personne *et al.*, 1982; Gayet, 1986). Of particular relevance to the VORTEX/MIGHT deployments is the tendency of the J-W to respond incompletely to cloud droplets larger than ~30 μm. Droplets this large, while not numerous in a relative sense, may account for a substantial fraction of the total cloud water content in warm-based convective clouds like those found in Oklahoma.

The J-W de-ice heaters were not operating at full power during the 1995 deployments and data obtained at temperatures below -5°C in 1995 should be analyzed carefully for evidence of the effects of icing.

King Probe

The T-28 facility was able to borrow a second heated-wire-type cloud water sensor for use during the 1995 deployments, after it was determined that the J-W probe could not be adequately de-iced and could not be repaired. The probe is known generically as a King or CSIRO probe, named after its developer, W. D. King, and his organization, the Commonwealth Scientific and Industrial Research Organization (CSIRO) of Australia. The heated element in this probe is a coil, rather than a straight wire, and its response to cloud water is measured somewhat differently than in the case of the J-W. King *et al.* (1978, 1981, 1985), and Biter *et al.* (1987), among others, have discussed the performance of this probe.

TABLE 4
FSSP Bead Tests, 1994-1995

Date	8 μm bead channel	32 μm bead channel
6 May 1994	1	6 & 7, evenly
8 Aug 1994	1 & 2, mostly 1	5 & 6, evenly
21 Aug 1994	1 & 2, mostly 1	5 & 6, evenly
30 Aug 1994	1 & 2, mostly 1	5. & 6, evenly
8 Nov 1994	1 & 2, mostly 1	6
14 Apr 1995	1 & 2, mostly 1	5 & 6, evenly
14 Jun 1995	1	5
23 Jun 1995	1	5

TABLE 5.
FSSP Channel Minimum Size Assignments VORTEX/MIGHT

Ch #	May, 1994	May, 1995	June ,1995
1	2.6	3	13
2	4.7	12	17
3	11.7	12	19
4	13.4	20	22
5	20.2	25	31
6	23.9	32	35
7	30.6	38	42
8	34.4	43	47
9	41.2	49	54
10	45.0	57	62
11	51.6	62	66
12	55.5	69	75
13	62.2	72	80
14	ignored	77	85
15	ignored	86	92

In general, the probe responds according to a fairly simple theoretical model, and responds to a much broader range of droplet sizes than the J-W due to its lower element temperature and greater element diameter.

Several companies and institutions have manufactured versions of this probe. The particular probe borrowed from NCAR was manufactured by PMS. Clear-air flight segments at several altitudes were used to calibrate its dry (background) readings for the new probe installation on the T-28. This installation is shown in Figure 7.

Intercomparisons

Figures 8-10 show examples of comparisons between cloud water concentration readings of the three cloud water probes discussed above. In weak updrafts, or higher in stronger updrafts, and with warmer cloud bases, the J-W tends to indicate lower concentrations than either of the other two probes. Near cloud base, and in stronger updrafts with cooler cloud bases, the J-W and King probes agree reasonably well. The FSSP reads somewhat lower concentrations than the other two probes in the latter case, probably due to undercounting in higher droplet concentrations.

3.2.2 PRECIPITATION PARTICLES

The primary data for the VORTEX/MIGHT deployments concerned precipitation particle population characteristics. Four instruments were employed to obtain this information.

2D-P

A PMS optical array probe, model OAP-2D-P, was borrowed from the NOAA Office of Aircraft Operations for use during the Oklahoma deployments in 1994 and 1995. This type of probe has been used in the cloud physics community since the 1970's. It produces shadow images of precipitation-size particles with 0.2 mm resolution. A brief discussion of how the probe works is given in Detwiler and Hartman (1991). The data were not analyzed in detail by the T-28 facility, but some preliminary quality checks and noise elimination procedures were applied, as described below.

The following processing was applied to the 2D-P data which were collected during the '94 and '95 Vortex operations in Oklahoma. The corrections apply to both seasons unless otherwise noted.

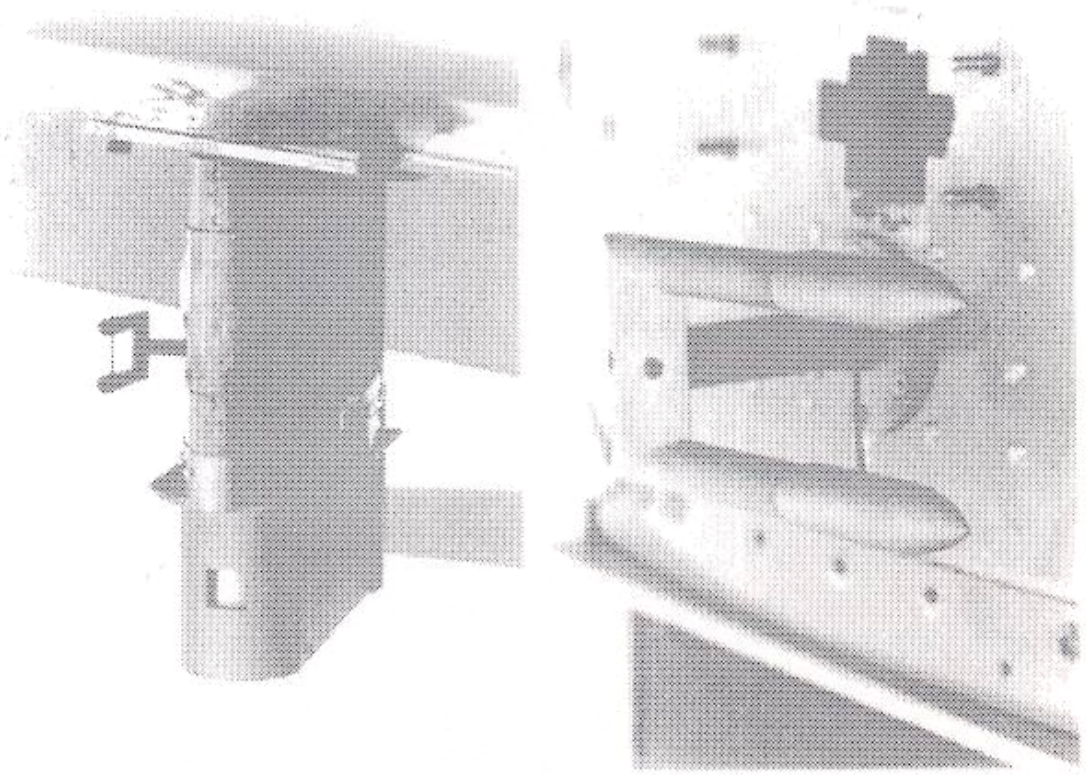

Figure 7. Photographs showing the King probe attached to the outboard side of the foil impactor pylon under the right wing.

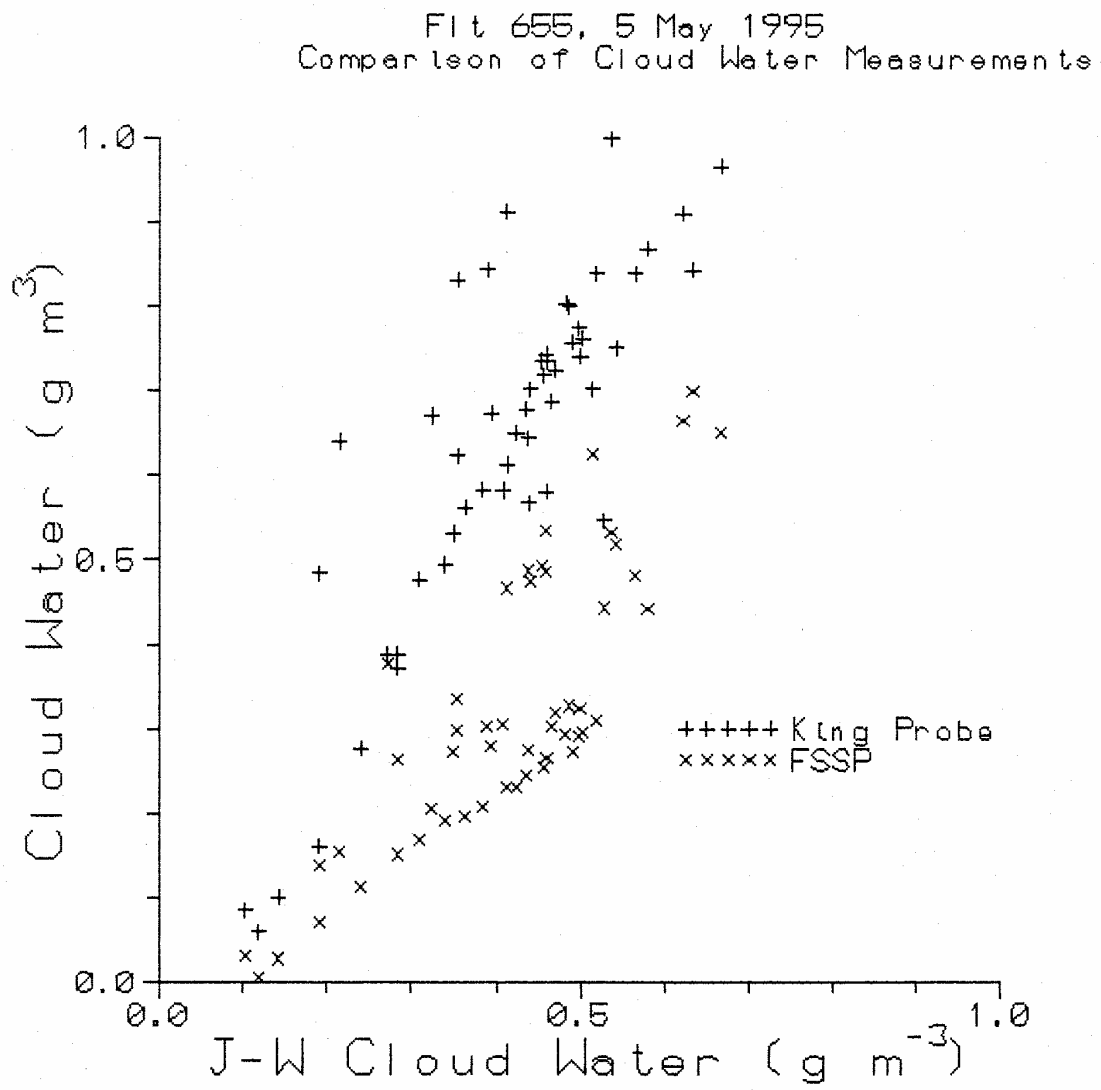

Figure 8a. Comparison of 1-second cloud water concentrations obtained during descent through a layer of small cumulus clouds trapped under an inversion capping the planetary boundary layer in Oklahoma.

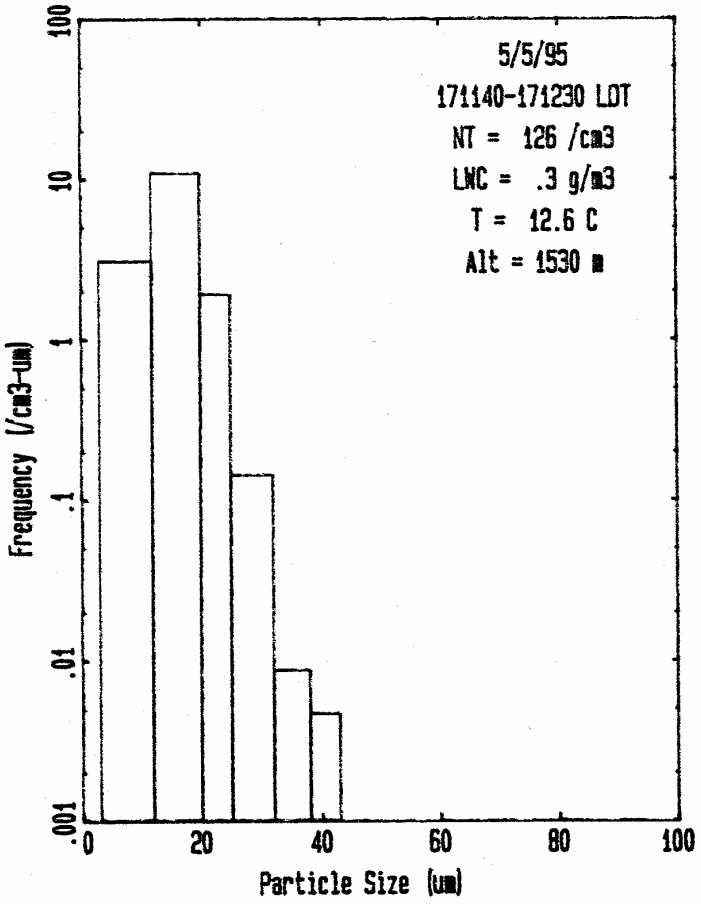

Figure 8b. Average FSSP droplet spectrum corresponding to Fig. 8a.

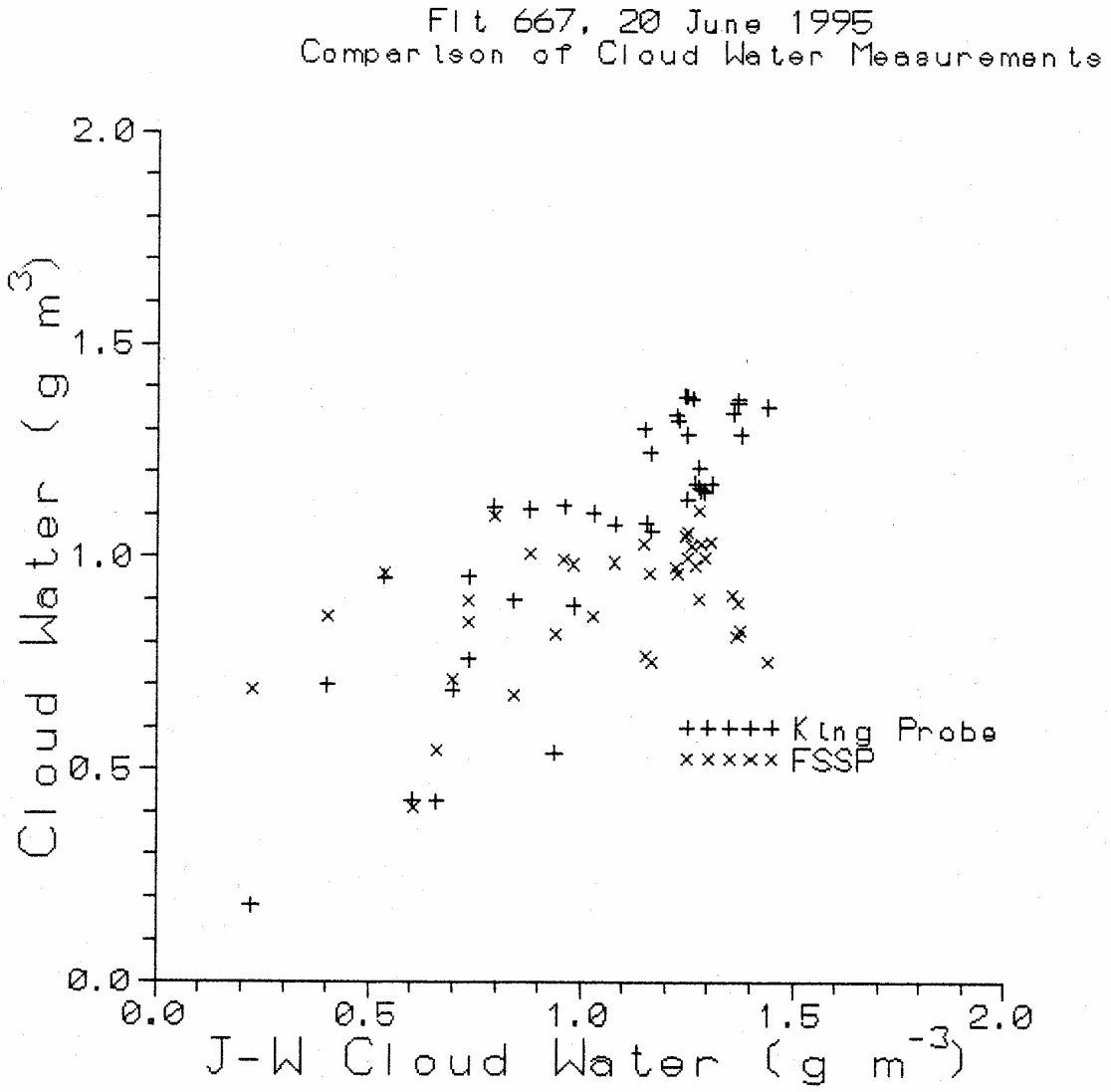

Figure 9a. Comparison of 1-second cloud water concentrations obtained during a thunderstorm updraft penetration at the -8°C level, in a Colorado storm.

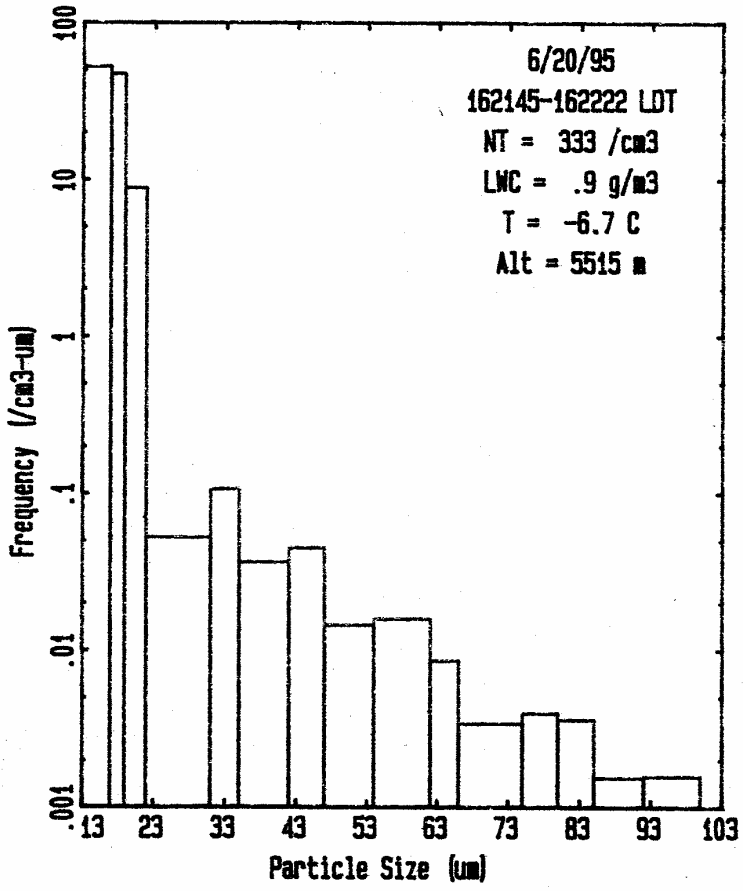

Figure 9b. Average FSSP droplet spectrum corresponding to Fig. 9a. The counts in the first three channels are 2 to 3 orders of magnitude higher than those in the higher channels and represent actual cloud droplets. Counts in the higher channels are predominantly artifacts due to passage of ice particles through the sample volume (see, e.g., Baumgartner and Spowart, 1990).

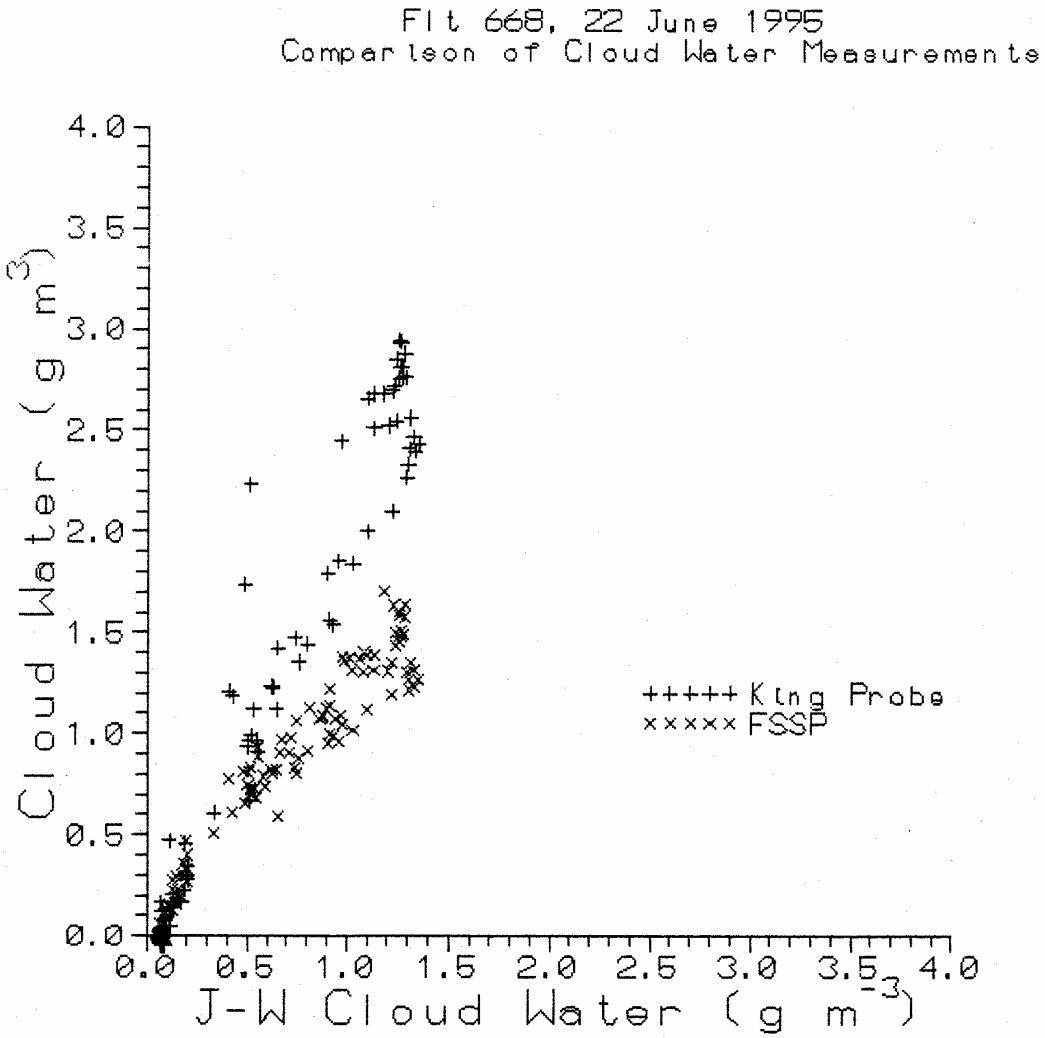

Figure 10a. Comparison of 1-second cloud water concentrations measured during a thunderstorm updraft penetration at the freezing level in a Colorado storm.

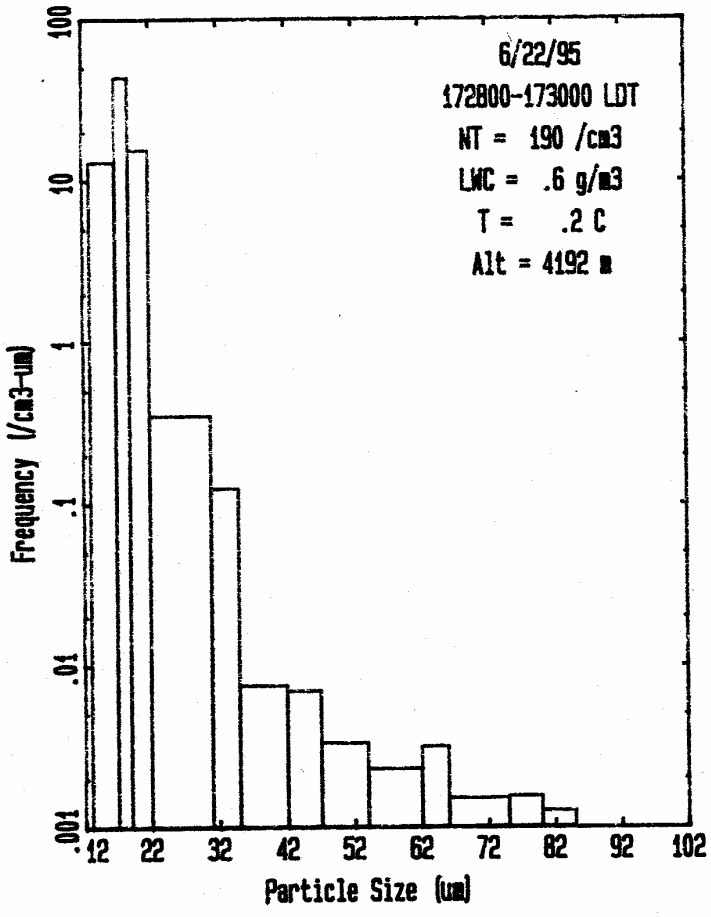

Figure 10b. Average FSSP spectrum corresponding to Fig. 10a. Contamination by artificial counts due to ice appears to be less compared to Fig. 9b, predominating only above channel 5. The droplet portion of the spectrum is much broader than that in Fig. 9b, probably accounting for the underestimate of water concentration by the J-W compared to the other two probes.

1) Shifted buffers were created by splicing together the second half of each buffer (slices 513-1024) with the first half (1-512) of each succeeding buffer. The data acquisition system buffer start and duration times seem to agree very well with the summed interparticle elapsed times once this is done. During this process the first half of the very first buffer, which is always pure noise anyway, and the last half of the final buffer, are discarded.

2) In 1995 there were two bits which always seemed to be stuck in the "on" state (non-occluded). These were the ninth bit from the bottom and, for every other buffer, the fifth bit from the top. Whenever the two bits on either side of each of these bits were both zero, the offending stuck bit was cleared, i.e., a 010 pattern was replaced with 000.

3) An attempt was made to remove speckles in the data. Single pixels or very small clusters separate from the main group of occluded bits were removed.

4) When a diode appeared to be stuck continuously (in the occluded state), its pixel state would be modified, as long as that original state was the opposite of the pixels immediately above and below it. The main method for detecting stuck bits made use of the fact that there normally should be several blank slices preceding the time slice. Any bit that was occluded in these slices generally corresponded to a stuck bit. This condition arose more frequently in '95 than in '94.

Examples of raw image buffers and their "cleaned" counterparts are shown in Figure 11 and 12. The "cleanup" procedure may result in the elimination or slight reduction in size of a few valid images, but it renders many "noisy" buffers analyzable.

Periodic checks were done in the field while running the probe on the ground, passing objects of known size through the probe sample volume to verify the size calibration of images obtained from the probe. The probe behaved consistently throughout the 1994 and 1995 deployments, with an equivalent diode size of 0.2 mm.

HVPS

The PMS OAP-2D-P discussed above was replaced for the 1995 Colorado deployment by a SPEC, Inc., High-Volume Particle Sampler (HVPS). This instrument, which actually belongs to the Cloud Physics Research Division, Atmospheric Environment Service of Canada, was obtained by CSU, and installed on the T-28 and maintained in the field by SPEC. Its data were acquired using a computer supplied by SPEC and installed in the rear cockpit

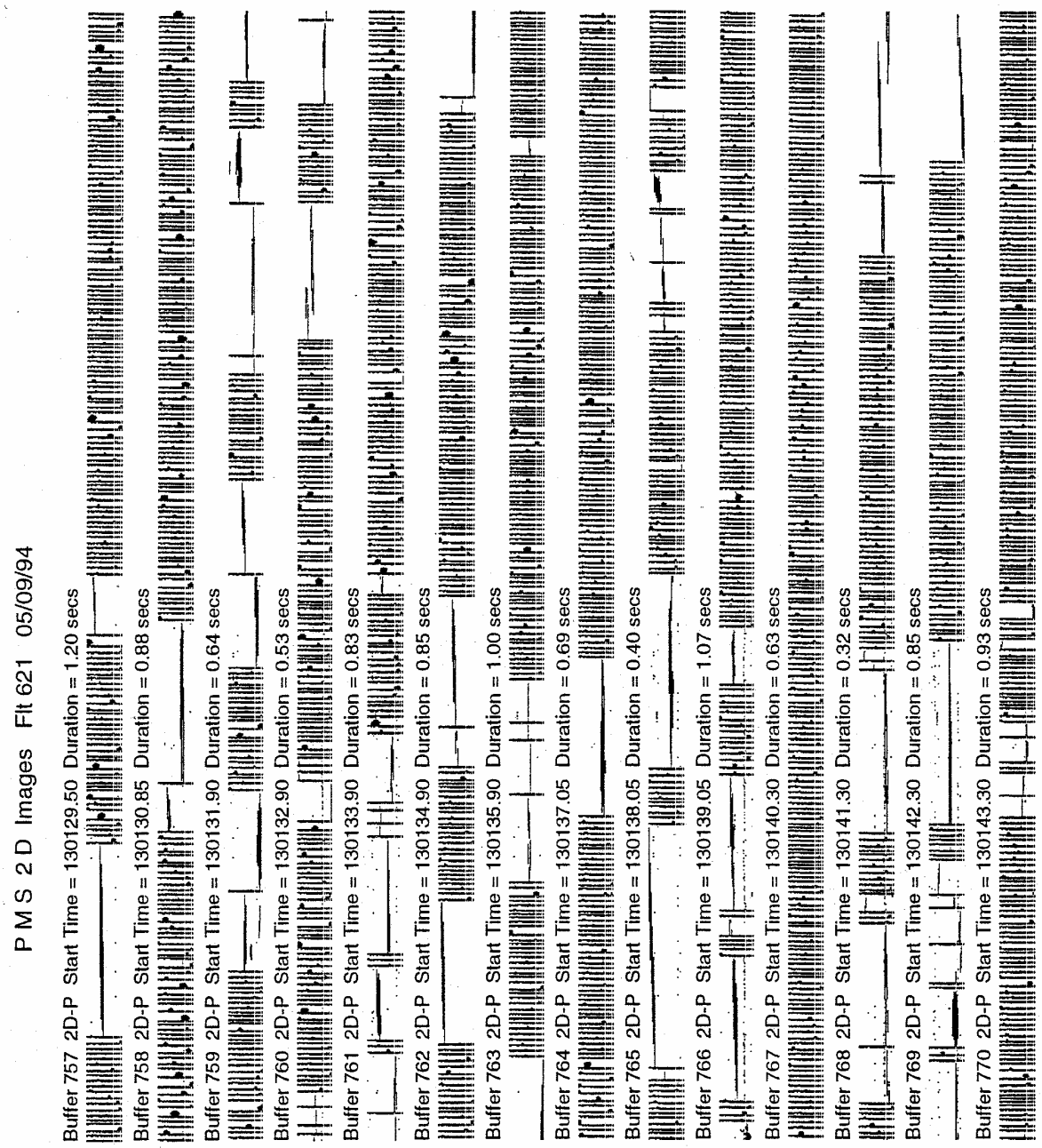

Figure 11a. Raw 2D-P image buffers obtained during an Oklahoma flight through light rain.

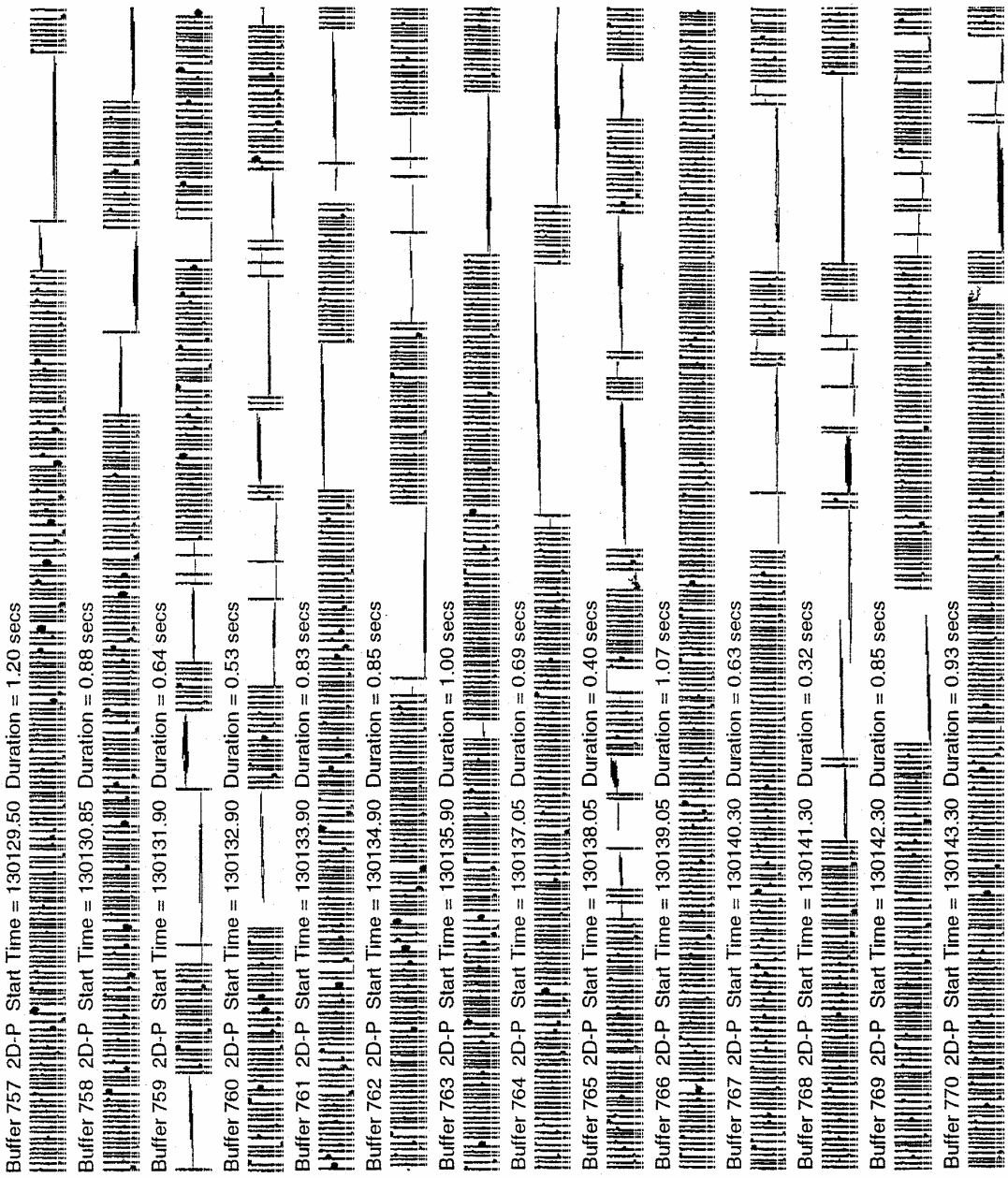

Figure 11b. The image buffers in Fig. 11a after "cleanup".

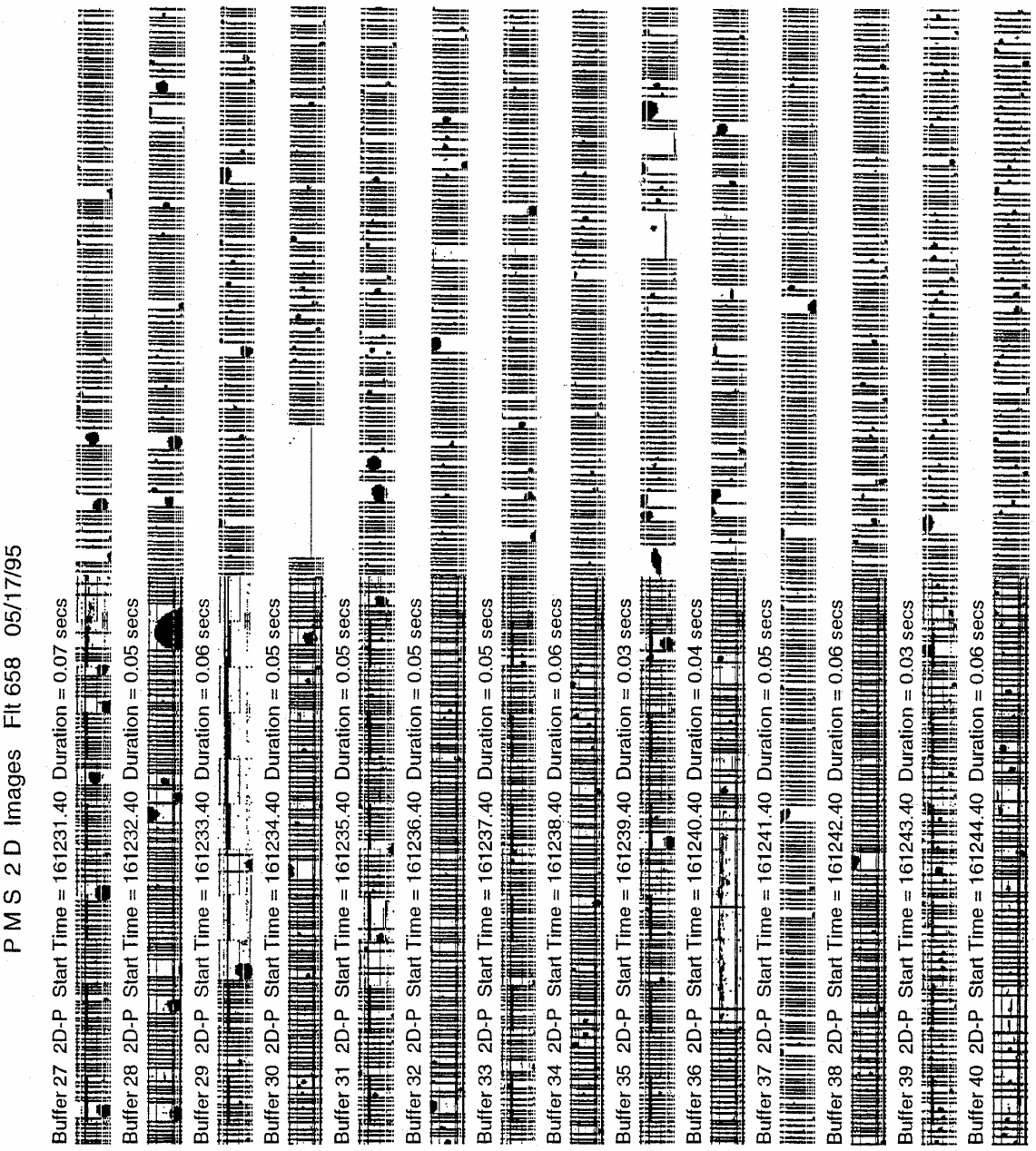

Figure 12a. Raw 2D-P image buffers obtained during an Oklahoma flight through a mixture of rain and graupel.

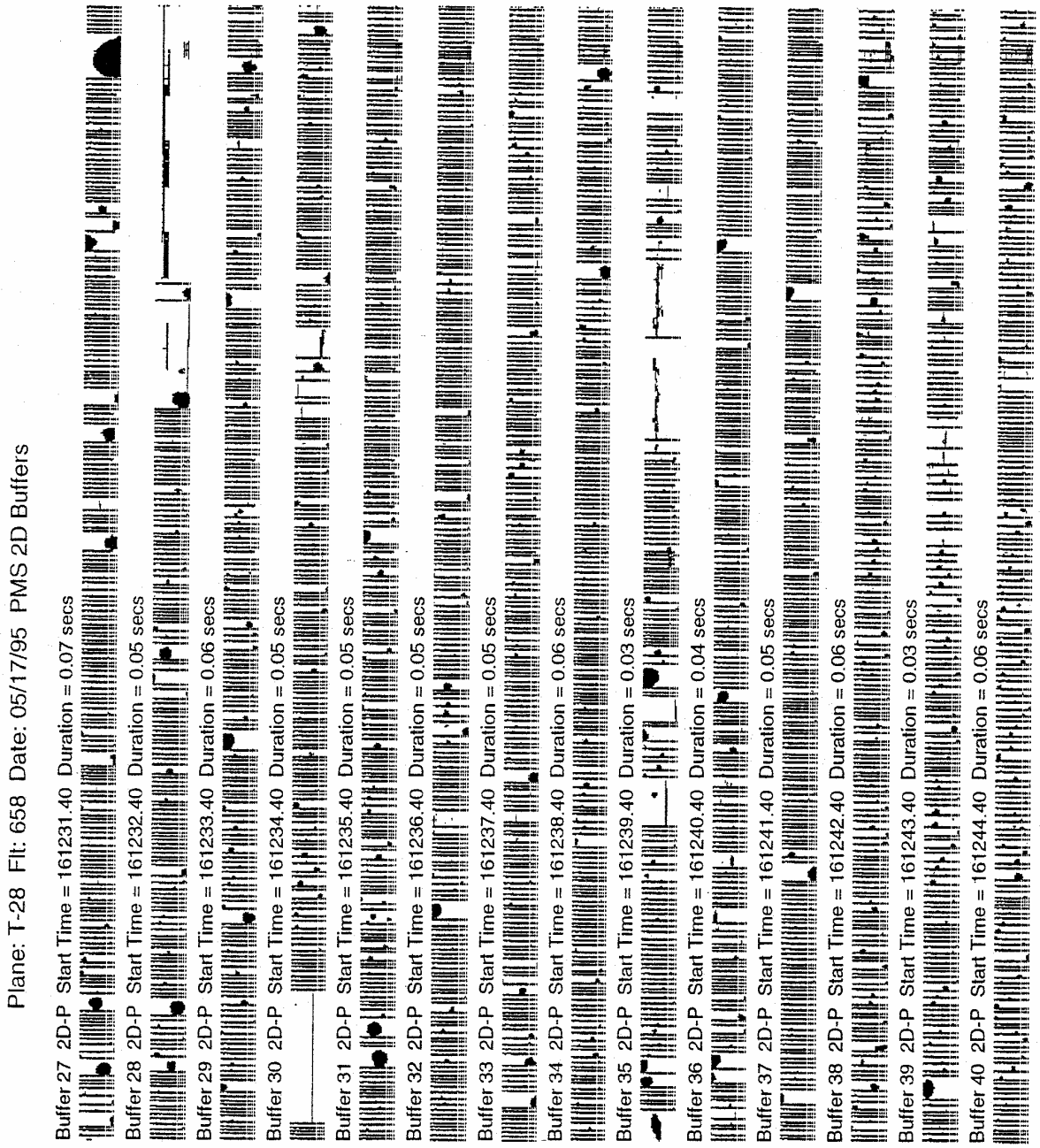

Figure 12b. The image buffers in Fig. 12a after "cleanup".

of the T-28. These data are archived independently of all other T-28 data and must be obtained through V. Chandrasekar, Department of Electrical Engineering, CSU. A similar instrument is described in Lawson *et al.* (1993).

The HVPS functions somewhat similarly to a 2D-P, producing shadow images of precipitation particles passing through an illuminated volume. This volume is roughly 6 times the volume sampled by a 2D-P, yielding better sampling statistics for larger, less-numerous particles, compared to the 2D-P. Size resolution is 0.2 mm in the vertical and 0.4 mm in the horizontal. A photograph of the HVPS installed under the right wing of the T-28 (in the same position in which the 2D-P was installed for the Oklahoma deployments) is shown in Figure 13, and example images are shown in Figure 14.

Hail spectrometer

This instrument is a large optical array probe, operating in a manner similar to the 2D-P and HVPS, but having a volume sampling rate roughly 10 times that of the HVPS. It has a size resolution of 0.9 mm in the vertical and horizontal (along-track) directions, and is used to obtain population statistics on the largest and rarest particles in convective clouds. The imaging interface to the data acquisition system functioned poorly throughout the 1994 and 1995 deployments, yielding only small samples of useful image data. An example is shown in Fig. 15. However, the probe also supplies numerical counts of particles larger than ~4.5 mm (5 diodes in the vertical) resolved into 15 size categories telescoping up to 4.5 cm and larger. These data were generally of high quality during all deployments.

Foil impactor

This instrument and the J-W are the oldest instruments on the T-28, dating from the initial outfitting of the T-28 for hailstorm research missions in 1968. Foil impactors were a common precipitation particle sampling tool in this era. The T-28 instrument is mounted under the right wing on a pylon just inboard of the pylon carrying either the 2D-P or HVPS, and can be seen in Fig. 7.

A 300 ft long roll of foil is scrolled past an open window at the front of the impactor where precipitation particles can hit the foil and leave an impression. The foil continues past the window and is rolled onto a take-up reel. The shutter covering this window is opened and foil is transported and exposed only when activated by the pilot upon entering a cloud. A punch mark is made in the foil and a flag is set in the data record every time the

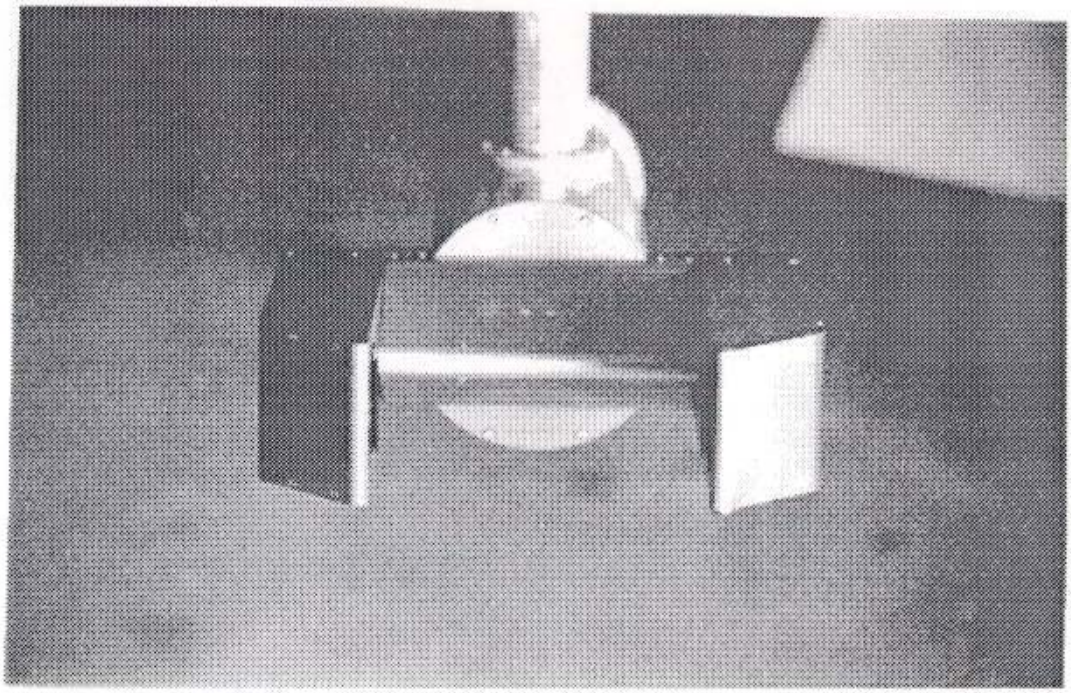

Figure 13: HVPS precipitation-imaging probe installed under the right wing of the T-28.

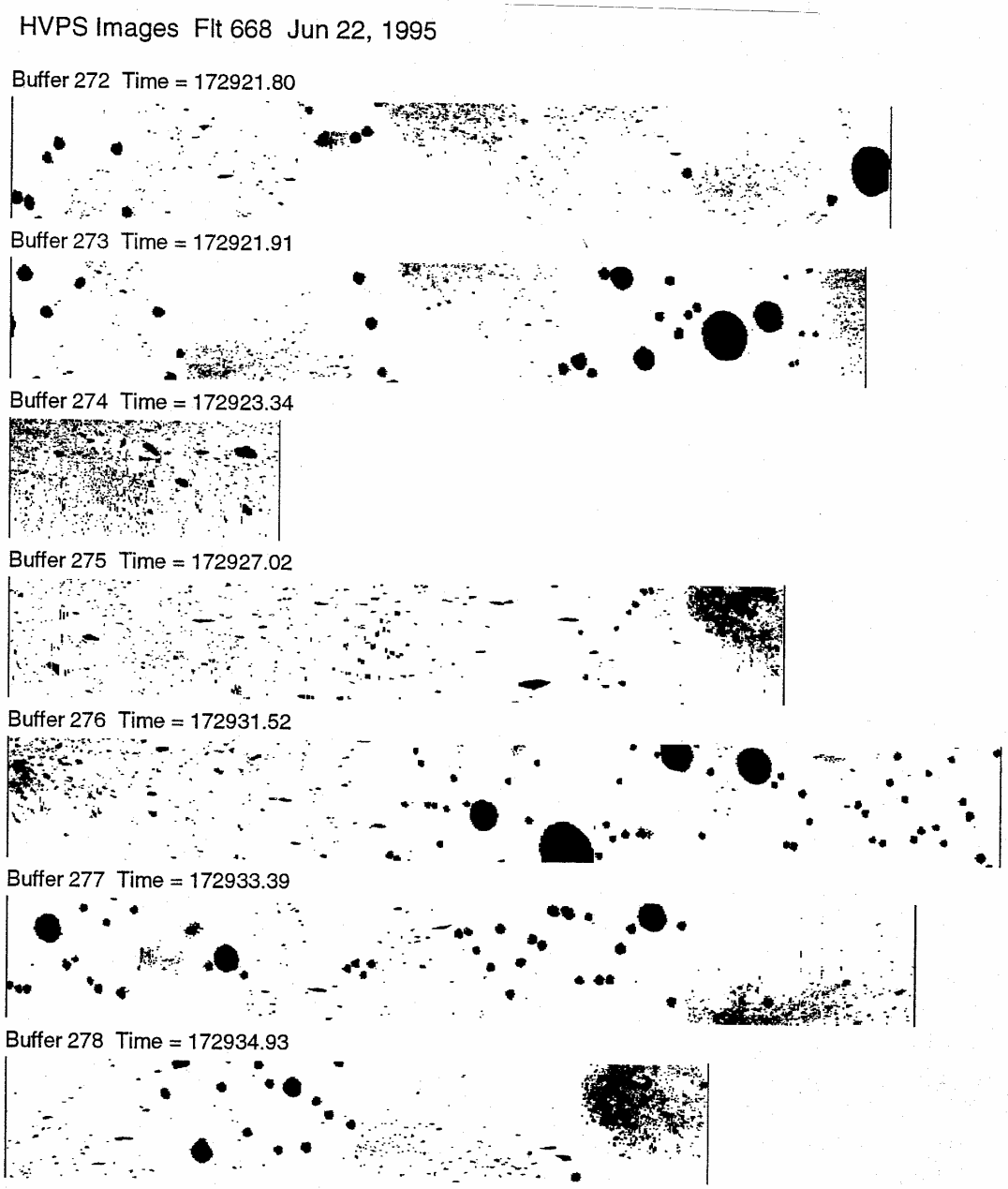

Figure 14: HVPS images of hail obtained in a Colorado thunderstorm. The vertical bars represent a size of 5 cm.

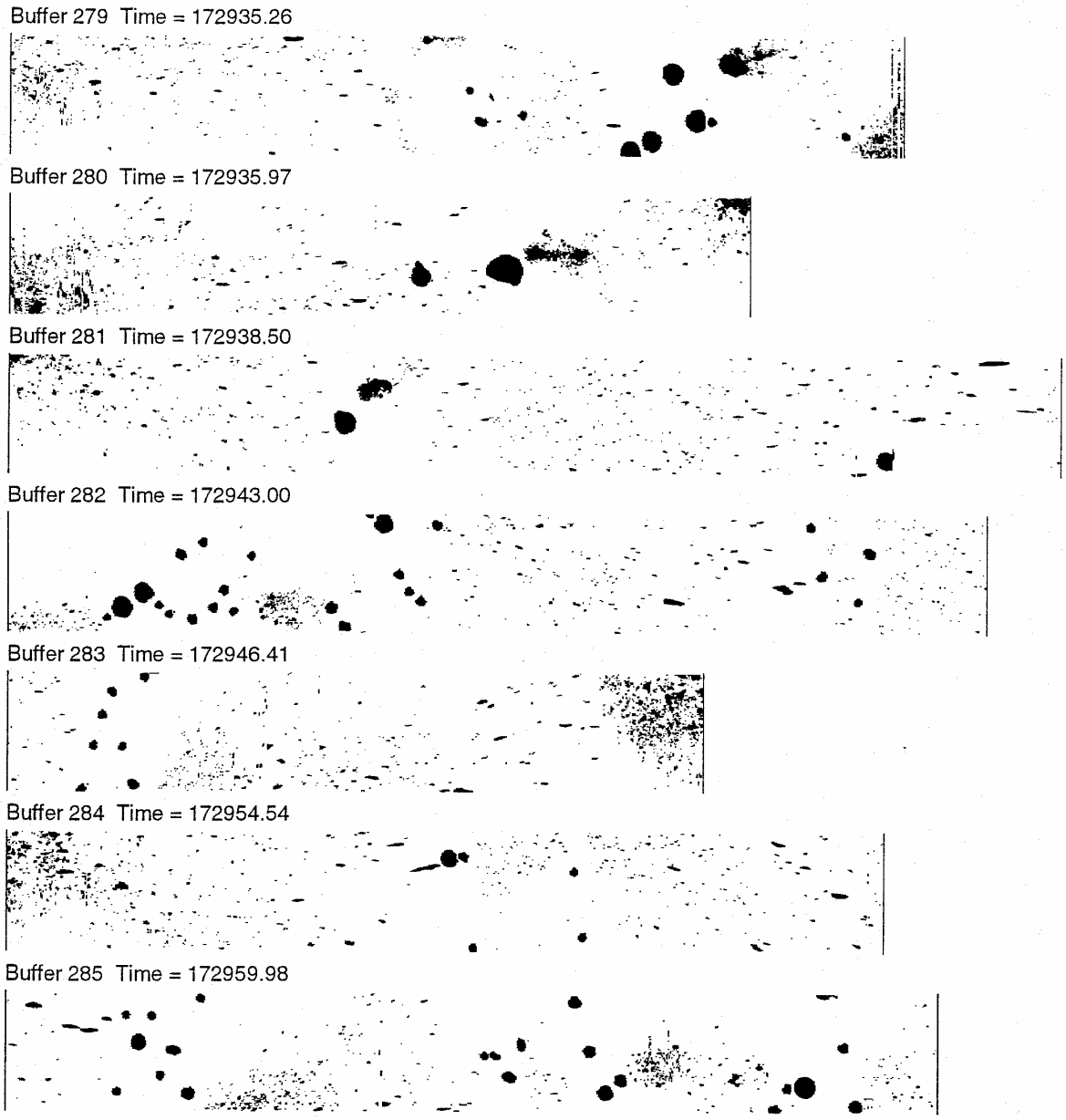

Figure 14: (Continued)

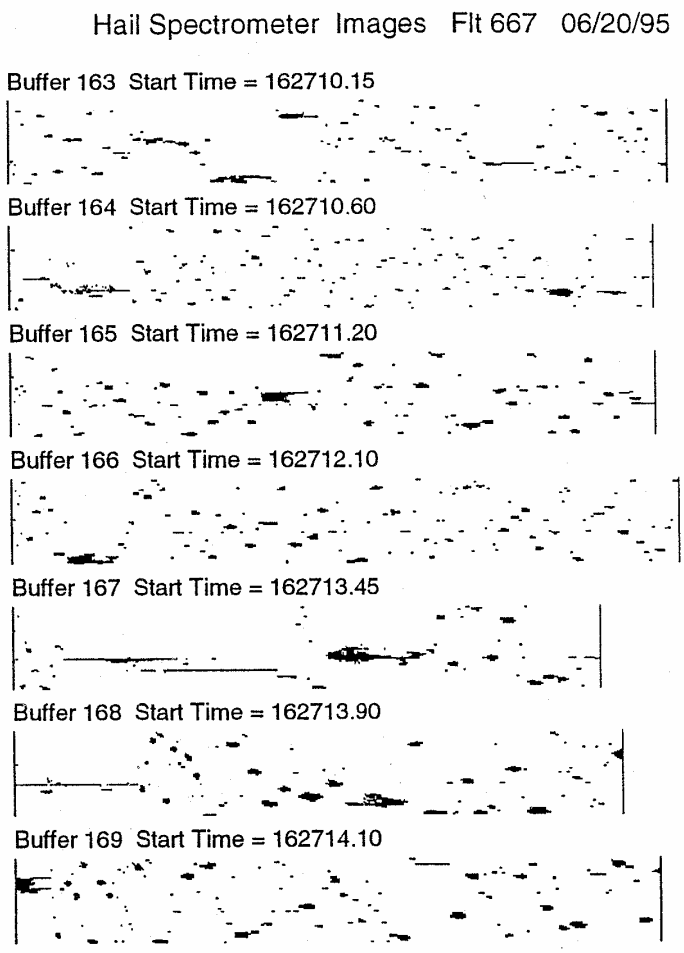

Figure 15: Hail spectrometer images of rimed aggregates and rimed clumps of aggregates observed at the -8°C level in a Colorado thunderstorm. The vertical bars represent a size of 11.8 cm.

pilot de-activates the probe and the window closes. Thus, a punch mark separates data obtained during one cloud pass from that obtained on the subsequent one. After a flight, the foil is examined manually. The punch marks and corresponding times recorded on the data system are used to assign a unique time to each portion of the exposed foil.

Particle impressions from ~0.5 mm to several cm can usually be resolved. Heavy icing can result in build-up of ice around the window and in ice being rolled up between the foil layers on the take-up spool. This can result in wrinkling of the foil and loss of data quality.

Further discussion of analysis of foil impressions can be found in Schecter and Russ (1970) and Knight *et al.* (1977).

Intercomparisons

Preliminary intercomparisons in the field between particle concentrations in various size categories sampled by the different precipitation probes yielded reasonable agreement. In general, a probe tends to undersample particles close in size to its minimum resolution. It is better to rely on a probe for which the size of interest is in the mid-range of its size range, if possible. Further intercomparisons would be desirable for those episodes of highest interest, as analysis proceeds. Although the foil data are the least amenable to automated analysis, Walsh (1993) found foil data to be generally superior to that from optical array probes in comparing *in situ* precipitation observations to radar signatures.

3.2.3 OTHER

Several other quantities were observed using instrumentation on the T-28 that may be of interest to users of its VORTEX/MIGHT data.

Electric fields

Ambient electric field components in directions vertical and horizontally transverse to the aircraft heading can be obtained from a suite of 5 electric field meters mounted on the T-28. In addition, a signal proportional to aircraft charging and to the sign of the electric field component along the heading can also be obtained. A detailed description of this system and interpretation of data from it is in preparation. A summary description is contained in an appendix to Ramachandran *et al.* (1996).

The performance of this system is periodically checked by artificially charging the aircraft in clear-air flight using an on-board high voltage power supply. The ratio of the responses of the 5 mills to each other during these

tests was consistent within ~ 10% throughout both 1994 and 1995 deployments, indicating that the data reduction equations contained in Appendix C should produce estimates of ambient field components of comparable accuracy for all flights, in the absence of interference from the effects of aircraft charging. When the aircraft is highly-charged, the retrieval of ambient field components is subject to more uncertainty. A good rule-of-thumb is to compare the magnitudes of the computed ambient components to that of the computed component due to charge on the aircraft. As long as the charge component is moderate or small compared to the ambient components, the ambient component can be relied upon. When the charge component approaches the ambient components in magnitude, the estimates of the ambient components should be examined more carefully, and T-28 facility personnel should be consulted.

Vertical Winds

An estimate of the vertical wind is obtained from the observed rate of change of aircraft pressure altitude by inverting the aircraft equation of motion. This technique is described in Kopp (1985).

Temperature

There are two temperature sensors on the T-28. One is a standard, de-iced Rosemount aircraft temperature probe of a type flown on almost every large aircraft in the world. The other is a platinum-resistance element housed in a specially-designed probe known as a "reverse-flow" housing. Both probes are pictured in Figure 16. The Rosemount probe actually indicates the "total" temperature, which is higher than the ambient "static" temperature due to aerodynamic heating as the air in contact with the sensing element decelerates to rest from the free-stream velocity. The reverse-flow temperature probe indicates a temperature somewhere between the total and static temperature, as air coming into contact with the sensing element apparently does not come to complete rest. Tower fly-by exercises over the years have yielded empirical correction factors that allow an estimate of the ambient static temperature to be made from the indicated total temperature. The temperature archived in the T-28 datasets is the static temperature, computed from the total temperature using equations described in Appendix C.

The temperature estimates from the two probes typically agree within a few tenths of a degree C in clear air. There occasionally may be larger deviations, sometimes exceeding 1 degree C, between the reverse-flow temperature and the Rosemount temperature in clear air. These can be attributed to variations in the angle at which the free stream strikes the probe housings, different exposures to sunlight, and perhaps additional

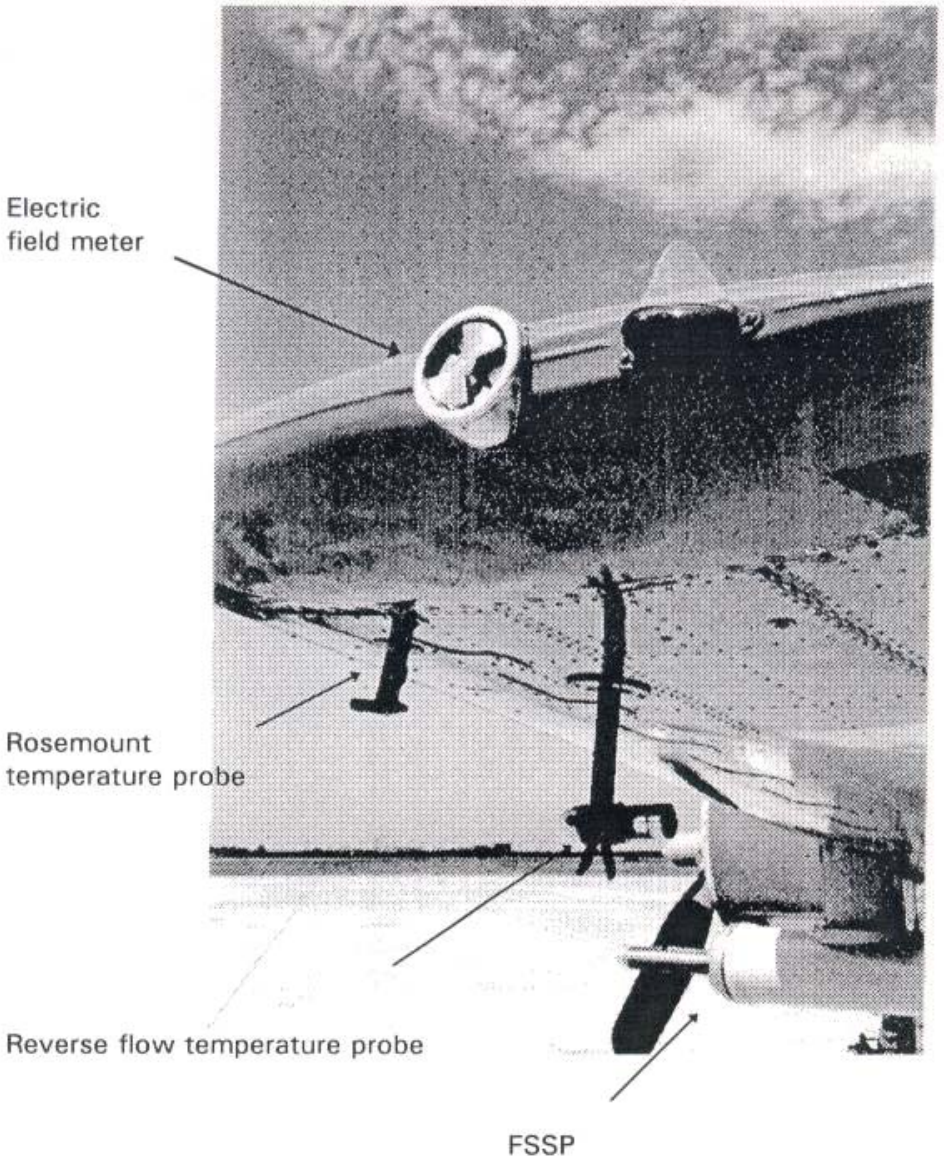

Figure 16: The left wing-tip of the T-28, showing a field meter, the Rosemount temperature probe, the reverse-flow temperature probe, and the FSSP.

miscellaneous factors. The reverse-flow system is more sensitive to angle-of-attack than is the Rosemount system. Clear-air comparisons with nearby aircraft and balloon packages typically show agreement to within 1 degree C between the T-28 Rosemount sensor and sensors on other vehicles, in steady flight.

The de-iced Rosemount probe is reliable out-of-cloud, and semi-reliable in-cloud in the presence of less than ~0.5 g m^{-3} cloud water. At higher water concentrations the temperature-sensing element can be wetted and the computed static temperature will then be somewhere between the dry and wet-bulb temperatures. The reverse-flow temperature sensor is intended to yield better readings in-cloud by shielding the sensing element from cloud and precipitation water. This appears usually to be the case in supercooled cloud, but not in warm cloud (Lawson and Cooper, 1990).

IV. SUMMARY

A prelimary discussion of T-28 observations obtained during VORTEX/MIGHT deployments in 1994 and 1995 has been presented. A variety of cloud environments was sampled, ranging from hail-containing convective storms to quiescent stratiform regions. The temperature range sampled extended from -12°C to below the melting layer. T-28 facility personnel look forward to working with VORTEX/MIGHT analysts as they compare these observations to co-located radar signatures from the Cimarron and CSU-CHILL polarization-diversity radars.

V. ACKNOWLEDGEMENTS

Facility staff involved in these deployments included Dan Custis, Charles Summers, and Tom Root (pilots), Jon Leigh (mechanic), Gary Johnson (instrumentation engineer), Ken Hartman (software engineer), and Dennis Musil and Andy Detwiler (meteorological forecasting and flight guidance, and data quality analysis). The facility is grateful to the NOAA Office of Aircraft Operations for loan of the Particle Measuring Systems, Inc., OAP-2D-P optical array probe for both Oklahoma deployments; the NCAR Research Aviation Facility for loan of a King cloud water probe for the 1995 deployments; and CSU, Atmospheric Environment Service (Canada), SPEC, Inc., and OU, for arranging to make available the High Volume Particle Sampler (HVPS-1) used during the Colorado deployment in 1995. Support for the deployments came from the NSF ATM facilities deployment pool. Base support for the T-28 facility came from NSF and SDSM&T through cooperative agreements ATM-9104474 and ATM-9401117. Special thanks to Connie Crandall for processing the manuscript.

6. REFERENCES

Baumgardner, D., and M. Spowart, 1990: Evaluation of the forward scattering spectrometer probe. Part III: Time response and laser inhomogeneity limitations. *J. Atmos. Ocean. Tech.*, **7**, 666-672.

Biter, C. J., J. E. Dye, D. Huffman, and W. D. King, 1987: The drop-size response of the CSIRO liquid water probe. *J. Atmos. Ocean. Tech.*, **2**, 359-367.

Cooper, W. A., 1988: Effects of coincidence on measurements with a forward scattering spectrometer probe. *J. Atmos. Ocean. Tech.*, **5**, 823-832.

Detwiler, A. G., and K. R. Hartman, 1991. IAS Method for 2D Data Analysis on PC's. Bulletin 91-5, Institute of Atmospheric Sciences, South Dakota School of Mines and Technology, 501 East St. Joseph Street, Rapid City, SD 57701-3995. (variously paged)

Gayet, J. F., 1986: Calibration of Johnson-Williams and PMS ASSP probes in a wind tunnel. *J. Atmos. Ocean. Tech.*, **3**, 381-390.

King, W. D., D. A. Parkin, and R. J. Handsworth, 1978: A hot-wire liquid water device having fully calculable response characteristics. *J. Appl. Meteor.*, **17**, 1809-1813.

King, W. D., C. T. Maher and G. A. Hepburn, 1981: Further performance tests on the CSIRO liquid water probe. *J. Appl. Meteor.*, **20**, 195-202.

King, W. D., J. E. Dye, J. W. Strapp, D. Baumgardner, and D. Huffman, 1985: Icing wind tunnel tests on the CSIRO liquid water probe. *J. Atmos. Ocean. Tech.*, **2**, 340-358.

Knight, C. A., N. C. Knight, W. Grotewold, and T. W. Cannon, 1977: Interpretation of foil impactor impressions of water and ice particles. *J. Appl. Meteor.*, **16**, 997-1002.

Kopp, F. J., 1985: Deduction of vertical motion in the atmosphere from aircraft measurements. . *J. Atmos. Ocean. Tech.*, **2**, 684-688.

Lawson, R. P., and W. A. Cooper, 1990: Performance of some airborne thermometers in clouds. *J. Atmos. Ocean. Tech.*, **7**, 480-494.

Personne, P., J. L. Brenguier, J. P. Pinty, and Y. Pointin, 1982: Comparative study and calibration of sensors for the measurement of the liquid water content of clouds with small droplets. *J. Appl. Meteor.*, **21**, 189-196.

Ramachandran, R., A. Detwiler, J. Helsdon, Jr., P. L. Smith, and V. N. Bringi, 1996: Precipitation development and electrification in Florida thunderstorm cells during CaPE. *J. Geophys. Res.* (in press).

Rasmussen, E. N., J. M. Straka, R. Davies-Jones, C. A. Poswell III, F. H. Carr, M. D. Eilts, and D. R. MacGorman, 1994: Verification of the Origins of Rotation in Tornadoes Experiment: VORTEX. *Bull. Amer. Meteor. Soc.,* **75**, 995-1006.

Schecter, R. M., and R. G. Russ, 1970: The relationship between imprint size and drop diameter for an airborne drop sampler. *J. Appl. Meteor.*, **9**, 123-126.

Spyers-Duran, P. A., 1968: Comparative measurements of cloud liquid water using heated wire and cloud replicating devices. *J. Appl. Meteor.*, **3**, 450-460.

Strapp, J. W., and R. S. Schemenauer, 1982: Calibrations of Johnson-Williams liquid water content meters in a high-speed icing tunnel. *J. Appl. Meteor.*, **21**, 98-108. [The T-28 J-W probe was designated "G" in this intercomparison study.]

Walsh, T. M., 1993. Dual-polarization radar and particle probe measurements in an Oklahoma hailstorm. M. S. Thesis, Department of Electrical and Computer Engineering, The Graduate School, The Pennsylvania State University, State College, PA. 89 pp.

APPENDIX A
Basic T-28 Instrumentation

VARIABLE	INSTRUMENT	RANGE	ACCURACY	RESOLUTION (as recorded)	NOTES
STATIC PRESSURE	ROSEMOUNT 1301-A-4B	0-15 psi (0-103 kPa)	±0.015 psi (±0.1kPa)	0.0002 psi (0.002 kPa)	• Bench calibration, 6/93
	ROSEMOUNT 1301-A-4B	5-15 psi (35-103 kPa)	±0.015 psi (±0.1kPa)	0.0002 psi (0.002 kPa)	• Bench calibration, 6/93
TOTAL TEMPERATURE	ROSEMOUNT 102AU2AP	-30 - +30°C	±0.5°C	0.001°C	• Platinum wire • -2 s time constant
	NCAR REVERSE FLOW	-30 - +30°C	±0.5°C	0.001°C	• Platinum wire • Several seconds time constant • Bench calibration, 6/93 • Recovery factor adjusted, 6/93
CLOUD WATER AND CLOUD DROPLETS	JOHNSON-WILLIAMS LIQUID WATER CONCENTRATION	0 - 6 g/m^3	±20% for narrow size spectra	0.0001 g/m^3	• Accurate if all droplets have d <30 μm
	PARTICLE MEASURING SYSTEMS, INC. FORWARD SCATTERING SPECTROMETER PROBE	Size ~1 ~90 μm Concentration 0-2000 droplets/ cm^3	±1 size channel in size and ±1% in concentration at ~50/cm^3	1 size channel	• 15 discrete size channels spread over an adjustable range • Sampling rate ~300 cm^3/km • Accuracy of computed liquid water concentration ~ ±20%. Depends on processing.
	PMS KING LIQUID WATER PROBE	0-10 g m^{-3}	± 20%	0.001 g m^{-3}	• Borrowed from NCAR RAF for 1995 deployments

APPENDIX A BASIC T-28 INSTRUMENTATION (Continued)

VARIABLE	INSTRUMENT	RANGE	ACCURACY	RESOLUTION (as recorded)	NOTES
PRECIPITATION PARTICLE SIZES AND CONCENTRATIONS	WILLIAMSON FOIL IMPACTOR	1 - 20 mm	0.2 mm	0.2 mm	• Sampling rate 1.4 m^3/km
	PARTICLE MEASURING SYSTEMS, INC. 2D Precipitation Probe	Size 200 - 6400 μm	±200 μm	200 μm	• Computed ice and water concentration can vary ±50% with processing technique • Sampling rate: 1.66 m^3/km; DAS can accept ~250 particles/s (2500/km) • Borrowed from NOAA OAO for use during 1994 and 1995 OK deployments
	HAIL SPECTROMETER	Size 4.5 - 45 mm Concentration 0 - 100/m^3	± 1 size class	1 size class	• 14 size classes • Sampling rate 100 m^3/km
	SPEC HIGH VOLUME PARTICLE SAMPLER 1	0.2 - 48 mm size	0.2 mm vertical 0.4 mm horizontal	0.2 mm vertical 0.4 mm horizontal	• Volume sampling rate ~1 m^3 s^{-1} ~10 m^3 km^{-1} • Provided by CSU and AES Canada for use in Colorado deployment

APPENDIX A BASIC T-28 INSTRUMENTATION (Continued)

VARIABLE	INSTRUMENT	RANGE	ACCURACY	RESOLUTION (as recorded)	NOTES
AIRCRAFT MOTION	NCAR TRUE AIRSPEED COMPUTER	0 - 250 kts (0 - 130 m/s)	±3 kts (±1.5 m/s)	0.125 kt (0.07 m/s)	• True airspeed
	HUMPHREY SSA09-D0101-1 VERTICALLY STABILIZED ACCELEROMETER	± 2 g's pitch -50° to +50° roll -50° to +50°	0.004 g 0.2° 0.2°	0.00006 g 0.002° 0.002°	
	ROSEMOUNT 1301-D-1B DYNAMIC PRESSURE	-3 to +3 psi (-20 to +20 kPa)	±0.1%	0.0001 psi (0.0006 kPa)	• Indicated airspeed • Bench calibration, 6/93
	ROSEMOUNT 1221-F-2A DYNAMIC PRESSURE	-2.5 to +2.5 psi (-18 to +18 kPa)	±0.1%	0.0001 psi (0.0006 kPa)	• Indicated airspeed • Bench calibration, 6/93
	GIANNINI 45218YE MANIFOLD PRESSURE	0 to 50 in Hg	±2%	0.008 in Hg (0.03 kPa)	• Used in one vertical velocity calculation • Bench calibration, 3/93
	BALL ENGINEERING 101A VARIOMETER	-6000 to +6000 ft/min (-30 to +30 m/s)	±200 ft/min (±1 m/s)	0.2 ft/min (0.001 m/s)	
AIRCRAFT LOCATION	NARCO NAV-122 VOR	0 - 360°	±2°	0.005°	
	CESSNA 400 DME	0 - 100 nmi (0 - 185 km)	0.1 nmi (185 m)	0.002 nmi (3 m)	• Maximum 2 s to lock on and acquire range
	TRIMBLE TNL2000 GPS	(global)	30 m	18 m	

APPENDIX A BASIC T-28 INSTRUMENTATION (Continued)

VARIABLE	INSTRUMENT	RANGE	ACCURACY	RESOLUTION (as recorded)	NOTES
ELECTRIC FIELD	NMIMT Model E-100 DC Electric Field Meter	top/bot ± 650 wings ± 3200 5th ± 340 kV/m		(coarse resolution) 0.01 $\frac{kV}{m}$	
NOTE: Many of these instruments do not behave as ideal instruments. The use of one measure of accuracy over the entire range of measurement is, in many cases, questionable. An accuracy representative of the most useful part of the range is given here.					

Revised 12/95

APPENDIX B

List of Variables Recorded or Routinely Computed
from T-28 Observations

Each different variable in the data stream is indexed with a unique tag number. Those used for the VORTEX/MIGHT deployment are listed here.

Tag	Variable	Remarks
100	**Time**	The T-28 data system is always set to local time, and recorded in a 24-hour format. It is maintained daily within a second of WWV unless otherwise noted.
101	**Dynamic Pressure 1**	
102	**Dynamic Pressure 2**	Both dynamic pressures are read from the same pitot tube line (with the inlet out on the right wing) using two different but nearly identical sensors. [hPa]
103	**Static Pressure 1**	
104	**Static Pressure 2**	Both static pressures are read from the same static pressure line (inlet on the rear fuselage) using two different but nearly identical sensors. [hPa]
105	**Rate of Climb**	The instantaneous rate of change of aircraft altitude, read from a standard aircraft variometer. The recorded data are unfiltered and much noisier than the damped cockpit display. [$m\ s^{-1}$]
106	**Rosemount Temperature**	This is static temperature computed from the reading of a standard, deiced, Rosemount aircraft total air temperature probe. It commonly suffers from wetting and reads low in clouds. [°C]

107	**Reverse Flow Temperature**	This is static temperature computed from the reading of a platinum resistance element placed inside a custom-design "reverse-flow" housing. It normally does not get wet in cold clouds or in regions of high precipitation water concentration. Apparently, ice may sometimes build up to such an extent on the housing that temperature readings are affected even though the sensor is not wetted. Its response to changes in angle of attack is greater than that of the Rosemount probe. [°C]
108	**Manifold Pressure**	Pressure inside the engine manifold (an indicator of power being developed by the engine) is recorded from a standard aircraft engine presssure sensor. [inches of mercury]
109	**Acceleration**	Vertical acceleration is determined by a Humphrey gyro/accelerometer. [g's]
110	**Pitch**	The accelerometer also gives angle of the fuselage relative to horizontal. [deg]
111	**Roll**	Finally, the accelerometer gives angle of the wings relative to horizontal. Angle is positive for a left bank (left wing down). [deg]
112	**J-W liquid water**	The J-W probe yields concentration of water in clouds represented in droplets less than approximatley 30 μm diameter. [g m^{-3}]
113	**VOR**	The VOR gives the direction to the VORTAC (a radio direction-finding beacon used by aircraft) to which it is tuned. [deg]
114	**DME1**	This is distance to the VORTAC to which the #1 DME is tuned. [n mi]

116	**Voltage Regulator**	Voltage of power source for some instruments. [volts]
117	**Heading**	Indicates direction (from magnetic north) towards which the aircraft is heading. [deg]
119	**PMS End Element 1**	Voltage readings of PMS end diodes.
120	**PMS End Element 2**	
121	**Interior Temperature**	Temperature inside the data acquisition system computer in the baggage bay. [°C]
124	**Heater Current**	Total current consumed by de-icing circuits (A).
125	**King liquid water**	Cloud liquid water concentrations sensed by the King Probe (also known as CSIRO probe). This probe responds to a broader range of droplet sizes than the J-W probe, and typically indicates higher concentrations than the J-W unless the cloud droplet spectrum is very narrow (i.e. near cloud base, or in the lower portion of a very strong updraft) This unit was borrowed from NCAR for use during 1995 only. [g m^{-3}]
128	**Discharging Forward**	Signal proportional to electrical discharge from an experimental probe mounted on the lower fuselage, just behind the engine compartment. A positive signal corresponds to the discharge of negative ions. Borrowed from SRI International, for use during 1995. [V]
129	**Discharging Aft**	Signal proportional to electrical discharge from an experimental probe mounted on the lower fuselage, under the tail. A positive signal corresponds to the discharge of negative ions. Borrowed from SRI International, for use during 1995. [V]

130	**Event Bits**	Bits corresponding to various events recognized by the data system, including an indication that the system is running, that the in-cloud switch is activated by the pilot (when visually entering cloud), that the foil impactor is running, and that the cockpit voice recorder is activated.
131	**GPS Warning Codes**	Bits corresponding to various status messages from the GPS system.
140	**FSSP size counts**	This tag contains information concerning the number of counts in each of the 15 available FSSP size channels. [number per channel per second]
141	**FSSP total counts**	The total number of droplets counted by the FSSP during a second.
142	**FSSP average diameter**	The arithmetic average diameter of all droplets recorded during a second. [μm]
143	**FSSP concentration**	The actual concentration of droplets computed from FSSP counts divided by the volume sampled in 1 s ("Standard method"). A rudimentary correction for probe activity is made. [# cm^{-3}]
144	**FSSP Water**	The liquid water concentration computed from the FSSP data for a second ("Standard method"). [g m^{-3}]
145	**FSSP Activity**	The fraction of time the FSSP is active during the current second.
147	**PMS 2DP Shadow Or Count**	The number of times the 2D-P probe was triggered out of its wait state by the passage of a new particle. The 2D-P was flown during deployments to Norman during May of 1994 and 1995, but was not flown during the deployment to Greeley in June, 1995. [# s^{-1}]

148 **FSSP Equivalent Diameter** $\sum_{i=1}^{15}\left[\frac{n_i \cdot d_i^3}{n_i \cdot d_i^2}\right]$ at one second intervals, using "standard method" counts and sizes.

149 **Variance in FSSP Equivalent Diameter** Variance around the equivalent diameter, computed as

$$\frac{\sum_{i=1}^{15} n_i \cdot d_i^2 \cdot \left(d_i - d_{eqv}\right)^2}{d_{eqv}^2 \cdot \left(\sum_{i=1}^{15} d_i\right)^2}$$

using "standard method" counts and sizes.

150 **Hail size counts** This tag contains information on the number of particles in each of the 14 hail spectrometer size channels. [number per channel per second]

151 **Slow Particle** The number of particles rejected because they passed through the hail spectrometer too slowly (indicating they were probably water or ice shed from the probe structure rather than airborne hydrometeors). [number per second]

152 **Hail total counts of (150)** Total number of particles accepted by the hail spectrometer. [number per second]

153 **Hail average diameter** The average diameter of all particles accepted by the hail spectrometer in the last second. [cm]

154 **Hail concentration** The computed concentration corresponding to all particles accepted by the hail spectrometer in the last second. [number per cubic meter]

155 **Hail Water** The mass concentration computed from the observed particle spectrum assuming spherical particles and a bulk particle density of 0.9 grams per cubic centimeter. [grams per cubic meter]

160 **Top Field Mill (low res)** The electric field indicated by the low sensitivity channel on the field mill mounted in

		the aircraft canopy looking up. Field mill data are recorded at 20 Hz. [kV m^{-1}]
161	**Bottom Field Mill (low res)**	The electric field indicated by the low sensitivity channel on the field mill located in the baggage bay door looking down. [kV m^{-1}]
162	**Left Field Mill (low res)**	The electric field indicated by the low sensitivity channel on the field mill mounted in the left wing tip facing outward. [kV m^{-1}]
163	**Right Field Mill (low res)**	The electric field indicated by the low sensitivity channel on the field mill mounted in the right wing tip facing outward. [kV m^{-1}]
164	**Top Field Mill (high res)**	The electric field indicated by the high sensitivity channel on the top field mill. [kV m^{-1}]
165	**Bottom Field Mill (high res)**	The electric field indicated by the high sensitivity channel on the bottom field mill. [kV m^{-1}]
166	**Left Field Mill (high res)**	The electric field indicated by the high sensitivity channel on the left field mill. [kV m^{-1}]
167	**Right Field Mill (high res)**	The electric field indicated by the high sensitivity channel on the right field mill. [kV m^{-1}]
168	**Fifth Field Mill (low res)**	The electric field indicated by the low sensitivity channel on the fifth field mill, located in one of the hail spectrometer pylons under the left wing. [kV m^{-1}]
172	**Latitude**	Computed internally in the GPS receiver. [deg]
173	**Longitude**	Also computed internally in the GPS receiver. [deg]

174	**Groundspeed**	Computed internally in the GPS receiver (by differentiating the position data with respect to time). [m/s]
175	**Ground Track Angle**	The direction towards which the aircraft is moving relative to the ground, with respect to magnetic north. [deg]
176	**Magnetic Deviation**	The difference between magnetic north and true north as indicated automatically by the GPS receiver based on the current position. [deg]
177	**Time Since Solution**	The time since the GPS was last able to compute an accurate position solution based on a sufficient number of satellites. The GPS updates position based on dead reckoning if it does not have a sufficient number of satellites in view. [s]
178	**GPS Altitude**	Geometric aircraft altitude. [m]
190	**FSSP Gated Strobes**	Number of accepted droplet counts. [s^{-1}]
191	**FSSP Total Strobes**	Total number of droplet counts. [s^{-1}]
192	**FSSP Reference Voltage**	Reference voltage for FSSP opto-electronics.
200	**Date**	As indicated by the data acquisition system computer clock. [yymmdd]
201	**Month**	mm [integer number]
202	**Day**	dd [integer number]
203	**Year**	yy [integer number]
204	**Flight**	A serial number assigned to each T-28 flight beginning with the "first" research flight. (Flight #1 occurred in 1972.)
205	**Altitude**	The altitude in a standard atmosphere corresponding to the recorded static pressure. [m]

206	θ_e	The equivalent potential temperature corresponding to the recorded temperature and assuming saturation with respect to liquid water (should be valid in-cloud). [K]
207	**Saturation Mixing Ratio**	The mixing ratio of water vapor corresponding to saturation with respect to liquid water at the recorded temperature. [g kg^{-1}]
208	**Point dz/dt**	The rate of change of altitude of the aircraft computed by differentiating the pressure altitude with respect to time. This represents an independent estimate of the rate of climb to be compared to tag 105. [m s^{-1}]
209	**Indicated Air Speed**	What the airspeed would be if the aircraft were flying at sea level and indicating the observed dynamic presure. [m s^{-1}]
210	**Updraft (uncorrected)**	The estimated upward speed of the air relative to the ground computed from changes in the aircraft altitude and other factors, but not corrected for horizontal aircraft acceleration. [m s^{-1}]
211	**Calculated TAS**	The true speed of the aircraft relative to the air computed from the observed dynamic and static pressures, and temperature. [m s^{-1}]
212	**Updraft Correction Factor**	A correction to tag 210, the simple (uncorrected) updraft calculation, that accounts for horizontal accelerations of the aircraft. [m s^{-1}]
213	**Cooper Updraft**	The sum of the uncorrected updraft and the correction factor. [m s^{-1}]
214	**Kopp Updraft**	An updraft calculated somewhat differently than the Cooper updraft [Kopp, 1985]. In most situations, it yields a less noisy and more physically plausible updraft result for the T-28 than the Cooper method. [m s^{-1}]

215	**Geopotential Altitude**	Altitude computed from changes since takeoff in static pressure and temperature, using the hydrostatic equation. *[Not routinely computed, but can be computed upon request.]* [m]
216	**Turbulence**	The turbulent energy dissipation rate estimated from observed fluctuations in true airspeed. [$cm^{2/3}$ s^{-1}]
217	**Air Density**	Computed from the recorded temperature and static pressure. [kg m^{-3}]
218	**J-W Mixing Ratio**	The mixing ratio of cloud water per unit mass of dry air based on the J-W reading and computed air density. [g kg^{-1}]
219	**FSSP Mixing Ratio**	The mixing ratio of cloud water per unit mass of dry air calculated from the FSSP water concentration. [g kg^{-1}]
220	**Hail Mixing Ratio**	The mixing ratio of hail mass per unit mass of dry air based on the computed hail water and air density. [g kg^{-1}]
244	**FSSP equivalent J-W Liquid Water**	An estimate of the liquid water concentration the J-W probe should record, based on the observed FSSP droplet spectrum and the assumption that the J-W responds incompletely to droplets larger than 30 μm diameter. [g m^{-3}]
260	**Ambient Vert Electric Field**	The component of the ambient electric field that is vertical in the aircraft frame of reference. Positive means a positive test charge would drift upward relative to the aircraft in the field. [kV m^{-1}]
261	**Plane Vert Electric Field**	The field due to charge on the aircraft, computed by summing the readings of the top and bottom mill and normalizing based on self-charging tests. Positive means a positive test charge would be repelled away

		from the aircraft due to its charge. [kV m^{-1}]
262	**Ambient Hor Electric Field**	The ambient field oriented perpendicular to the aircraft along the wings, positive meaning a positive test charge would drift to the right in the field. [kV m^{-1}]
263	**Plane Hor Electric Field**	The field due to charge on the aircraft, computed by summing the wingtip mill readings and normalizing. Positive means a positive charge would be repelled away from the aircraft due to its charge. [kV m^{-1}]
264	**Ambient Vert Field (roll cor)**	The component of the ambient field that is truly vertical with respect to earth coordinates. [kV m^{-1}]
265	**Ambient Hor Field (roll cor)**	The component of the ambient field perpendicular to the aircraft path and truly horizontal with respect to earth coordinates. [kV m^{-1}]
272	**Latitude (deg)**	GPS coordinates broken into separate degree and minute components.
273	**Latitude (min)**	GPS coordinates broken into separate degree and minute components.
274	**Longitude (deg)**	GPS coordinates broken into separate degree and minute components.
275	**Longitude (min)**	GPS coordinates broken into separate degree and minute components.
276	**Ground Track Angle (True N)**	The direction of motion relative to the ground with respect to true north, derived from the GPS ground track angle with respect to magnetic north.

[Tags 341 - 349 computed only for May, 1995, FSSP data, as of the date of this report. Can be computed for other flights upon request.]

341	**Calculated FSSP Total Count**	Observed FSSP total counts with minor corrections made in an attempt to correct for the effects of ice particles on FSSP droplet spectra. Not fully proven. [s^{-1}]
342	**Calculated FSSP Average Diameter**	FSSP average droplet diameter estimated from spectra calculated using the Baumgardner FSSP data reduction procedure. [μm]
343	**Calculated FSSP Concentration**	Droplet concentration estimated using the Baumgardner FSSP data reduction procedure. [# cm^{-3}]
344	**Calculated FSSP Water**	Liquid water concentration estimated using the Baumgardner FSSP data reduction procedure. [g m^{-3}]
345	**Calculated FSSP Mixing Ratio**	Computed from "calculated FSSP water" (tag 344) and "air density" (tag 217). [g kg^{-1}]
348	**Calculated FSSP Equivalent Diameter**	Computed as for tag 144, but using FSSP spectra derived using the Baumgardner FSSP data reduction procedure. [μm]
349	**Variance of the Calculated FSSP Equivalent Diameter**	Computed as for tag 149, but using FSSP spectra derived using the Baumgardner FSSP data reduction procedure.

APPENDIX C: FORMULAE

Reduced Data Items Computed for VORTEX/MIGHT, Norman, OK May, 1994 and May, 1995; Ft.Collins, CO June, 1995 *0

Tag #	*Description*	*# Values Output*	*Units*		*Method of Computation*	*Last Mod (if this project)*	
101	Dynamic Pressure #1	(10 Hz)	1	mb	6.30452E-3 * Raw - 0.0489		
102	Dynamic Pressure #2	(10 Hz)	1	mb	5.28371E-3 * Raw - 1.5768		
103	Static Pressure #1	(2 Hz)	1	mb	1.5791E-2 * Raw + 530.37		
104	Static Pressure #2	(2 Hz)	1	mb	1.0917E-2 * Raw + 691.92		
105	Rate of Climb	(2 Hz)	1	m/s	5.625E-4 * Raw, for Raw > = 0		
					5.287E-4 * Raw, for Raw < 0		
106	Rosemount Temp		1	deg C	mach2 = 5*((1+dyn_pr/stat_pr)**(2/7)-1)		
					divisor = 1 + 0.195 * mach2		
					temp = (1.83105E-3*Raw+243.16)/divisor-273.16		
107	Reverse Flow Temp		1	deg C	divisor = 1 + 0.1594 * mach2		
					temp = (3.02109E-3*Raw+222.06)/divisor-273.16	5/19/94	
108	Manifold Pressure		1	" Hg	3.1098E-3 * Raw + 0.159275		
109	Acceleration	(10 Hz)	1	g's	6.25E-5 * Raw [prior to 7/14/94]		
					6.25E-5 * Raw + 1.0 [after 7/14/94]	7/14/94	
110	Pitch	(5 Hz)	1	deg	-3.05175E-3 * Raw + 50		
111	Roll	(5 Hz)	1	deg	3.05175E-3 * Raw - 50		
112	J.W.Liquid Water		1	g/m3	1.83125E-4 * Raw		
113	VOR		1	deg	1.117534E-2 * Raw - 1.155475		
114	DME #1		1	naut mi	3.03269E-3 * Raw - 0.24536		
116	Voltage Regulator		1	volts	1.5258789E-4 * Raw		
117	Heading	(5 Hz)	1	deg	interpolation from lookup table		
118	NCAR true? air speed		1	m/s	3.96744E-3 * Raw		
121	Interior Temp (computer)		1	deg C	3.05175E-2 * Raw		
124	Heater current		1	amp	3.05175E-3 * Raw	5/7/94	
125	King liquid water		1	g/m3	P = -3.05175E-3 * Raw	1995	*1
					A = 2.973E-4; B = 0.501; Ts = 188.16		
					Pwet = P - A * (Ts - temp) * (pres * tas)**B		
					Kwater = Pwet / (0.099 * tas)		

Tag #	Description	# Values Output	Units		Method of Computation	Last Mod (if this project)	
128	Discharging (Forward)		1		1.52588E-4 * Raw		
129	Discharging (Aft)		1		-1.52588E-4 * Raw		*2
130	Event Code bits		1	flags	bit 0 = 1 --> system running bit 1 = 0 --> in cloud bit 2 = 0 --> foil on bit 3 = 0 --> voice recorder on		
131	GPS warning codes		1	flags	11 bit codes		
140	FSSP counts		15	number	Raw		
141	FSSP total counts		1	number	Sum of tag 140s		
142	FSSP ave diameter		1	microns	sum of diams / number		*3
143	FSSP concentration		1	#/cm3	vol = 0.22275 * tas denom = 1 - .55 * activ / 100 conc = tot_count / vol / denom	5/25/94	*3
144	FSSP water		1	g/m3	mass = sum of counts * volumes water = mass/vol/denom*1.E6		*3
145	Probe Activity		1	%	Raw / 10		
146	PMS 2DP Shd Or		1	number	Raw		
148	FSSP equivalent diameter		1	microns	Ratio of sum of diam**3 to sum of diam**2		*3
149	FSSP equivalent diameter variance		1	microns	Consult REDUCE.C listing		*3
150	Hail counts		14	number	Raw		
151	Hail slow particle count		1	number	Channel 15		
152	Hail total counts		1	number	Sum of tag 150s		
153	Hail ave diameter		1	cm	sum of diams / number		
154	Hail concentration		1	#/m3	conc = counts / (0.1 * tas)		
155	Hail water		1	g/m3	mass = sum of counts * volumes * 0.9 water = mass / (0.1 * tas)		
160	Top field mill, low res	(20 Hz)	1	kV/m	-2.1117E-2 * Raw + 0.094	Jan, '94	
161	Bottom field mill, low res	(20 Hz)	1	kV/m	-2.091E-2 * Raw + 0.181	Jan, '94	*4
162	Left field mill, low res	(20 Hz)	1	kV/m	-9.6722E-2 * Raw - 0.975	Jan, '94	
163	Right field mill, low res	(20 Hz)	1	kV/m	-9.7641E-2 * Raw - 2.076	Jan, '94	
164	Top field mill, hi res	(20 Hz)	1	kV/m	-3.4082E-4 * Raw - 0.007	Jan, '94	*5
165	Bottom field mill, hi res	(20 Hz)	1	kV/m	-3.3032E-4 * Raw + 0.215	Jan, '94	*4 *5
166	Left field mill, hi res	(20 Hz)	1	kV/m	-1.5364E-3 * Raw + 0.102	Jan, '94	*5
167	Right field mill, hi res	(20 Hz)	1	kV/m	-1.5414E-3 * Raw + 0.029	Jan, '94	*5
168	Fifth field mill, low res	(20 Hz)	1	kV/m	-9.9154E-2 * Raw + 6.49	Jan, '94	*4

Tag #	Description	# Values Output	Units		Method of Computation	Last Mod (if this project)
169	Fifth field mill, hi res	(20 Hz)	1	kV/m	-1.5428E-3 * Raw - 0.22	Jan, '94 *4 *5
172	GPS latitude		1	deg	degree + (minute + hundredths/100)/60	
173	GPS longitude		1	deg	degree + (minute + hundredths/100)/60	
174	GPS groundspeed		1	m/s	1852 / 36000 * Raw	
175	GPS grnd track angle (mag N)		1	deg	Raw / 10	
176	GPS magnetic deviation		1	deg	Raw / 10 (Raw is 32-bits, not 16)	
177	GPS time since solution		1	s	Raw / 10	
178	GPS altitude		1	meters	Raw / 10 (Raw is 32-bits, not 16)	
185	GPS ROC		1	m/s	10ths of ft/min to m/s	5/1/94
190	FSSP gated strobes		1	number	Raw	
191	FSSP total strobes (div by 10)		1	number	Raw	
192	FSSP reference voltage		1	volts	Raw / 25.5	
200	Date		1	yymmdd		
201	Month		1	number		
202	Day		1	number		
203	Year		1	2-dig		
204	Flight number		1	number		
205	Altitude		1	meters	4.43077E4*(1-(stat_pr/1013.3027)**.190284)	
206	Theta e		1	K	tempk = RFT temp in K svp = 6.1078*exp(17.26939*rft/(tempk-35.86)) smr = svp / (stat_pr - svp) * 0.622 ts = tempk * (1000/stat_pr)**0.286 thetae = ts*exp(597.3*smr)/(0.24*tempk))	
207	Saturation mixing ratio		1	g/kg	smr from above	
208	Point dz/dt		1	m/s	alt - prev_alt	
209	Indicated airspeed		1	m/s	c = 1 + dyn_pr / 1013.3027 ias = sqrt(5.79E5*(c**(2/7)-1))	
210	Updraft (uncorrected)		1	m/s	u1 = change in alt ((i+1)-(i-1))/2 u2 = (27 - man_pr) * 92 u3 = (1.94254 * ias - 140) * 17.7 updr = u1 + (u2 + u3) * 0.00508	
211	Calculated TAS		1	m/s	sqrt(rftuc*mach2*401.856/divisor)	
212	Updraft correction factor		1	m/s	calc_tas*(change in calc_tas)/2/9.775	
213	Cooper Updraft		1	m/s	updraft + updraft correction	

Tag #	Description	# Values Output	Units		Method of Computation	Last Mod (if this project)	
214	Kopp Updraft		1	m/s	dens = 0.34838 * stat_pr /tempk ang = pitch * 0.0174533 Kopp=u1+62.12*accel*9.775/(dens*calc_tas) -(0.02028+ang)*calc_tas		
215	Geopotential altitude		1	meters	stepwise integration of hydrostatic equation		*6
216	Turbulence		1	cm**2/3/s	Much too complicated to write here. Static and dynamic pressure values, along with RFTs, are fed into a fast Fourier transform routine. Consult program listing.		
217	Air density		1	kg/m3	0.34838 * stat_pr / tempk		
218	JW mixing ratio		1	g/kg	jw_water / density		
219	FSSP mixing ratio		1	g/kg	FSSP_water / density		
220	Hail mixing ratio		1	g/kg	hail_water / density		
221	RFT uncorrected		1	deg C	Reverse flow temp without divisor term		
244	JW equiv water		1	g/m3	mass = sum of counts * volumes, where diams > 30 microns are treated as equal to 30 water = mass/vol/denom*1.E6	10/7/94	*7
260	Ambient vert EF		1	kV/m	(tfm - 2 * bfm) / 11.2		*8
261	Plane vert EF		1	kV/m	(tfm + 2 * bfm) / 11.2		*8
262	Ambient lateral EF		1	kV/m	(rfm - lfm) / 44.8		*8
263	Plane lateral EF		1	kV/m	(rfm + lfm) / 32.48		*8
264	Ambient vert EF (with roll)		1	kV/m	cosr = cos(roll_rad) sinr = sin(roll_rad) t264 = t260 * cosr + t262 * sinr		
265	Ambient lat EF (with roll)		1	kV/m	t265 = -t260 * sinr + t262 * cosr		
272	GPS deg lat		1	deg	integer portion of tag 172 (t172)		
273	GPS min lat		1	min	fractional part of t172 * 60		
274	GPS deg long		1	deg	integer portion of tag 173 (t173)		
275	GPS min long		1	min	fractional part of t173 * 60		
276	GPS true bearing		1	deg	mod(t175+t176+360,360)		
340	Adjusted FSSP counts		15	number	Raw		*9
341	Adjusted FSSP total counts		1	number	Sum of tag 340s		*9
342	Adjusted FSSP ave diameter		1	microns	sum of diams / number		*9

Tag #	Description	# Values Output	Units		Method of Computation	Last Mod (if this project)	
343	Adjusted FSSP concentration		1	#/cm3	vol = 0.22275 * tas denom = 1 - .55 * activ / 100 conc = tot_count / vol / denom	5/25/94	*9
344	Adjusted FSSP water		1	g/m3	mass = sum of counts * volumes		*9
345	Adjusted FSSP mixing ratio		1	g/kg	FSSP_water / density		*9
348	Adjusted FSSP equiv diam		1	microns	Ratio of sum of diam**3 to sum of diam**2		*9
349	Adjusted FSSP equiv diam variance		1	microns	Consult REDUCE.C listing		*9

*0 In some cases the equation variables are averages. Consult the listing of REDUCE.C for exact details. All quantities are recorded at 1 Hz unless otherwise noted.

*1 The King probe was added for the 1995 OK and CO projects.

*2 Prior to 5/12/95, the coefficient term was positive (same as tag 128). Tags 128 and 129 were recorded only for the '95 flights.

*3 Calibration of the FSSP (via bead test) led to different channel assignments in file FSSP.CHN for each month.

*4 On 5/6/95 the bottom field mill was physically swapped with the "fifth" field mill. Thus, for flights after this date, the equations for bottom<-->5th should be interchanged.

*5 Some high resolution field mill data were stored on various flights (usually left and right), but not all, due to the limited analog channels available.

*6 Some data files include this variable. It is computed during an optional second phase of processing, using static pressure and temperature changes.

*7 Computation added prior to 1995 projects.

*8 These numerical equations have varied slightly from one season to the next.

*9 Adjusted FSSP values are computed as described in Baumgardner and Spowart (1990). The adjustment algorithm was run to produce a second, enlarged reduced data file. These adjusted data currently are included only for flights during the OK '94 project.

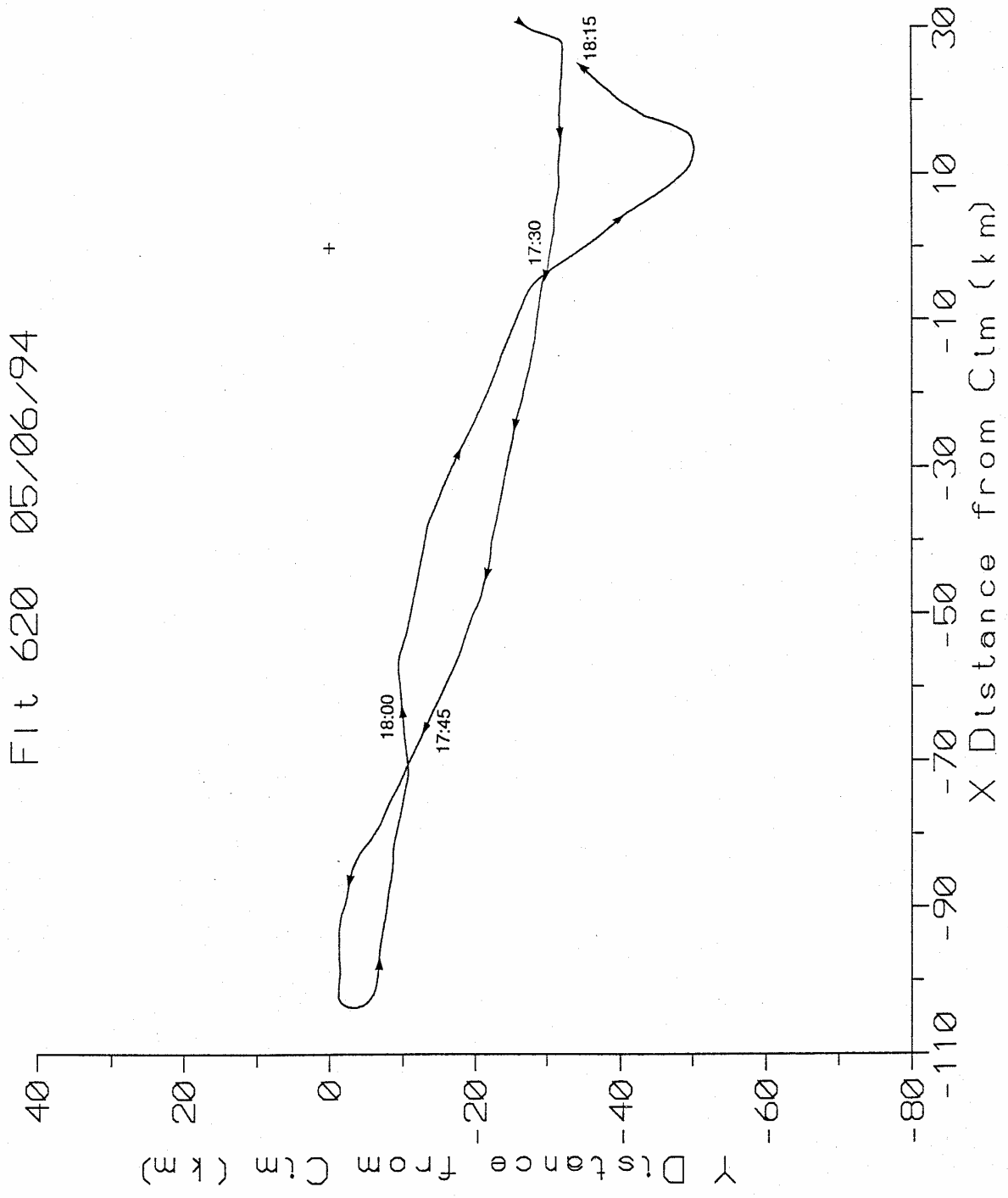
Flt 620 05/06/94
18:00
17:45
17:30
18:15
Y Distance from Clm (km)
X Distance from Clm (km)
40
20
0
-20
-40
-60
-80
-110
-90
-70
-50
-30
-10
10
30

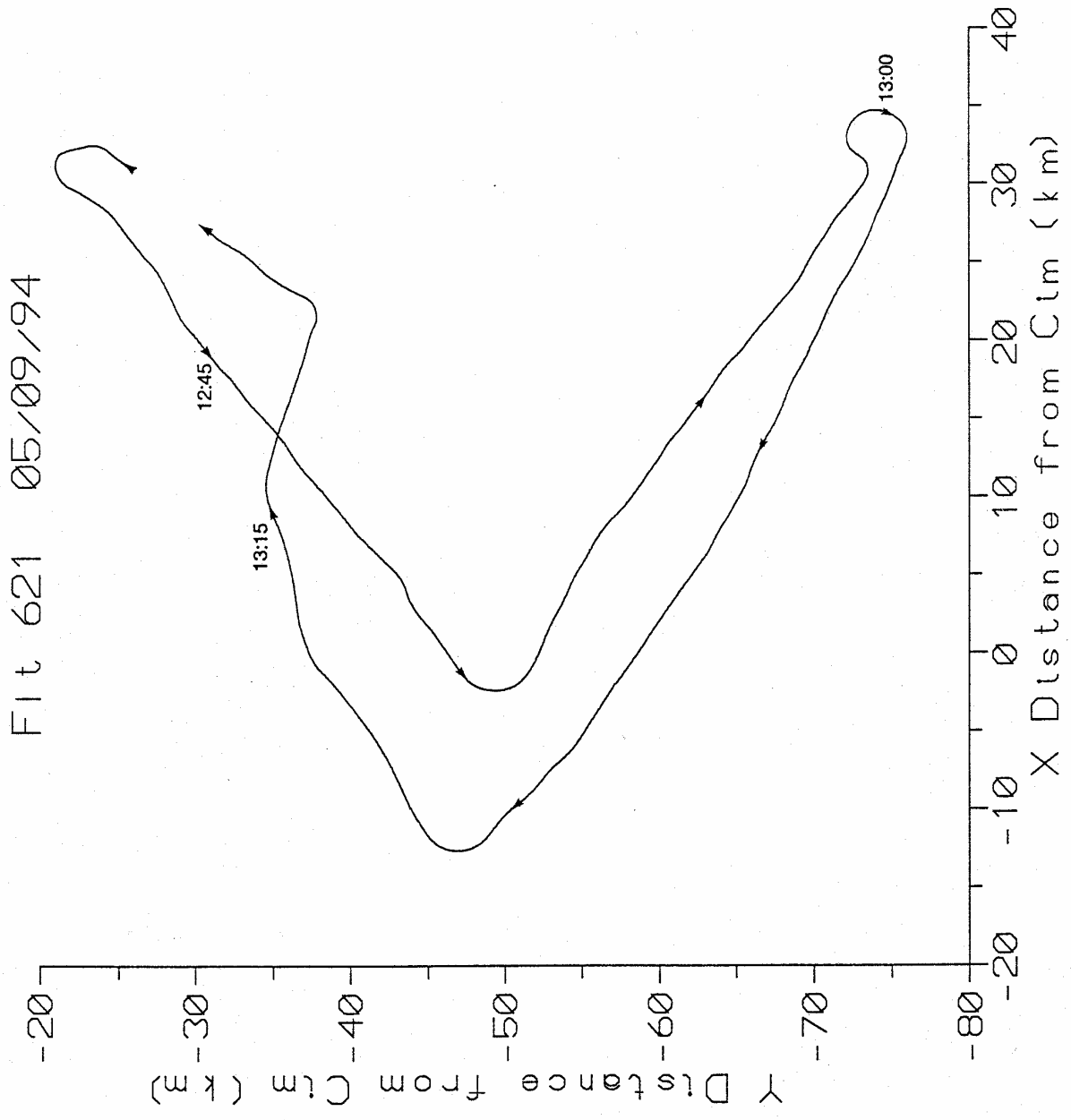
Flt 621 05/09/94
12:45
13:15
13:00
Y Distance from Clm (km)
-20
-30
-40
-50
-60
-70
-80
X Distance from Clm (km)
-20
-10
0
10
20
30
40

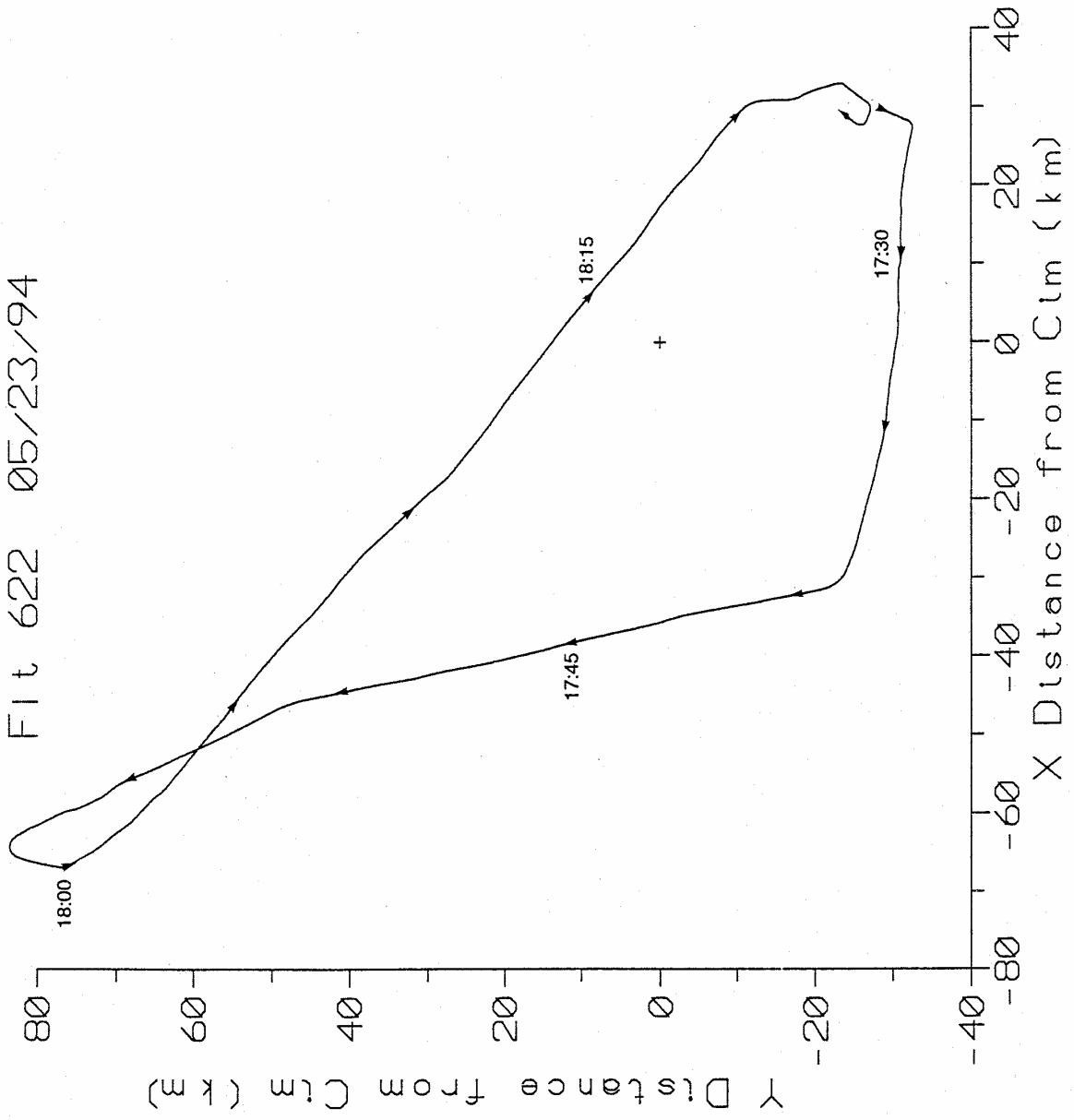
Flt 622 05/23/94
18:00
17:45
18:15
17:30
Y Distance from Clm (km)
X Distance from Clm (km)
80
60
40
20
0
-20
-40
-80
-60
-40
-20
0
20
40

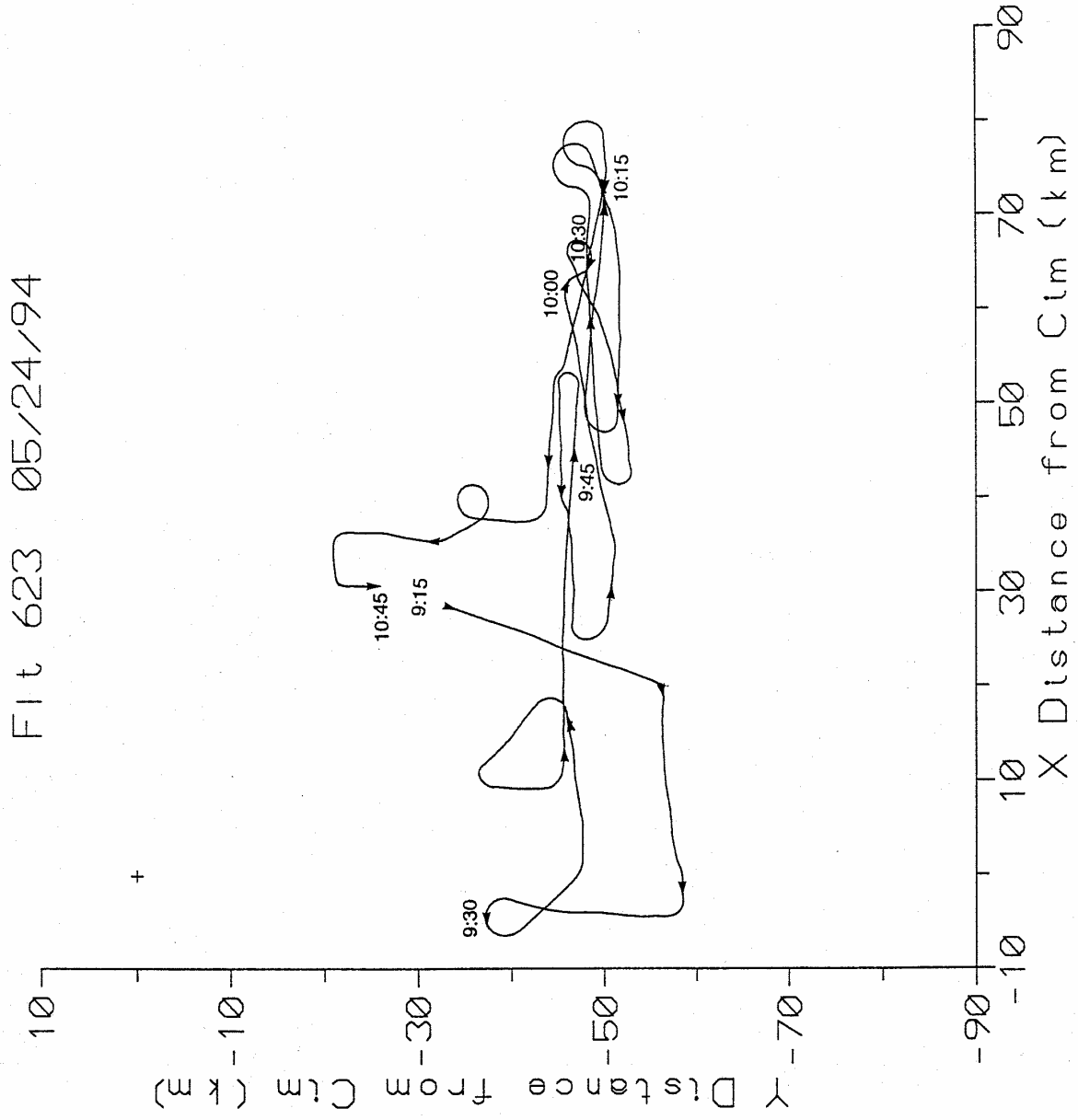
Flt 623 05/24/94
9:30
9:15
9:45
10:00
10:30
10:15
10:45
Y Distance from Clm (km)
X Distance from Clm (km)
10
-10
-30
-50
-70
-90
-10
10
30
50
70
90

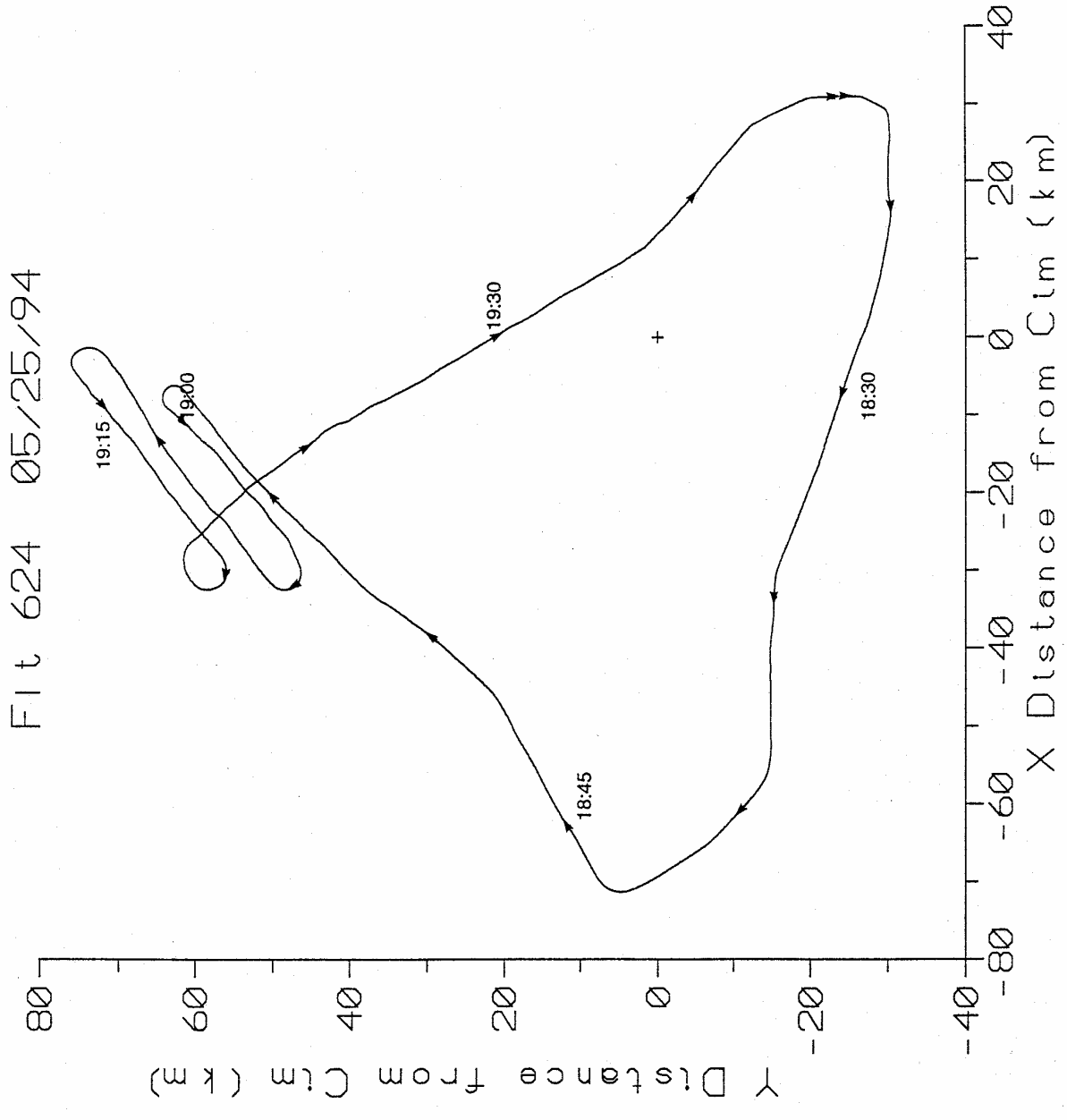
Flt 624 05/25/94
19:15
19:00
19:30
18:30
18:45
+
Y Distance from Clm (km)
80
60
40
20
0
-20
-40
X Distance from Clm (km)
-80
-60
-40
-20
0
20
40

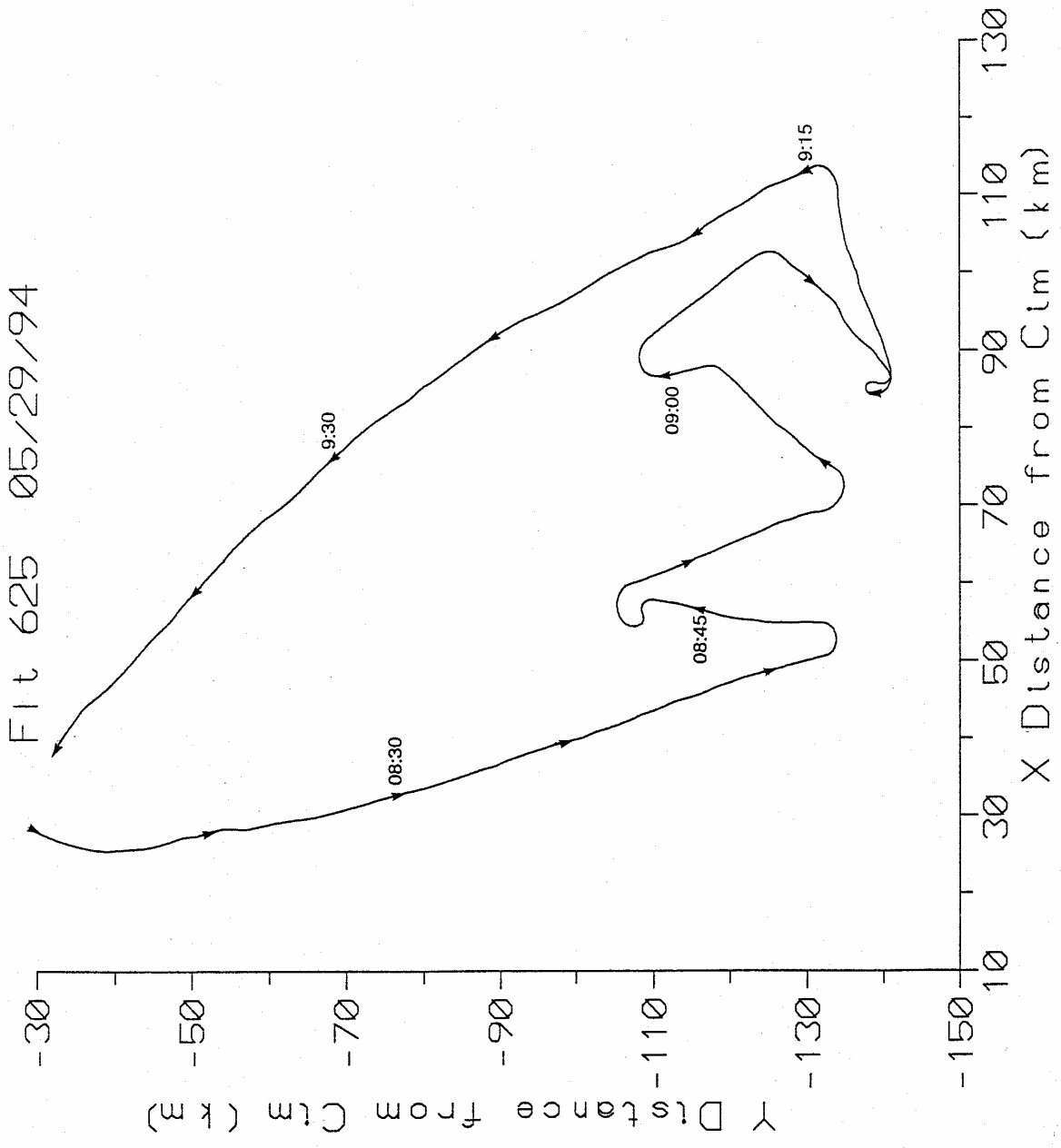
Flt 625 05/29/94
08:30
9:30
08:45
09:00
9:15
Y Distance from Clm (km)
X Distance from Clm (km)
-30
-50
-70
-90
-110
-130
-150
10
30
50
70
90
110
130

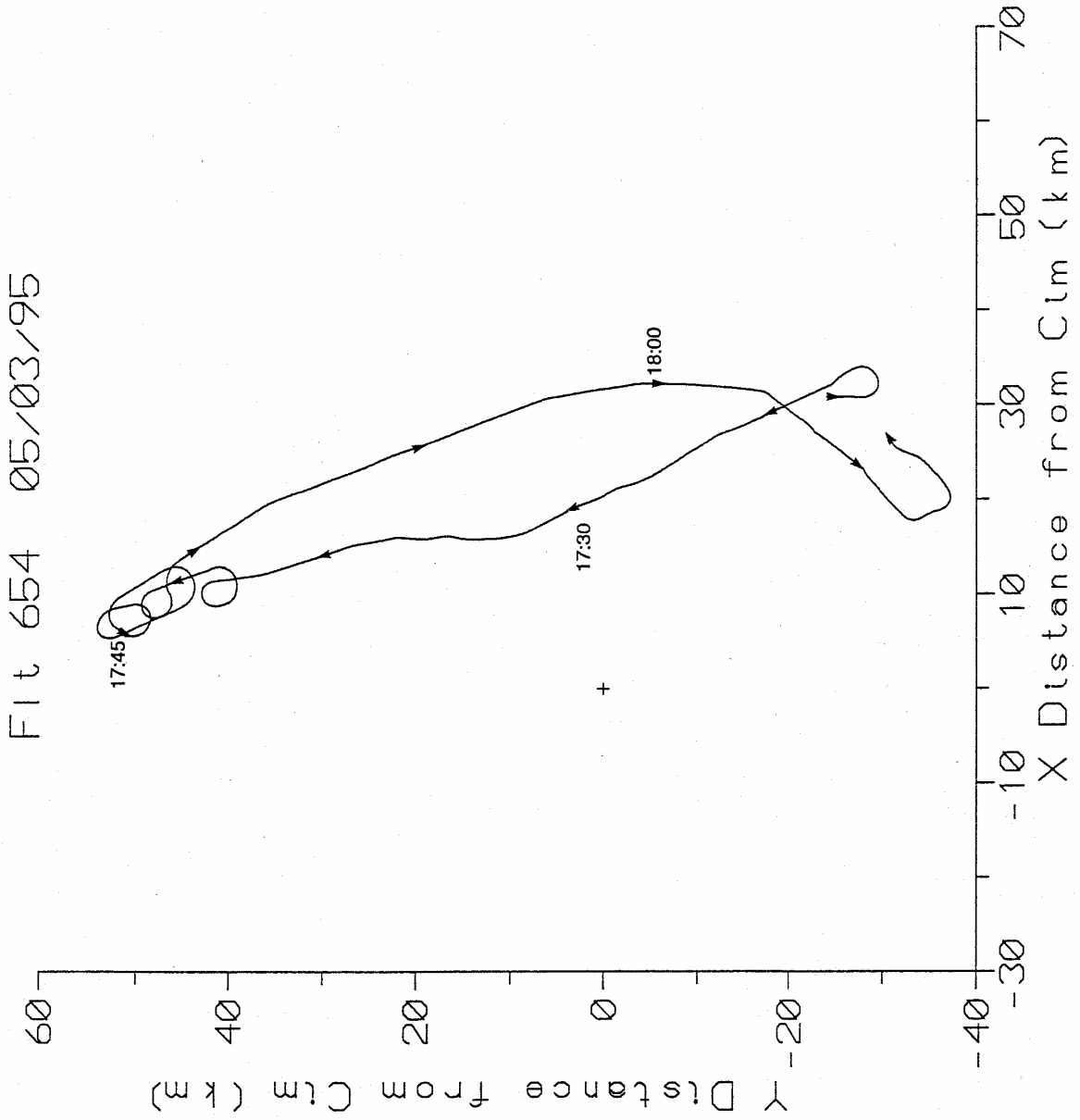
Flt 654 05/03/95
17:45
18:00
17:30
Y Distance from Clm (km)
X Distance from Clm (km)
60
40
20
0
-20
-40
-30
-10
10
30
50
70

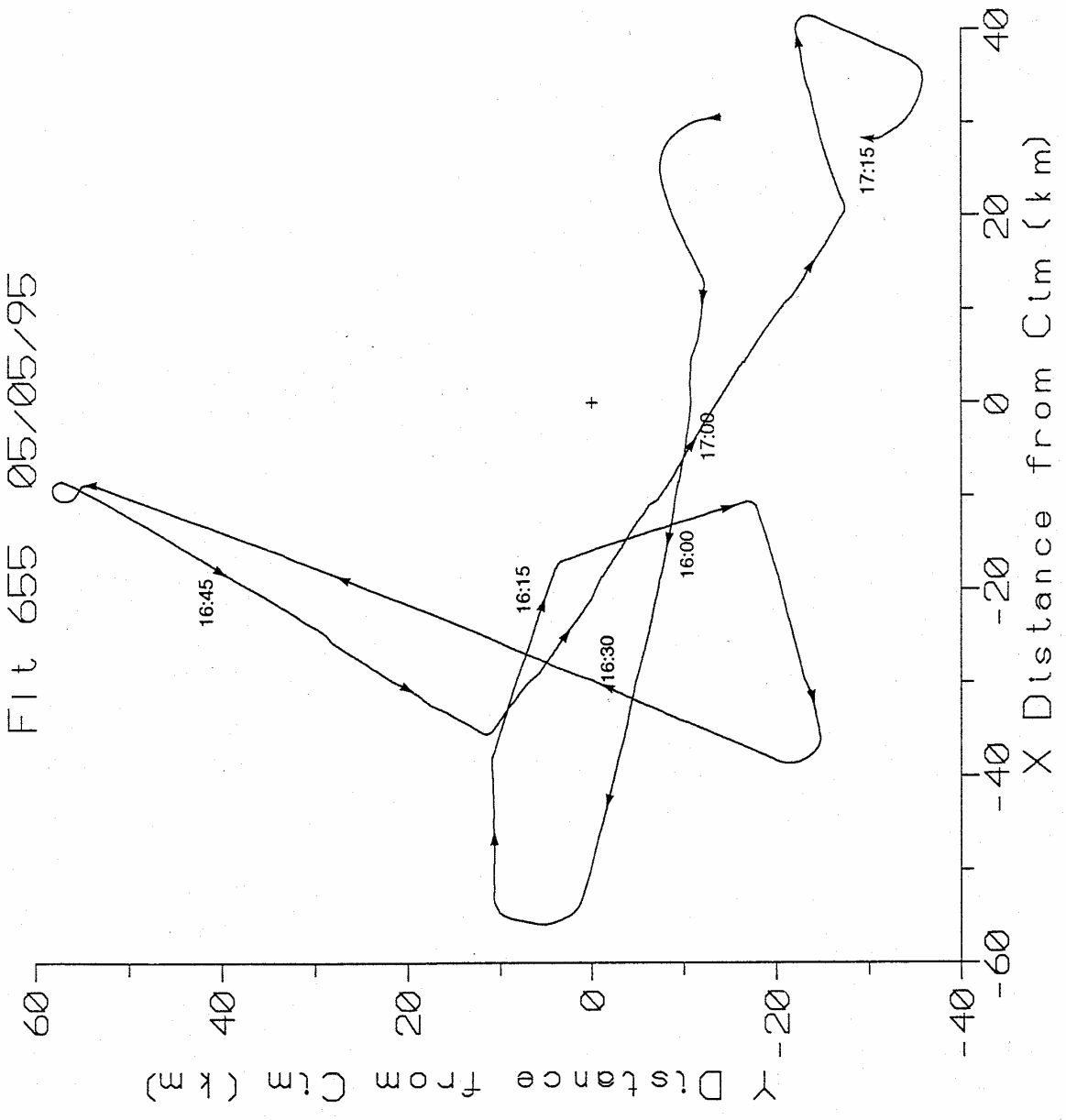
Flt 655 05/05/95
16:45
16:15
16:30
16:00
17:00
17:15
Y Distance from Clm (km)
X Distance from Clm (km)
60
40
20
0
-20
-40
-60
-40
-20
0
20
40

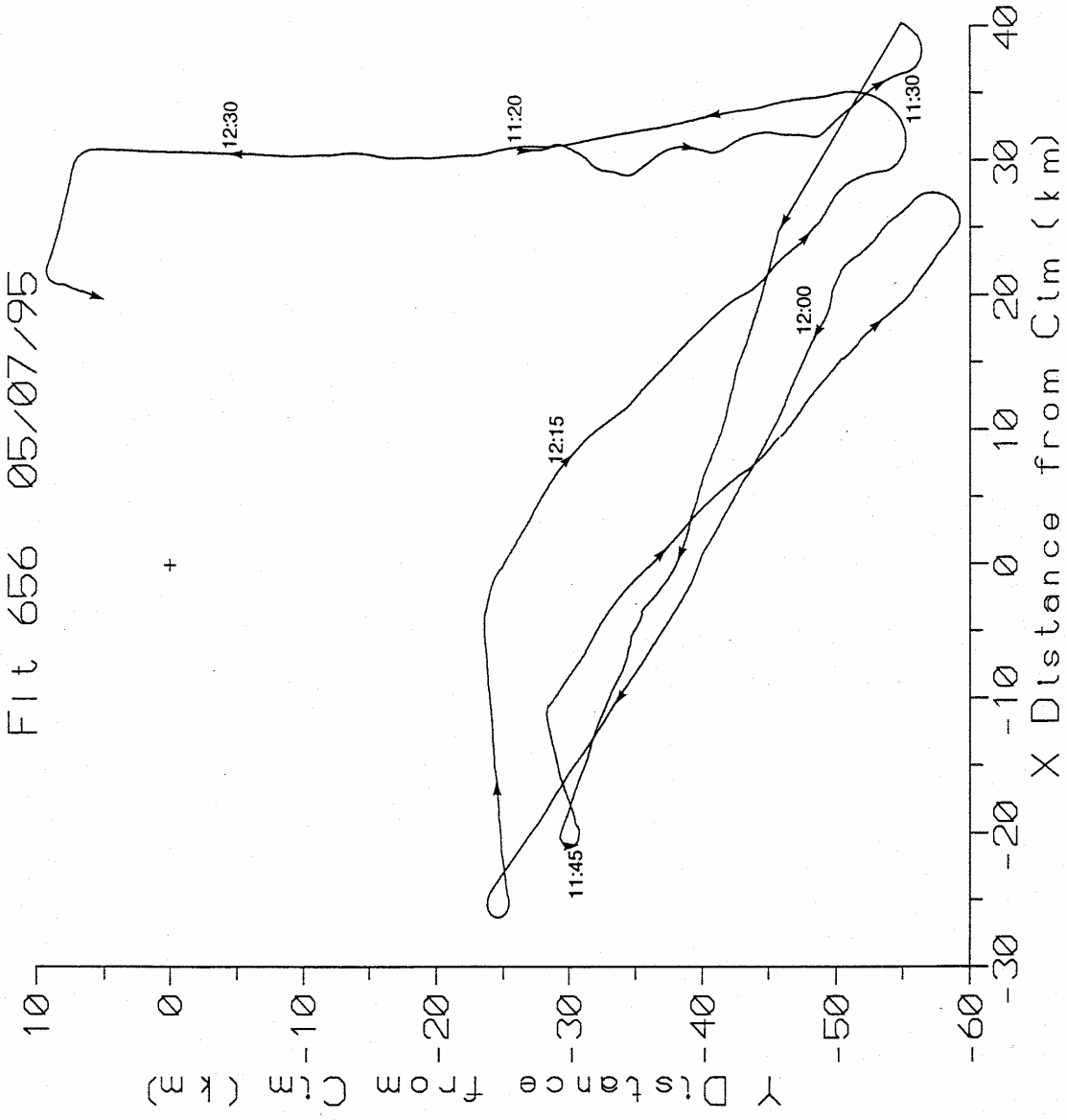
Flt 656 05/07/95
12:30
11:20
11:30
12:00
12:15
11:45
Y Distance from Clm (km)
X Distance from Clm (km)
10
0
-10
-20
-30
-40
-50
-60
40
30
20
10
0
-10
-20
-30

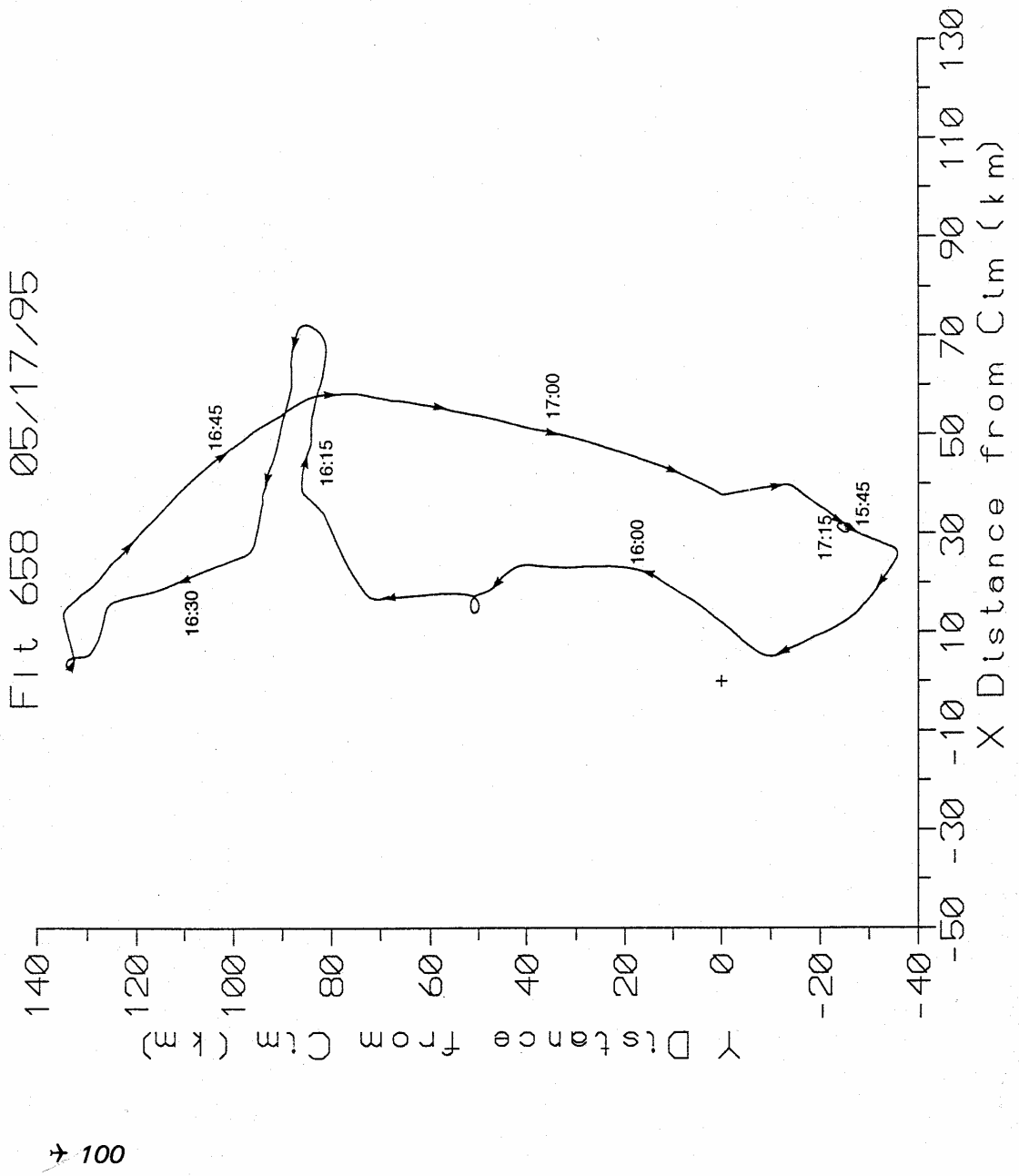
Flt 658 05/17/95
16:45
16:30
16:15
17:00
16:00
17:15
15:45
Y Distance from Clm (km)
X Distance from Clm (km)
140
120
100
80
60
40
20
0
-20
-40
-50
-30
-10
10
30
50
70
90
110
130

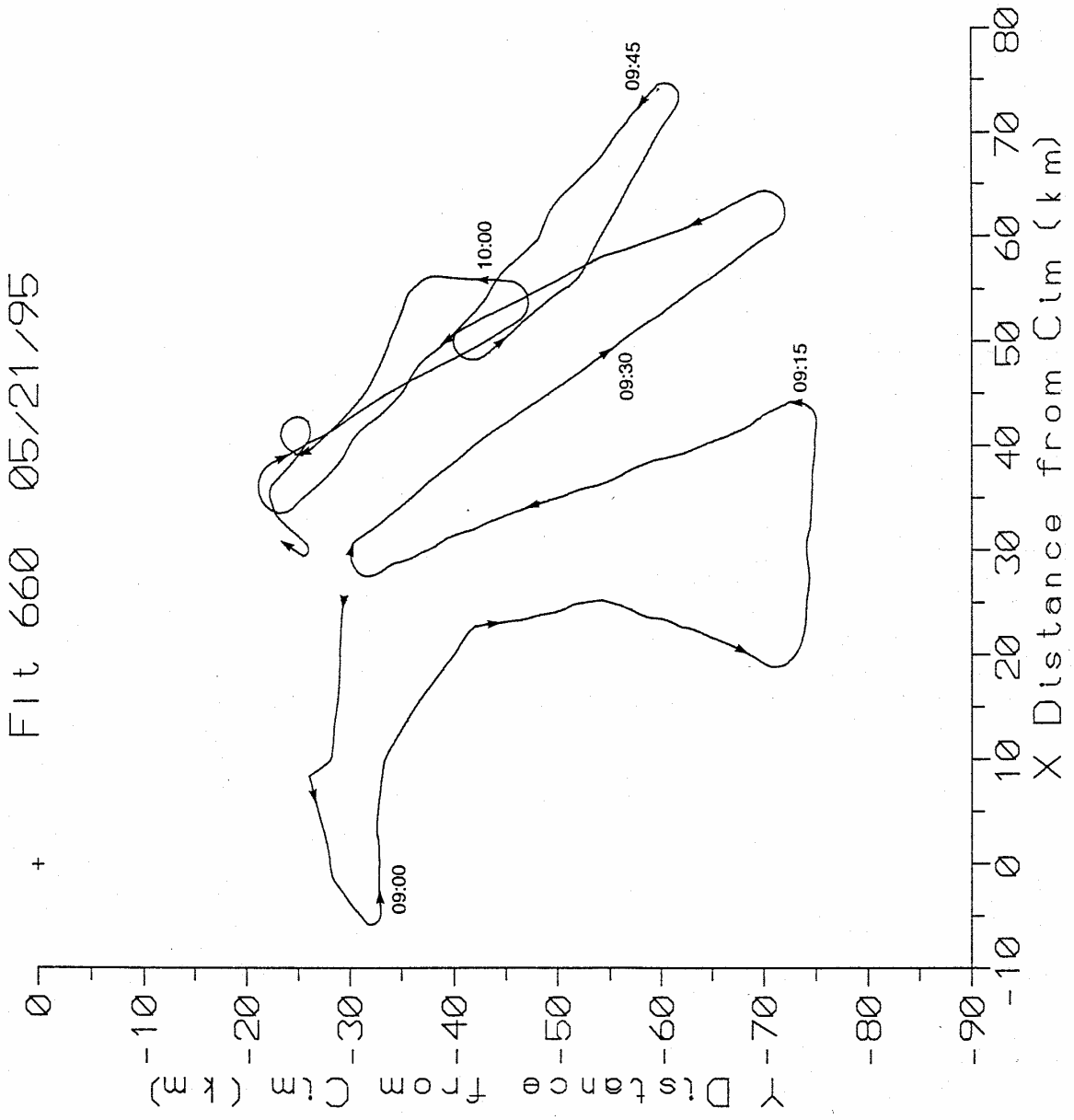
Flt 660 05/21/95
09:00
09:15
09:30
09:45
10:00
Y Distance from Clm (km)
X Distance from Clm (km)
0
-10
-20
-30
-40
-50
-60
-70
-80
-90
-10
0
10
20
30
40
50
60
70
80

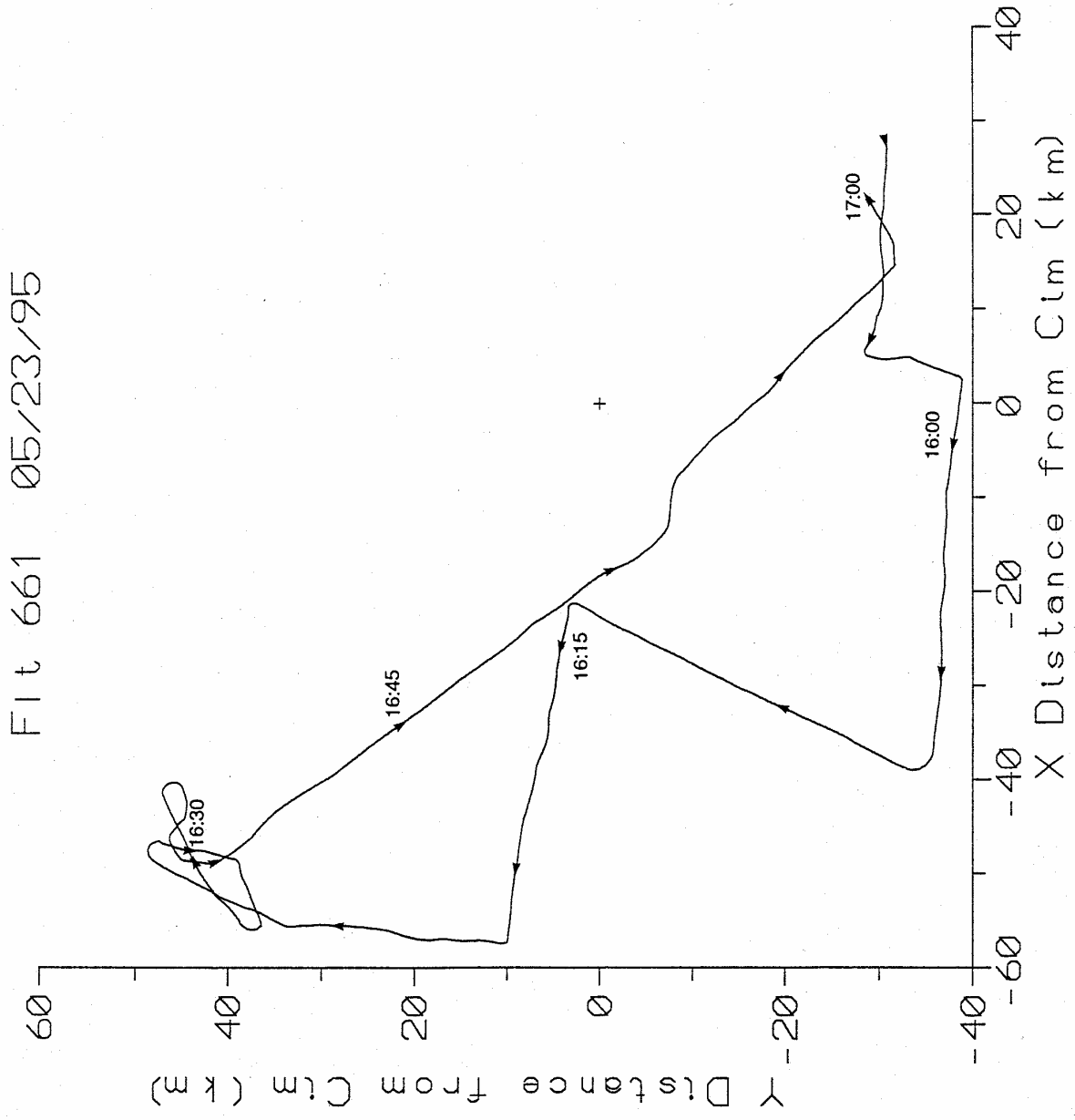
Flt 661 05/23/95
Y Distance from Clm (km)
X Distance from Clm (km)
60
40
20
0
-20
-40
-60
-40
-20
0
20
40
16:30
16:45
16:15
16:00
17:00

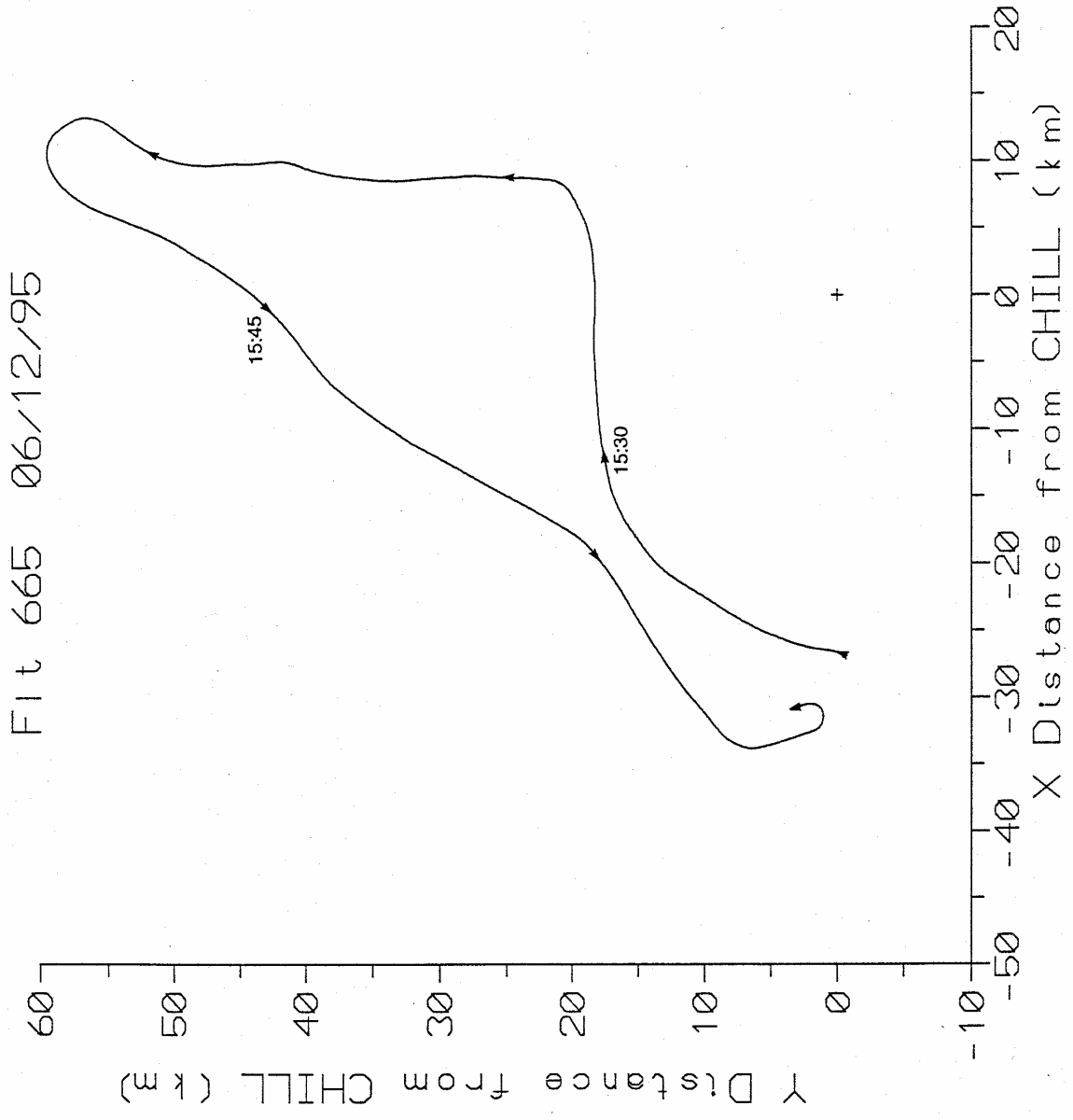
Flt 665 06/12/95
15:45
15:30
Y Distance from CHILL (km)
X Distance from CHILL (km)
60
50
40
30
20
10
0
-10
-50
-40
-30
-20
-10
0
10
20

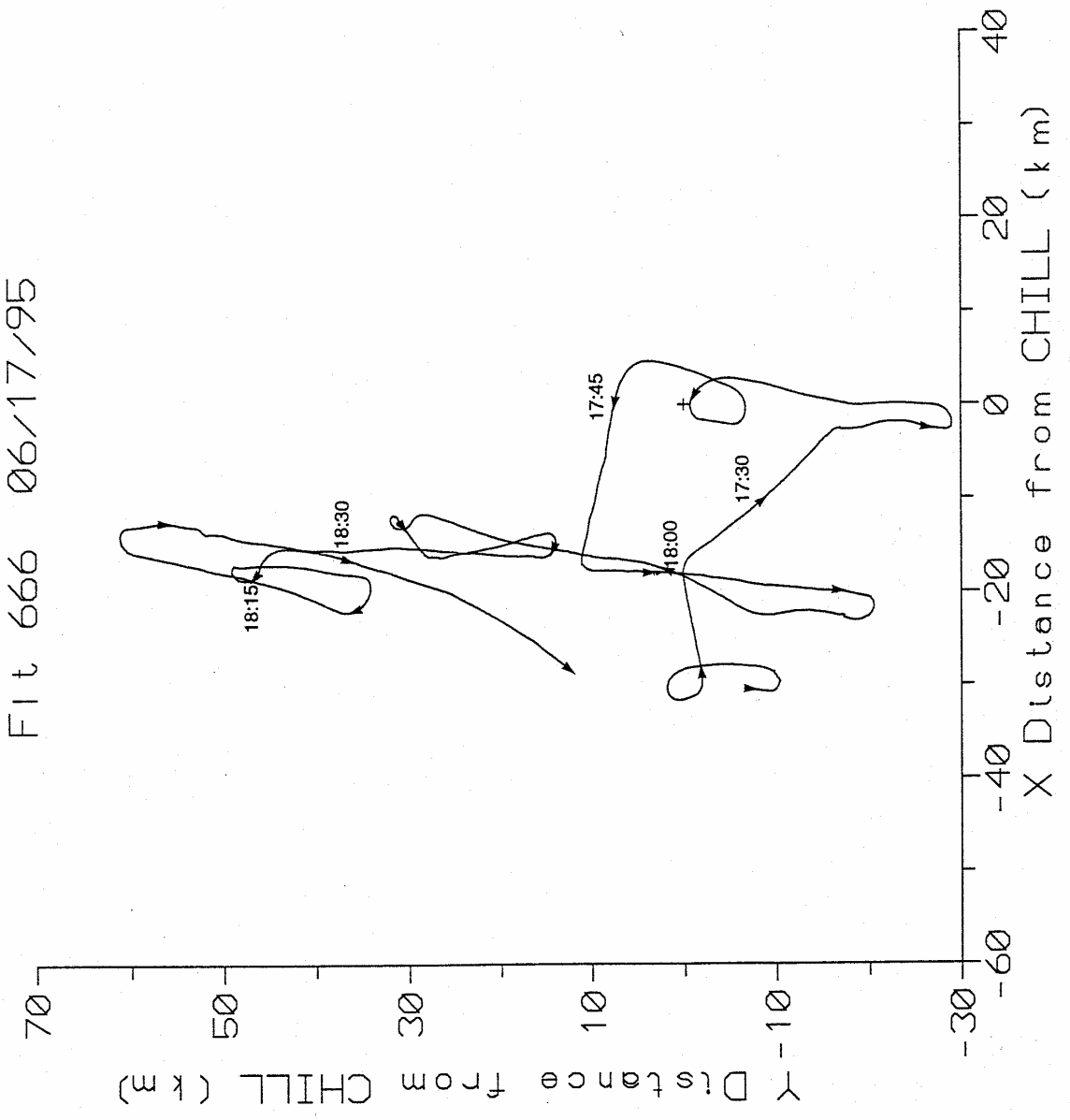
Flt 666 06/17/95
18:15
18:30
17:45
18:00
17:30
70
50
30
10
-10
-30
-60
-40
-20
0
20
40
Y Distance from CHILL (km)
X Distance from CHILL (km)

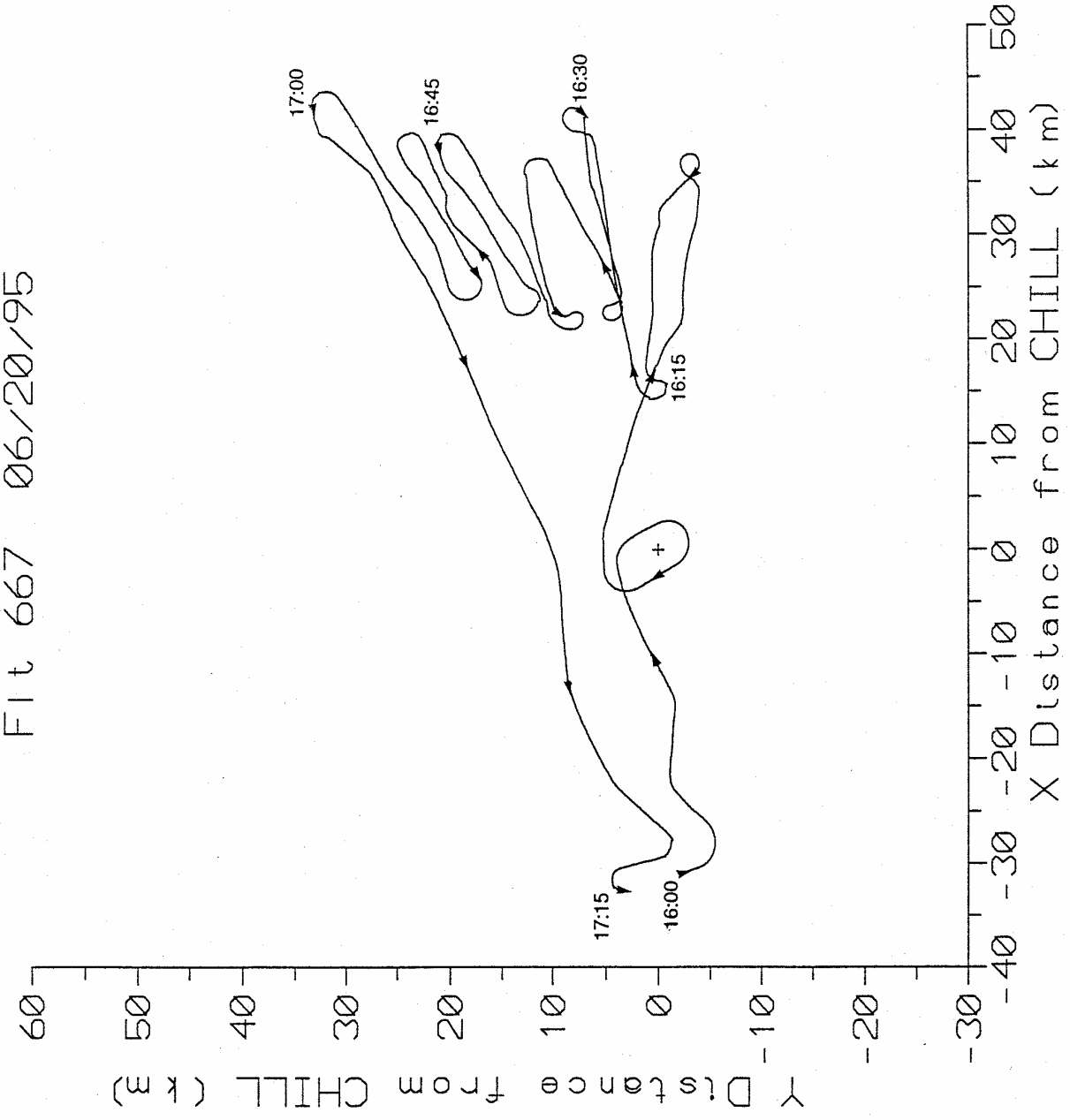
Flt 667 06/20/95
17:00
16:45
16:30
16:15
17:15
16:00
Y Distance from CHILL (km)
X Distance from CHILL (km)
60
50
40
30
20
10
0
-10
-20
-30
-40
-30
-20
-10
0
10
20
30
40
50

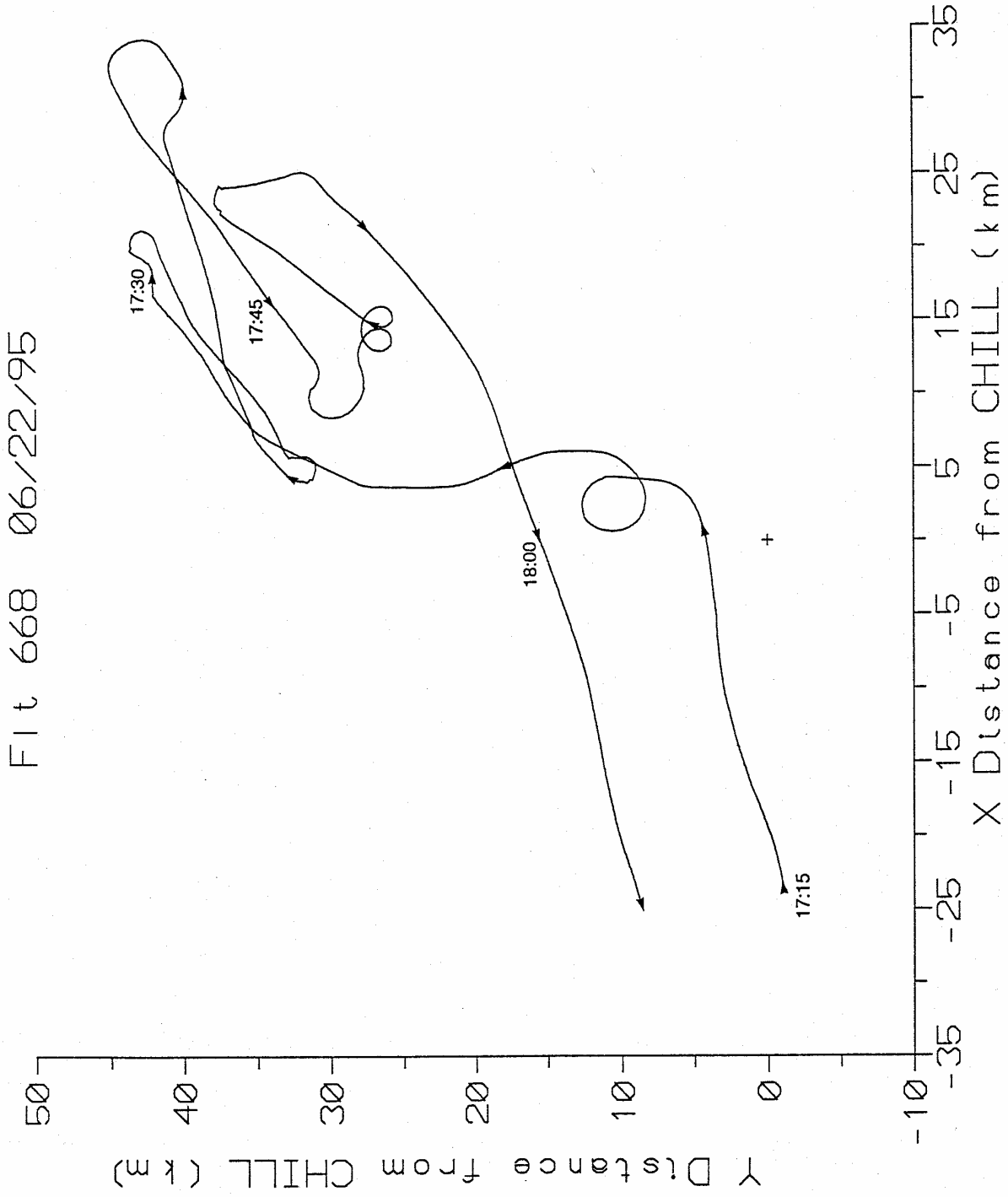
Flt 668 06/22/95
17:30
17:45
18:00
17:15
+
X Distance from CHILL (km)
Y Distance from CHILL (km)
-35
-25
-15
-5
5
15
25
35
-10
0
10
20
30
40
50

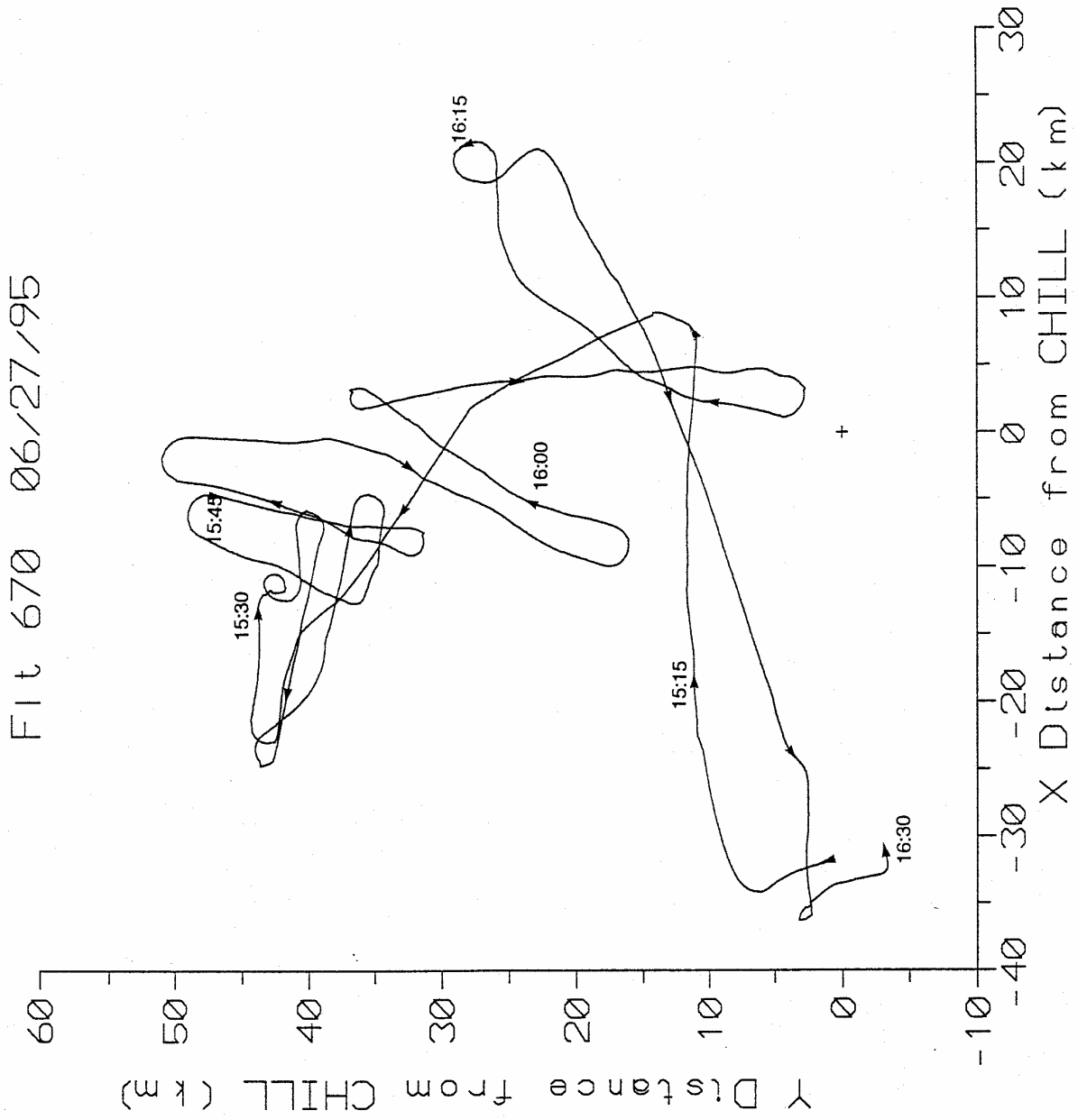
Flt 670 06/27/95
Y Distance from CHILL (km)
X Distance from CHILL (km)
60
50
40
30
20
10
0
-10
-40
-30
-20
-10
0
10
20
30
15:30
15:45
16:00
16:15
15:15
16:30

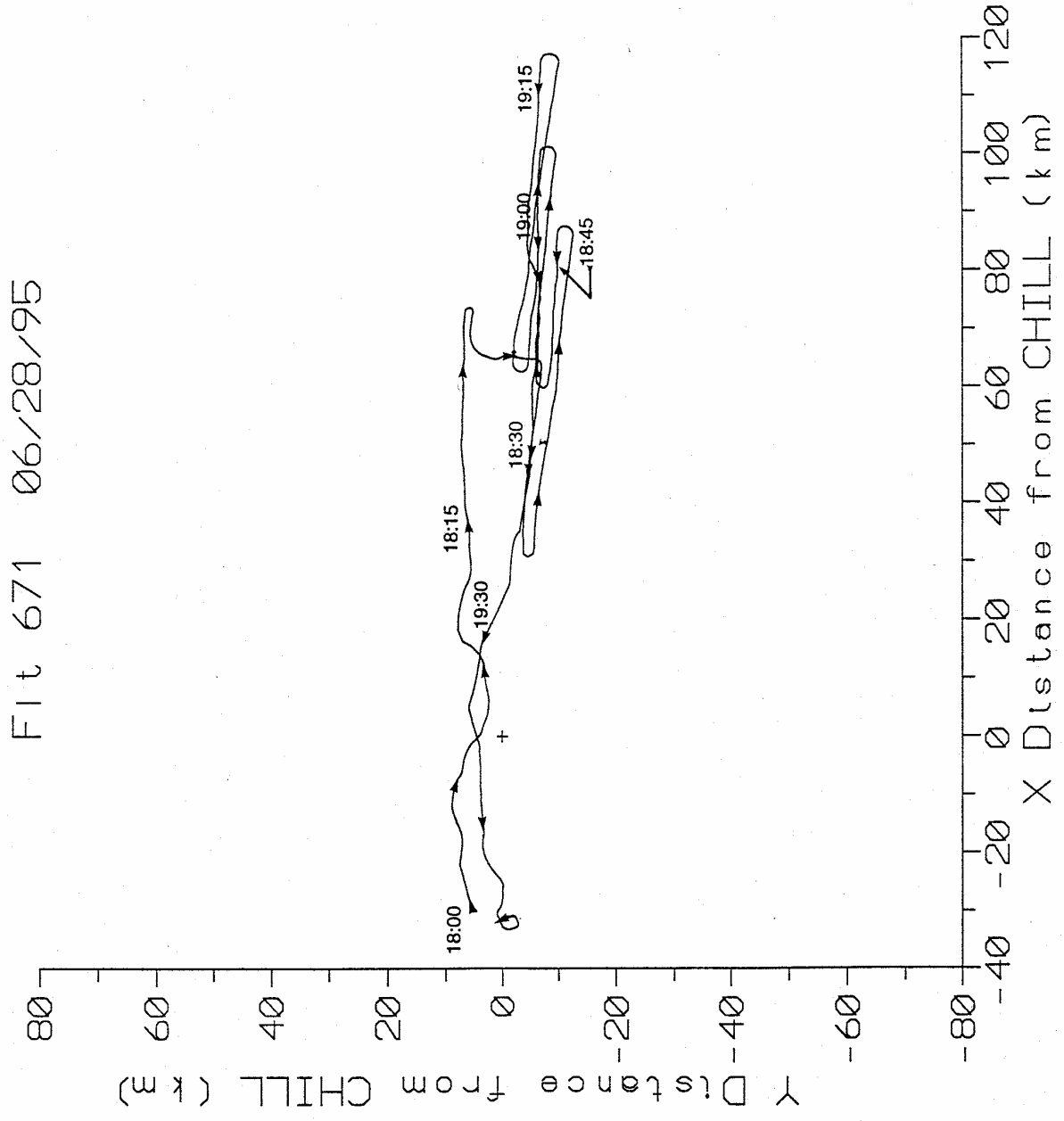
Flt 671 06/28/95
18:00
18:15
18:30
18:45
19:00
19:15
19:30
X Distance from CHILL (km)
Y Distance from CHILL (km)
-40
-20
0
20
40
60
80
100
120
80
60
40
20
0
-20
-40
-60
-80